Memoirs of the Faculty of Engineering, Nagoya University
Vol. 32, No. 1. (1980)

THEORY OF STREAMLINE ANALYSIS METHOD REFERRED TO THE ORTHOGONAL CURVILINEAR COORDINATES

SHIGEO UCHIDA

Department of Aeronautical Engineering

(Received June 2, 1980)

Abstract

Fundamental concepts of the theory of streamline analysis method and its applications are presented. Controlling the form of curvilinear coordinates close to the estimating pattern for the solution, the partial differential equation can be divided into series of ordinary ones, and thus integration is simplified. To improve the approximations iterative procedures are employed. In the flux analysis method the coordinates are corrected by the patterns of approximate solution in each step of iterations. Applications to the compressible flow through a nozzle of predicted wall velocity, cascade flows, the supersonic flow around a blunt body and swirling flow through arbitrary pipe are presented.

A brief notice on the explicit solution of mixing layer referring to the stream-surface coordinates are also given. Fundamental equations of fluid mechanics referred to generalized coordinates with twist of axes and to other coordinate system are presented in Appendices.

CONTENTS

Chapter 1. Introduction

Many problems in fluid dynamics are highly non-linear, even if the effect of viscosity is excluded. The non-linearities are frequently originated from the large deformation of flow patterns by finite disturbances. On the way of investigation on highly deformed compressible flow through a turbine cascade in 1944~47, the

present author[1] devised an idea of the use of orthogonal curvilinear coordinates adapting to the flow patterns to be solved. When the coordinates can be selected sufficiently close to the patterns of solution, the partial differnetial equation can be approximated by an ordinary one, which can be integrated by the theory of ordinary differential equation. In many cases only a simple integration containing the extension parameters specifying the coordinates is sufficient to proceed the further analysis. Since the fundamental concept is based on the mathematical imagination the present theory[1] will be superior to the stream curvature method[4,5], which is originated from the early study made by Flügel[2,3] in 1915. Thus the application of the present method can be extended to the general forms of partial differential equations.

In recent years many ideas of computational procedure for solving differential equations are presented to give individual values of numerical solutions. As these results are called the numerical experiment, phenomenological images can not be obtained directly from such methods of numerical computation. Since considerations on flow patterns are inherent in the computational procedure, the present method is closely connected with physical imaginations.

Introducing the fundamental concepts and revising some early works on the flux analysis method, further developments of the present theory are presented in this paper, in which applications to the design of the nozzle with prescribed velocity distributions along the wall and the calculation of swirling flow through an arbitrary form of circular pipe are performed by computerizing the whole procedure.

Closely relating to the present subject a brief notice on some fully analytical solutions for the boundary layer equation referred to stream-surface coordinates is described in supplementary remarks. Fundamental equations referred to the general orthogonal curvilinear coordinates with twist of axes and other systems are given in appendices.

Chapter 2. Fundamental concepts of streamline analysis for solving the boundary value problem.

The method of streamline analysis or flux analysis[1] is to solve the flow field by transforming the partial differential equation approximately into the ordinary one referring to an appropriate system of orthogonal curvilinear coordinates, which enables us to select predominant terms being matched boundary condition. Integrating the approximated ordinary differential equation along a specified component of coordinates, values of the dependent variable are calculated being satisfied the boundary conditions. The convergent final solution is obtained by the iterative procedure.

2. 1. A partial differential equation referred to orthogonal curvilinear coordinates

The method of streamline analysis is started by transforming the independent variables of Cartesian coordinates into a general system of orthogonal curvilinear coordinates, for instance, α, β and γ, whose extension parameters are h_α, h_β and h_γ, respectively. The partial differential equation for a dependent variable ϕ (α, β, γ) is expressed by an equation of function of ϕ and its various orders of partial

derivatives:

$$\boldsymbol{D}[\psi,\ \psi_\alpha,\ \psi_\beta,\ \psi_\gamma,\ \psi_{\alpha\alpha},\ \psi_{\beta\beta},\ \psi_{\gamma\gamma},\ \psi_{\alpha\beta},\ \psi_{\beta\gamma},\ \psi_{\gamma\alpha},\ \cdots]=0. \tag{1}$$

This form of equation can be derived, for instance, from the fundamental equations referred to orthogonal curvilinear coordinates as shown in the Appendices of the present paper. Introducing a schematical form of the boundaries as shown in Fig. 1, the boundary conditions for the present problem is assumed, for instance, to be $\psi=$constant along the boundary a and b, and $\partial\psi/\partial n=0$ along c and d, where n is normal length to these boundary.

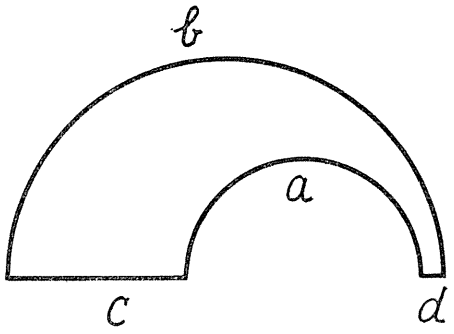

Fig. 1. Space and Boundaries.

Suppose that the form of surface $\beta=$constant is taken very close to that of the expecting final solution $\psi=$constant, which contains boundaries a and b, then the partial derivatives can be separated into two groups of different order of magnitude, in a general sence, predominant and minor ones, respectively:

$$(\psi,\ \psi_\beta,\ \psi_{\beta\beta},\ \cdots)\gg(\psi_\alpha,\ \psi_\gamma,\ \psi_{\alpha\alpha},\ \psi_{\gamma\gamma},\ \psi_{\alpha\beta},\ \psi_{\beta\gamma},\ \psi_{\gamma\alpha},\ \cdots)=0. \tag{2}$$

It is assumed that the concerning partial differential equation can be separated into two terms

$$D[\psi,\ \psi_\beta,\ \psi_{\beta\beta},\ \cdots]+D'[\psi_\alpha,\ \psi_\gamma,\ \psi_{\alpha\alpha},\ \psi_{\gamma\gamma},\ \psi_{\alpha\beta},\ \psi_{\beta\gamma},\ \psi_{\gamma\alpha},\ \cdots]=0, \tag{3}$$

where non-linear terms consisting of derivatives of the first group multiplied by the second group should be contained in D'. It is assumed that

$$D\gg D'. \tag{4}$$

Neglecting the minor term D' the equation for the first approximation is obtained by

$$D[\psi,\ \psi_\beta,\ \psi_{\beta\beta},\ \cdots]=0, \tag{5}$$

which can be integrated by the method for the ordinary differential equations.

There are two ideas for promoting the approximation, i.e. the method of fixed coordinates and that of correcting coordinates.

2. 2. The method of fixed coordinates

Referring to a suitably chosen system of orthogonal curvilinear coordinates, which is fixed throughout the computational procedure the term D' is regarded to be a complementary part to the predominant term D. Neglecting the term D' the first approximation $\psi^{(1)}$ is obtained from $D_1=0$. The term D_1', which is given by substituting $\psi^{(1)}$ into D', can be taken as the correcting term in the differential equation for the second approximation $\psi^{(2)}$ which is expressed by $D_2+D_1'=0$. The solution $\psi^{(2)}$ is substituted into D' and the succeeding approximation is calculated

from $D_3+D_2'=0$. These iterative processes should be continued until the converging solution is obtained.

Denoting the degree of approximation by superscript (m), the differential equations in each stage are

$$
\begin{aligned}
&D_1[\psi^{(1)},\ \psi_\beta{}^{(1)},\ \psi_{\beta\beta}{}^{(1)},\ \cdots]=0 \qquad \text{for } \psi^{(1)},\\
&D_2[\psi^{(2)},\ \psi_\beta{}^{(2)},\ \psi_{\beta\beta}{}^{(2)},\ \cdots]+D_1'[\psi_\alpha{}^{(1)},\ \psi_\gamma{}^{(1)},\ \psi_{\alpha\alpha}{}^{(1)},\ \psi_{\gamma\gamma}{}^{(1)},\\
&\quad \psi_{\alpha\beta}{}^{(1)},\ \psi_{\beta\gamma}{}^{(1)},\ \psi_{\gamma\alpha}{}^{(1)},\ \cdots]=0 \qquad \text{for } \psi^{(2)},\\
&\cdots\cdots\cdots\cdots\cdots\cdots\cdots\cdots\cdots\cdots \qquad (6)\\
&D_m[\psi^{(m)},\ \psi_\beta{}^{(m)},\ \psi_{\beta\beta}{}^{(m)},\ \cdots]+D_{m-1}'[\psi_\alpha{}^{(m-1)},\ \psi_\gamma{}^{(m-1)},\ \psi_{\alpha\alpha}{}^{(m-1)},\\
&\quad \psi_{\gamma\gamma}{}^{(m-1)},\ \psi_{\alpha\beta}{}^{(m-1)},\ \psi_{\beta\gamma}{}^{(m-1)},\ \psi_{\gamma\alpha}{}^{(m-1)},\ \cdots]=0 \quad \text{for } \psi^{(m)},\\
&\cdots\cdots\cdots\cdots\cdots\cdots
\end{aligned}
$$

These equations can be solved by the theory in ordinary differential equations. In each stage integration constants should be determined by satisfying the boundary conditions. They are generally expressed by functions of α and γ.

2. 3. *The method of correcting coordinates*

This is the original method of streamline analysis or of flux analysis, which is developed originally by the present author[1] improving the stream curvature method devised by Flügel[2,3]. The algorithm of the stream curvature method is recently developed by Bindon & Carmichael[4] and Barger[5]. Taking arc lengths of natural coordinates as independent variables Flügel referred the equation normal to the streamline. Velocity ratios are derived by integrating the streamline curvature along the arc normal to the flow. Since arc lengths in orthogonal curvilinear coordinates can not be taken as independent variables, Flügel's method is conceptually improper.

The fundamental idea of streamline analysis or of flux analysis[1] was developed by using the proper independent variables in orthogonal curvilinear coordinates.

In the method of correcting coordinates the curvilinear coordinates in each stage are corrected by the solution in preceding step of approximation, and only the predominant term D is considered in the differential equation.

Calculating the first approximation ψ_1 from $D_1=0$, the original curve of coordinate $\beta_0=$constant is corrected to give $\beta_1=$constant by replacing with the curve of $\psi_1=$constant. Then the second approximation ψ_2 is calculated from $D_2=0$ and the coordinate curve $\beta_1=$constant is replaced by the curve of $\psi_2=$constant, resulting in the revised coordinate curve $\beta_2=$constant. These iterative procedure is continued until convergent solution is obtained.

Denoting the degree of approximation by subscript m, the differential equations in each stage are

$$D_1\left[\psi_1,\ \frac{\partial\psi_1}{\partial\beta_0},\ \frac{\partial^2\psi_1}{\partial\beta_0^2},\ \cdots\right]=0 \quad \text{for} \quad \psi_1,$$

$$D_2\left[\psi_2,\ \frac{\partial\psi_2}{\partial\beta_1},\ \frac{\partial^2\psi_2}{\partial\beta_1^2},\ \cdots\right]=0 \quad \text{for} \quad \psi_2, \tag{7}$$

.....

$$D_m\left[\psi_m,\ \frac{\partial\psi_m}{\partial\beta_{m-1}},\ \frac{\partial^2\psi_m}{\partial\beta_{m-1}^2},\ \cdots\right]=0 \quad \text{for} \quad \psi_m,$$

.....

In each stage integration constants should be determined by satisfying the boundary conditions.

In the present method forms of other coordinates, i.e. $\alpha=$constant and $\gamma=$constant, should be determined by their conditions of othogonality. For the cases of two-dimensional or axisymmetrical field the orthogonal coordinates $\alpha=$constant are simply determined by geometry as the curves normal to those $\beta=$constant.

It is clear that a converged result can be taken as the correct solution, but the conditon of convergence is so complicated that it is left to the computation for the individual problem.

2. 4. The generation of orthogonal meshes for a group of given curves

In the early time normal curves to $\beta=$constant were drawn with graphical process. Since a FORTRAN Ⅳ program has been presented by McNally[6] recently, the orthogonal mesh for a group of given curves can be generated by a computational procedure.

Denoting the mesh point by suffix ij the concerning field is divided by n coordinate lines of $\beta=$constant, where $j=1$ and $j=n$ represent the boundaries a and b, respectively, shown in Fig. 1. In generating m orthogonals the boundaries c and d are taken as the upper and the lower end of orthogonals, which are denoted by $i=1$ and $i=m$, respectively. The curve of $\beta=$constant is represented by m-1 cubic spline curves, which are connected at the m-2 array points smoothly up to the second derivative in order to make curvature continuous. At the both end denoted by $i=1$ and m the coordinates and the first derivatives, which make the curve normal to the boundaries c and d, can determine the end spline curves.

According to McNally[6] the normal coordinate curves are obtained by means of a predictor-corrector technique in which normals to adjacent coordinate curve of $\beta=$constant is used. A normal line between $\beta_j=$constant and $\beta_{j+1}=$constant shown in Fig. 2 can be drawn by the following steps:

(1) A normal line to the curve of $\beta_j=$constant started at a desired point A intersects the curve of $\beta_{j+1}=$constant at point B.

(2) The tangent to the curve of $\beta_{j+1}=$

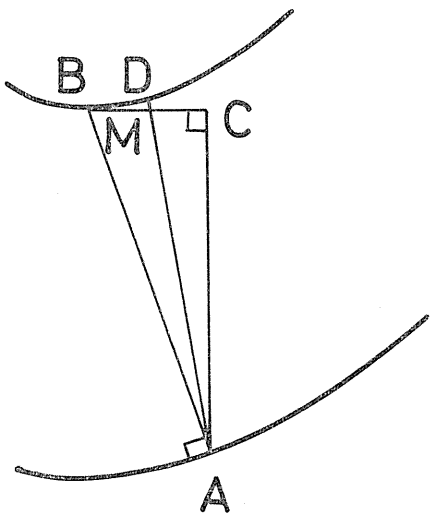

Fig. 2. Orthogonal line between two curves.

constant at this point B and the normal to it from the point A intersects at point C.
(3) Taking the mid point M between B and C, the line AM intersects the curve of $\beta_{j+1}=$constant at point D.
(4) The line AD is designated as the part of orthogonal line to the curve of $\beta=$ constant in this section.

Chapter 3. The compressible flow of an ideal gas through a channel

Fundamental concepts on streamline analysis have been applied to solve the compressible flow through a two-dimensional channel with circular wall. Comparing with the experiment, even the first approximation reveals an excellent agreement.

3. 1. Fundamental equations referred to orthogonal curvilinear coordinates

Referring to the plane orthogonal curvilinear coordinates: α and β, extension parameters

$$h_\alpha=\sqrt{x_\alpha^2+y_\alpha^2}\,,\quad h_\beta=\sqrt{x_\beta^2+y_\beta^2}\,, \tag{8}$$

are introduced. u, v denote the components of the velocity vector V in the α, β directions, respectively. The steady compressible flow of a inviscid fluid is governed by fundamental equations of continuity and irrotationality:

$$\text{div}\,(\rho V)\equiv(1/h_\alpha h_\beta)[(\rho u h_\beta)_\alpha+(\rho v h_\alpha)_\beta]=0, \tag{9}$$

$$\text{rot}\,V\equiv(1/h_\alpha h_\beta)[(v h_\beta)_\alpha-(u h_\alpha)_\beta]=0. \tag{10}$$

Introducing the stream function: ψ, defined by

$$u=\psi_\beta/\rho h_\beta,\quad v=-\psi_\alpha/\rho h_\alpha, \tag{11}$$

Eq. (9) is satisfied identically. Substituting Eq. (11) into Eq. (10), we have the non-linear partial differential equation for ψ:

$$\frac{\partial}{\partial\alpha}\left(\frac{h_\beta}{h_\alpha}\frac{1}{\rho}\frac{\partial\psi}{\partial\alpha}\right)+\frac{\partial}{\partial\beta}\left(\frac{h_\alpha}{h_\beta}\frac{1}{\rho}\frac{\partial\psi}{\partial\beta}\right)=0. \tag{12}$$

The equation of total energy to-gether with the relation of adiabatic change furnishes the formula of density:

$$\frac{\rho}{\rho_0}=\left[1-\frac{\gamma-1}{2c_0^2}\left\{\left(\frac{1}{h_\alpha}\frac{1}{\rho}\frac{\partial\psi}{\partial\alpha}\right)^2+\left(\frac{1}{h_\beta}\frac{1}{\rho}\frac{\partial\psi}{\partial\beta}\right)^2\right\}\right]^{\frac{1}{\gamma-1}}, \tag{13}$$

where ρ_0 and c_0 are the density and the velocity of sound in stagnation, respectively, and γ is the ratio of specific heats for constant pressure and for constant volume: $\gamma=c_p/c_v$.

Denoting the values of coordinate for the boundaries a, b and c, d by β_a, β_b and α_c, α_d, respectively, the boundary conditions are, for instance,

$$\psi=\psi_a\quad\text{at}\ \beta=\beta_a\ ;\quad\psi=\psi_b\quad\text{at}\ \beta=\beta_b, \tag{14}$$

$$\psi_\alpha=0 \quad \text{at } \alpha=\alpha_c \ ; \quad \psi_\alpha=0 \quad \text{at } \alpha=\alpha_d. \tag{15}$$

3. 2. Integrations by the method of fixed coordinates

In the narrow path of a nozzle flow patterns of compressible flow do not deviate much from those of incompressible flow. Hence, the coordinate axis $\beta=$constant can be assumed to be sufficiently close to the expected solution. If there are no singular point in the concerning field, $(\psi_\alpha, \psi_{\alpha\alpha}, \ldots.)$ may be very small quantities comparing with $(\psi, \psi_\beta, \psi_{\beta\beta}, \ldots.)$, and therefore, the first approximation ψ_1 can be obtained by neglecting the first term of Eq. (12) :

$$\frac{\partial}{\partial\beta}\left(\frac{h_\alpha}{h_\beta}\frac{1}{\rho_1}\frac{\partial\psi_1}{\partial\beta}\right)=0. \tag{16}$$

Substituting ψ_1 into the term initially neglected, the second approximation ψ_2 is calculated from

$$\frac{\partial}{\partial\beta}\left(\frac{h_\alpha}{h_\beta}\frac{1}{\rho_2}\frac{\partial\psi_2}{\partial\beta}\right)=-\frac{\partial}{\partial\alpha}\left(\frac{h_\beta}{h_\alpha}\frac{1}{\rho_1}\frac{\partial\psi_1}{\partial\alpha}\right). \tag{17}$$

In the similar way the differential equation for the mth approximation is given by

$$\frac{\partial}{\partial\beta}\left(\frac{h_\alpha}{h_\beta}\frac{1}{\rho_m}\frac{\partial\psi_m}{\partial\beta}\right)=-\frac{\partial}{\partial\alpha}\left(\frac{h_\beta}{h_\alpha}\frac{1}{\rho_{m-1}}\frac{\partial\psi_{m-1}}{\partial\alpha}\right). \tag{18}$$

Since the term in wright hand side is a known function, Eq. (18) is an ordinary differential equation and it can be integrated resulting in

$$\frac{h_\alpha}{h_\beta}\frac{1}{\rho_m}\frac{\partial\psi_m}{\partial\beta}=\int_{\beta a}^{\beta}-\frac{\partial}{\partial\alpha}\left(\frac{h_\beta}{h_\alpha}\frac{1}{\rho_{m-1}}\frac{\partial\psi_{m-1}}{\partial\alpha}\right)d\beta+F_m(\alpha), \tag{19}$$

where $F_m(\alpha)$ is a function of α. Since $(h_\alpha/h_\beta)\,(1/\rho_m)\,(\partial\psi_m/\partial\beta)=h_\alpha u_m$, $F_m(\alpha)$ is the boundary value of $(h_\alpha u_m)_{\beta=\beta a}$.

$$\psi_m=\int_{\beta a}^{\beta}\frac{h_\beta}{h_\alpha}\rho_m d\beta\int_{\beta a}^{\beta}-\frac{\partial}{\partial\alpha}\left(\frac{h_\beta}{h_\alpha}\frac{1}{\rho_{m-1}}\frac{\partial\psi_{m-1}}{\partial\alpha}\right)d\beta$$

$$+\int_{\beta a}^{\beta}\frac{h_\beta}{h_\alpha}\rho_m F_m(\alpha)\,d\beta+G_m(\alpha), \tag{20}$$

where $F_m(\alpha)$ and $G_m(\alpha)$ are determined by the boundary condition, i.e. Eq. (14), resulting in $G_m(\alpha)=\psi_a$. $F_m(\alpha)$ is determined by

$$\psi_b=\int_{\beta a}^{\beta b}\frac{h_\beta}{h_\alpha}\rho_m d\beta\int_{\beta a}^{\beta}-\frac{\partial}{\partial\alpha}\left(\frac{h_\beta}{h_\alpha}\frac{1}{\rho_{m-1}}\frac{\partial\psi_{m-1}}{\partial\alpha}\right)d\beta$$

$$+\int_{\beta a}^{\beta b}\frac{h_\beta}{h_\alpha}\rho_m F_m(\alpha)\,d\beta+\psi_a. \tag{21}$$

$F_m(\alpha)$ is given by a function of α and $\psi_b-\psi_a$ which represents the total mass flow through the channel.

The mth approximation of density is calculated by

$$\frac{\rho_m}{\rho_0}=\left[1-\frac{\gamma-1}{2c_0}\left\{\left(\frac{1}{h_\alpha}\frac{1}{\rho_{m-1}}\frac{\partial\psi_{m-1}}{\partial\alpha}\right)^2+\left(\frac{1}{h_\beta}\frac{1}{\rho_m}\frac{\partial\psi_m}{\partial\beta}\right)^2\right\}\right]^{\frac{1}{\gamma-1}}. \tag{22}$$

The boundary conditions given by Eq. (15) are applied to Eqs. (17) and (18) on the boundaries c and d.

3. 3. Integrations by the method of correcting coordinates

The flux analysis method is to construct a set of orthogonal curvilinear coordinates, i.e. stream surface function and normals, following the flow. In order to achieve this process the streamline in the preceding approximation is taken for the coordinate curve of $\beta=$constant, and normals are computed by geometry. With the proceeding of approximation the set of orthogonal curvilinear coordinates and accordingly h_α and h_β are corrected in every step. Since $(\psi_\alpha, \psi_{\alpha\alpha}, \ldots.)$ are always considered to be small enough, these terms are neglected in the differential equation.

The differential equation for the mth approximation is

$$\frac{\partial}{\partial\beta_{m-1}}\left(\frac{h_{\alpha\cdot m-1}}{h_{\beta\cdot m-1}}\frac{1}{\rho_m}\frac{\partial\psi_m}{\partial\beta_{m-1}}\right)=0. \tag{23}$$

This equation can be integrated to give

$$\frac{h_{\alpha\cdot m-1}}{h_{\beta\cdot m-1}}\frac{1}{\rho_m}\frac{\partial\psi_m}{\partial\beta_{m-1}}=F_m(\alpha). \tag{24}$$

Denoting the mth approximation of velocity by u_m defined by

$$u_m=\frac{1}{h_{\beta\cdot m-1}}\frac{1}{\rho_m}\frac{\partial\psi_m}{\partial\beta_{m-1}}, \tag{25}$$

Eq. (24) can be rewritten in the form of

$$h_{\alpha\cdot m-1}u_m=F_m(\alpha), \tag{26}$$

which expresses the constancy of $h_{\alpha\cdot m-1}u_m$ along the normal line to the stream. Integration of Eq. (24) gives

$$\psi_m=\int_{\beta a}^{\beta_{m-1}}\frac{h_{\beta\cdot m-1}}{h_{\alpha\cdot m-1}}\rho_m F_m(\alpha)\,d\beta_{m-1}+G_m(\alpha). \tag{27}$$

$F_m(\alpha)$ and $G_m(\alpha)$ are determined by Eq. (14) of boundary condition. Obviously $G_m(\alpha)=\psi_a$, and $F_m(\alpha)$ is calculated from

$$\psi_b=\int_{\beta a}^{\beta b}\frac{h_{\beta\cdot m-1}}{h_{\alpha\cdot m-1}}\rho_m F_m(\alpha)\,d\beta_{m-1}+\psi_a. \tag{28}$$

The density ρ_m in these formulae is given by

$$\frac{\rho_m}{\rho_0}=\left[1-\frac{\gamma-1}{2c_0^2}\left(\frac{1}{h_{\beta\cdot m-1}}\frac{1}{\rho_m}\frac{\partial\psi_m}{\partial\beta_{m-1}}\right)^2\right]^{\frac{1}{\gamma-1}}. \tag{29}$$

The boundary condition given by Eq. (15) is satisfied by taking the coordinate line of $\beta=$constant normal to the boundary c and. d.

3. 4. The compressible flow through a channel of circular walls

For an illustrative example the flow of a compressible fluid past circular walls has been calculated. The streamline and equi-potential line for the incompressible flow are used to the fundamental coordinate curves. Introducing complex variables defined by $z=x+iy$ and $\zeta=\alpha+i\beta$, flow patterns are calculated by

$$\zeta=\pi+i\ln\frac{z+ic}{z-ic},\quad \text{or}\quad z=c\tan\frac{\zeta}{2}, \tag{30}$$

as shown in Fig. 3. The extension parameters are given by

$$h_\alpha=h_\beta=|dz/d\zeta|=c/(\cos\alpha+\cosh\beta). \tag{31}$$

Denoting the radius of boundary a by R, the case of circular walls given by $R/a=1$ is selected, and the lower half of the channel given by $\beta_a=-\ln(\sqrt{2}+1)$ and $\beta_b=0$ is taken for the present analysis.

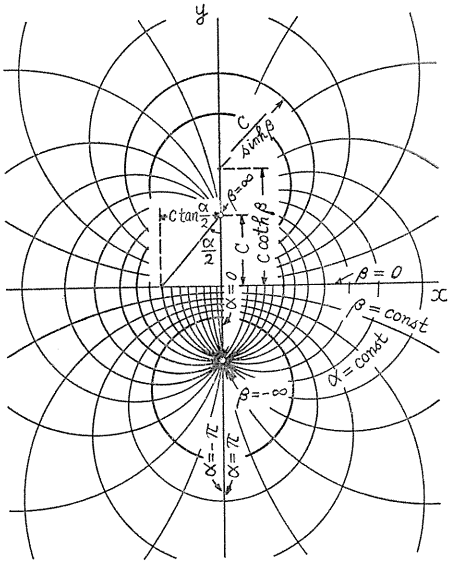

Fig. 3. Orthogonal curvilinear coordinates for the flow through circular walls.

3. 4. 1. Calculation by the method of fixed coordinates

Taking 11 streamlines with intervals of $\Delta\beta=(1/10)\cdot\ln(\sqrt{2}+1)$, calculations by the method of fixed coordinates are performed by the use of Simpson's rule for integration and of Collatz's method for differentiation.

In order to analyse the flow in choking condition the maximum value of $(\psi_b-\psi_a)$ attainable through the whole sections is calculated in every step.

The velocity distributions along the circular wall, u_a/c_0, for the maximum flow, where c_0 is the velocity of sound in the stagnation state, are shown in Table 1. The value of correcting term $D'(\psi_1)$ substituted by the first approximation is less than 0.01, and therefore, the calculation up to four effective figures as in the present case may be almost convergent in the third approximation. The accuracy of the present analysis depends on that of numerical differentiation.

3. 4. 2. Calculation by the method of correcting coordinates

The flow in choking condition is also calculated by the method of correcting

Table 1. Velocity distributions on the circular wall (maximum flow)

	α	Method of fixed coordinates		Method of correcting coordinates		Expts.
		1st approx.	2nd approx.	1st approx.	2nd approx.	
$\frac{u_a}{c_0}$	−0.2644	0.9144		0.916	0.912	0.89
	−0.1763	0.9534		0.954	0.948	0.92
	−0.0881	0.9928	0.9839	0.994	0.985	0.97
	0	1.0329	1.0204	1.034	1.022	1.00
	0.0881	1.0734	1.0600	1.074	1.060	1.03
	0.1763	1.1146		1.114	1.096	1.06
	0.2644	1.1564		1.155	1.134	1.10
$(\psi_b-\psi_a)/\rho_0 c_0 a$		0.2388	0.2390	0.2388	0.23916	

Table 2. Velocity distribution on the circular wall calculated by the method of correcting coordinates (maximum flow)

No. of section	θ	Incomp.	1st approx.	2nd approx.	by Characteristics
−12	−71° 19′	0.2481	0.252	0.252	
−11	−61° 13′	0.2909	0.298	0.298	
−10	−52° 33′	0.3366	0.349	0.349	
−9	−45° 0′	0.3837	0.405	0.405	
−8	−38° 20′	0.4308	0.464	0.464	
−7	−32° 21′	0.4765	0.526	0.526	
−6	−26° 45′	0.5194	0.591	0.592	
−5	−21° 52′	0.5581	0.659	0.660	
−4	−17° 9′	0.5916	0.730	0.730	
−3	−12° 40′	0.6187	0.803	0.802	
−2	− 8° 21′	0.6387	0.879	0.875	
−1	− 4° 9′	0.6510	0.955	0.949	
0	0°	0.6551	1.034	1.022	1.022
1	4° 9′	0.6510	1.113	1.096	1.098
2	8° 21′	0.6387	1.196	1.169	1.177
3	12° 40′	0.6187	1.282	1.241	1.259
4	17° 9′	0.5916	1.374	1.310	1.342
5	21° 52′	0.5581	1.467	1.372	1.425
6	26° 54′	0.5194	1.569	1.423	1.509
7	32° 21′	0.4765	1.679	1.463	1.591
8	38° 20′	0.4308	1.804	1.468	1.669
9	45° 0′	0.3837	1.950	1.382	1.748
10	52° 33′	0.3366	2.132	1.387	1.828
11	61° 13′	0.2909	2.380		
12	71° 19′	0.2481	2.756		

coordinates, i.e. by the flux analysis method. For this purpose the $(\psi_b-\psi_a)$ maximum attainable throughout the sections, which means the minimum value among the maximum of $\psi_b-\psi_a$ for individual sections, is calculated in every step of approximation.

The velocity distributions along the circular wall, u_a/c_0, for the maximum flow condition are given in Tables 1 and 2 and in Fig. 4. The manners of correcting coordinates, which are the progress of approximation of flow patterns started from those in incompressible flow, are shown in Fig. 5. In this case the construction of the orthogonal meshes are performed by graphical process. In spite of low accuracy the calculated values are close to those by the method of fixed coordinates as shown in Table 1.

The convergency of the present method is excellent in all subsonic regions and quite well in a part of supersonic region up to the section No. 2. Downstream from the section No. 4, however, a tendency of divergence is found, and therefore, around this section may be the limiting boundary of this solution. In order to get a convergent solution in the supersonic region calculations by the method of characteristics[5] are jointed from the conditions at the sonic line of second approximation. The velocity distribution u_a/c_0 by this method is given in Fig. 4 by a chain line.

Although starting from the incompressible flow pattern, it is noticed that

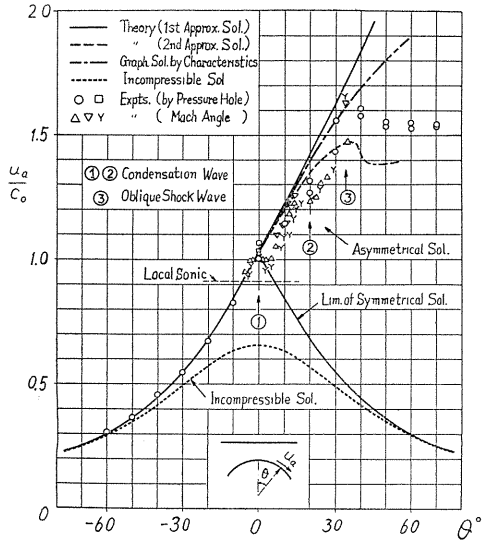

Fig. 4. Velocity distributions along the circular wall in choking condition.

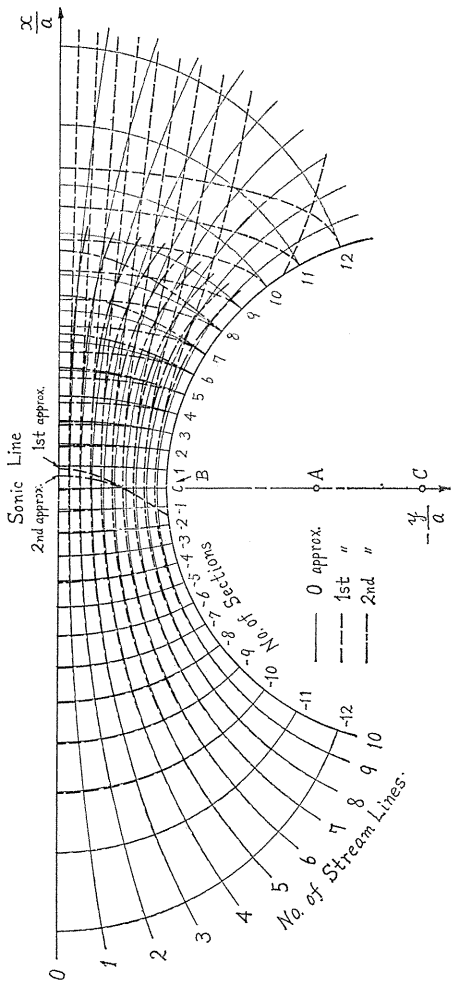

Fig. 5. Streamlines and orthogonals.

the velocity distribution by the first approximation deviates drastically from that of the incompressible flow to give a quite close value to the final result. Comparing with the observed value mentioned later, it is found that the present method gives an excellent consequence.

3. 4. 3. Experimental results

The channel used for the experimental study is shown in Fig. 6. Static pressures along the circular wall are measured by pressure holes at 14 stations. Neglecting the displacement effect of boundary layer the velocity along the circular wall, i.e. u_a/c_0, is calculated by the formula for ideal flow:

$$\frac{u}{c_0}=\sqrt{\frac{2}{\gamma-1}\left[1-\left(\frac{p}{p_0}\right)^{\frac{\gamma-1}{\gamma}}\right]}, \tag{32}$$

resulting in the values shown in Fig. 4.

The measured distribution of wall velocity in the choking condition (maximum flow) agrees very well with that given by the theory up to the middle section. In the supersonic region velocity distribution calculated from Mach angle in Schlieren photograph is also shown in Fig. 4. Two condensation shock waves observed in the lower supersonic region produce stepwise increase of pressure and slight sudden retardation.

Regulating the back pressure distributions of the wall velocity are measured as shown in Fig. 7, where the critical state of the symmetrical flow is also observed. Theoretical curves by the method of correcting coordinates show a good agreement with the observation.

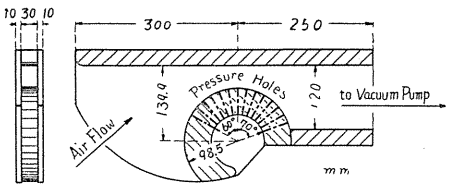

Fig. 6. Channel with a circular wall.

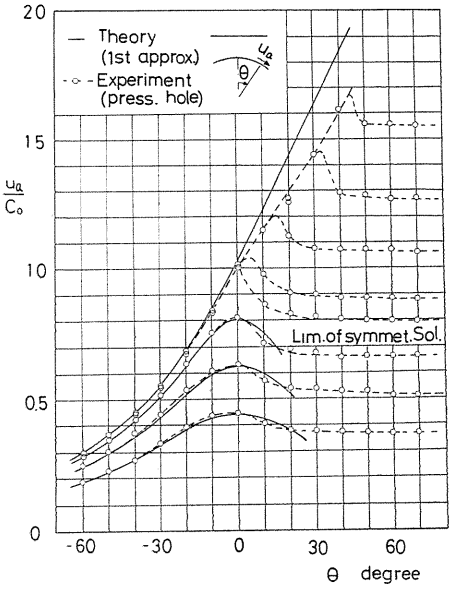

Fig. 7. Velocity distributions for various mass flows.

Chapter 4. The compressible flow through an axisymmetric pipe with a prescribed velocity distribution along the boundary

The pressure loss of a pipe is mainly originated from the friction of boundary layer which is developed along the wall. The flow condition in a boundary layer is governed by the velocity- or pressure distributions outside of the layer. Therefore, the performance of a pipe can be improved by an appropriate selection of the velocity distribution along the wall, with which the irrotational flow is calculated.

For this purpose, the computational algorithm of the flux analysis method is studied by Uchida and Kondo[8] to solve the compressible pipe flow of an inviscid fluid.

4. 1. Computation of the compressible flow through an axisymmetric nozzle with a prescribed velocity distribution.

Introducing an axisymmetric system of orthogonal curvilinear coordinates α, β, γ $(=\theta)$ as given in Appendix C, extension parameters and velocity components in $[\alpha, \beta, \theta]$ directions are $[h_\alpha, h_\beta, h_\gamma\ (=r)]$ and $[u, v, w\ (=0)]$, respectively. The coordinate lines in the meridian plane are shown in Fig. 8. From the equation of continuity:

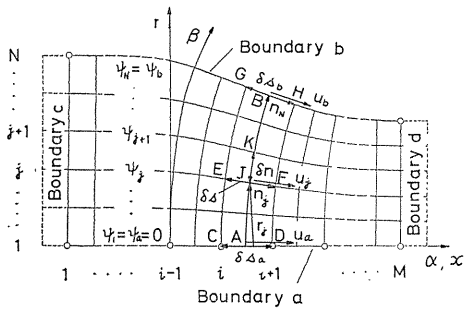

Fig. 8. Stream-surface coordinates for the axisymmetric flow.

$$(1/h_\alpha h_\beta r)[(\rho u r h_\beta)_\alpha + (\rho v r h_\alpha)_\beta] = 0, \tag{33}$$

the stream-surface function ϕ is defined by

$$u = (1/\rho r h_\beta)\phi_\beta, \quad v = -(1/\rho r h_\alpha)\phi_\alpha. \tag{34}$$

The Kelvin's conservation law of circulation holds for a barotropic flow. When the initial upstream is irrotational, then the flow keeps irrotational state in the entire field. Nullifying the γ component of vorticity the equation of irrotationality in the meridian plane is

$$(1/h_\alpha h_\beta)[(v h_\beta)_\alpha - (u h_\alpha)_\beta] = 0. \tag{35}$$

Now, referring the stream-surface coordinates, v is vanished and u becomes the meridian component of velocity, which is the total velocity in the present case. The equation of irrotationality (35) is reduced to

$$(u h_\alpha)_\beta = 0, \tag{36}$$

which is integrated to give

$$uh_\alpha = \text{constant} = u_a h_{\alpha a} = u_b h_{\alpha b}, \tag{37}$$

where subscripts a and b represent quantities on the boundary a and b, respectively. Introduclng an approximate form: $h_\alpha \fallingdotseq \delta s/\delta\alpha$, we have

$$\frac{u}{u_a} = \frac{h_{\alpha a}}{h_\alpha} = \frac{\delta s_a}{\delta s}, \quad \text{or} \quad \frac{u}{u_b} = \frac{h_{\alpha b}}{h_\alpha} = \frac{\delta s_b}{\delta s}. \tag{38}$$

The velocity ratio across the flow is given by the ratio of extension parameters for the coordinates of flow patterns.

Since $\psi_\alpha = 0$ from the equation of continuity referred to stream-surface coordinates, we have

$$d\psi/d\beta = \rho u r h_\beta, \tag{39}$$

which is integrated to give

$$\psi = \int \rho u r h_\beta d\beta + F(\alpha). \tag{40}$$

Since $h_\beta d\beta = dn$ along the β axis, ψ is expressed by

$$\psi(n\,;\,\alpha) = \int_0^n \rho u r dn, \tag{41}$$

where $\psi = 0$ is taken at $n = 0$. Referring to the radius of nozzle exit a, the speed of sound u_* and the density ρ_* at sonic state, i. e. the local Mach number unity, the non-dimensional form of stream function is expressed by

$$\frac{\psi(n\,;\,\alpha)}{\rho_* u_* a^2} = \int_0^{n/a} \frac{\rho u}{\rho_* u_*} \frac{r}{a} d\left(\frac{n}{a}\right), \tag{42}$$

where density and mass flow density are calculated from the equation of total energy and that of isentropic change as follows:

$$\frac{\rho}{\rho_*} = \left[1 + \frac{\gamma - 1}{2}\left(1 - \frac{u^2}{u_*^2}\right)\right]^{\frac{1}{\gamma - 1}}, \tag{43}$$

$$\frac{\rho u}{\rho_* u_*} = \frac{u}{u^*}\left[1 + \frac{\gamma - 1}{2}\left(1 - \frac{u^2}{u_*^2}\right)\right]^{\frac{1}{\gamma - 1}}. \tag{44}$$

The non-dimensional form of Eq. (38) is given by

$$\frac{u/u_*}{u_a/u_*} = \frac{h_{\alpha a}/a}{h_\alpha/a} = \frac{\delta s_a/a}{\delta s/a}, \quad \text{or} \quad \frac{u/u_*}{u_b/u_*} = \frac{h_{\alpha b}/a}{h_\alpha/a} = \frac{\delta s_b/a}{\delta s/a}. \tag{45}$$

The computational procedure of flux analysis (or flow line analysis) is started by assuming the zeroth approximation of stream-surface coordinates. Determining the form of nozzle wall (at $\psi = \psi_N$) by the theory of one-dimensional flow, the zeroth coordinates of stream-surface for $\psi = \psi_2, \psi_3, \ldots, \psi_{N-1}$ are obtained, for example, by dividing the radius between the wall ($\psi = \psi_N$) and the axis ($\psi = \psi_1 = 0$) into equal parts. Calculating the coordinates of orthogonal lines by McNally's method[6] as mentioned in chapter 2, coordinates of orthogonal mesh points are determined,

and arc lengths δs and δn or n are calculated.

Since the boundary value of velocity is given in the present problem, Eq. (45) gives the velocities at the mesh points along the normals to the flow ($\alpha=$ constant), which give the values of $\rho u/\rho_* u_*$ along n. Substituting these into Eq. (42) we have the values of ψ at the mesh points along n. Denoting the values of n corresponding to $\psi=\psi_2,\psi_3, \ldots, \psi_N$ by $n_2, n_3, \ldots, n_N$, respectively, these values are calculated by interpolations and thus the coordinates of the point, which the improved stream-surface has to pass, are determined. The similar calculations over all sections of α =constant furnish arrays of points for the corrected stream surface as shown in Fig. 9. By taking the orthogonal lines to this improved stream-surfaces, the mesh points for the first approximation of orthogonal stream-surface coordinates are determined. The arc length s_b of the corrected boundary is calculated to set the prescribed velocity distribution over again.

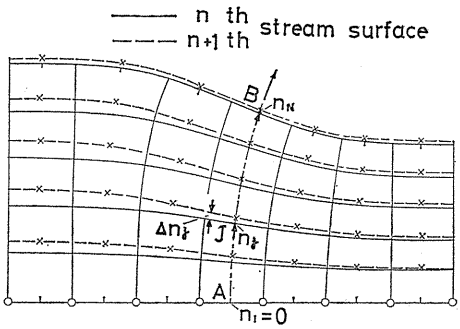

Fig. 9. Correction of stream-surface.

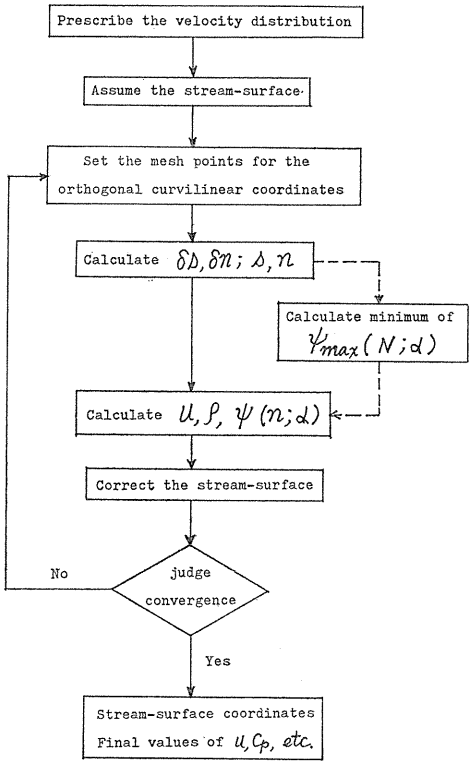

Fig. 10. Block diagram of flux analysis method.

The similar calulations are repeated and thus coordinates for the second approximation is obtained. These iterations are continued until the convergent value is obtained. When the maximum value of correction Δn of stream-surface in the whole field falls down under a small limiting value, the computation is regarded to be converged.

In case of the choking condition the mass flow through a pipe reaches its maximum value. When a set of orthogonal curvilinear coordinates is determined in every step of approximation, the minimum value of total mass flux among the maximum mass flow passable for every sections $\psi_{\max}(N;\alpha)$ is calculated by changing the wall velocities independently on the prescribed values. This minimum value is employed as the total mass flow ψ_N for the succeeding calculation of the concerning step of iteration.

The flow chart for the present calculation is shown in Fig. 10, where the route on a broken line represents the process of finding the total mass flow in choking condition. The input data

for the computation are the number of the mesh points ($M\times N$), condition of judgement for the convergence or the number of iterations and the velocity distribution prescribed along a boundary.

4. 2. Calculated examples

In a nozzle of high performance the flow along the wall is smoothly accelerated from the constant speed u_1 upstream to that u_2 downstream. In order to accelerate the flow from u_1 to u_2 in a distance l along the axis, the velocity distribution is prescribed in the form[8]:

$$\frac{u_b}{u_*}=\frac{u_1+u_2}{2u_*}+\frac{u_2-u_1}{2u_*}g\left(\frac{s_b}{a}\right), \tag{46}$$

where the function g is given by a power series of s_b/l. It becomes a function of s_b/a by designating the value of l/a. The smooth connection with the uniform velocities in both sides is attained by the conditions:

$$\begin{aligned} &g=-1, \quad g'=g''=0 \quad \text{at } x=0,\\ &g=1, \quad g'=g''=0 \quad \text{at } x=l. \end{aligned} \tag{47}$$

Taking the mesh number $M=15$ and $N=10$, some examples are calculated for $u_1/u_*=0.1$, $u_2/u_*=0.2$, 0.4, 0.6, 0.8 and $l/a=5.0$. To study the effect of location of main accelerating region four types of g:

$$\begin{aligned} &\text{(a)} \quad g(s_b/a)=12(s_b/l)^5-30(s_b/l)^4-20(s_b/l)^3-1,\\ &\text{(b)} \quad g(s_b/a)=-6(s_b/l)^4+8(s_b/l)^3-1,\\ &\text{(c)} \quad g(s_b/a)=-8(s_b/l)^5+10(s_b/l)^4-1,\\ &\text{(d)} \quad g(s_b/a)=-10(s_b/l)^6+12(s_b/l)^5-1, \end{aligned} \tag{48}$$

are examined.

For the first example the identical velocity distribution by Eq. (48 a) with $u_1/u_*=0.1$ and $u_2/u_*=0.6$ are prescribed on the axis as well as on the wall. The nozzle obtained by prescribing velocity on the axis is shown in Fig. 11. For this particular distribution of axial velocity, the nozzle wall swells at the entrance part and the velocity is first falling a little and then increasing. The boundary layer develops rapidly in the decelerating region, and therefore, a high performance can not be expected. The other nozzle obtained by prescribing the same velocity distribution on the wall is now shown in Fig. 12. The

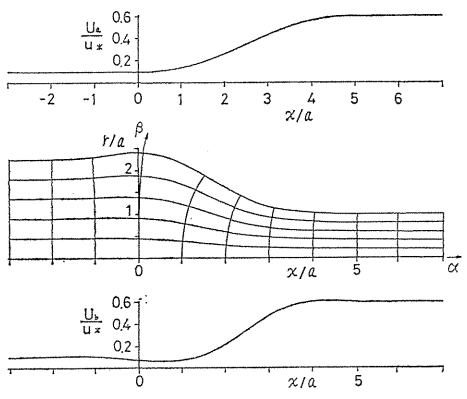

Fig. 11. Flow patterns and velocity distributions for a prescribed velocity along the axis.

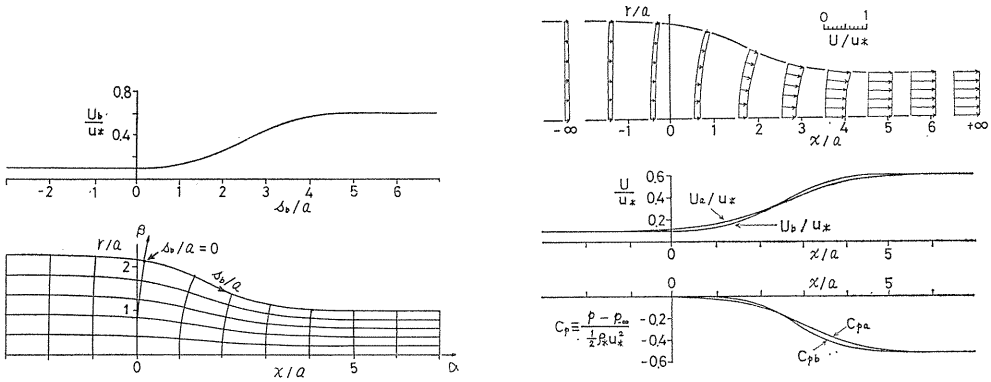

(a) Prescribed velocity and flow patterns, (b) velocity and pressure distributions.

Fig. 12. Flow patterns and velocity distributions for a prescribed velocity along the wall.

flow is accelerated smoothly towards downstream and higher performance is expected. It is found that the velocity distribution along the axis is flattened and widely spread comparing with the prescribed velocity distribution along the wall.

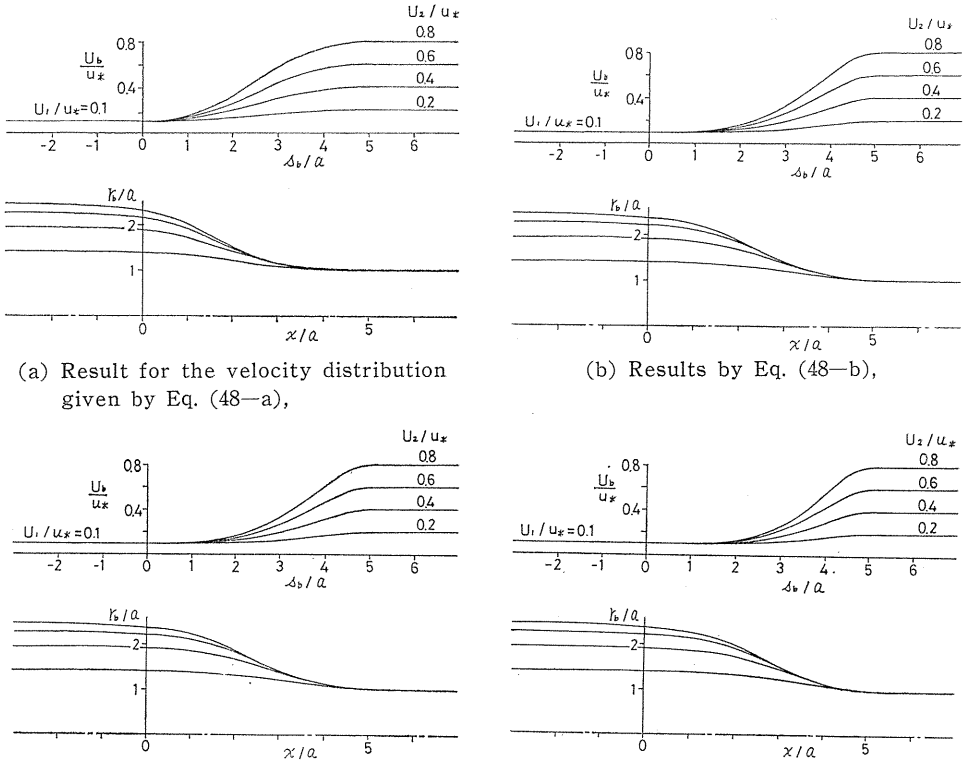

(a) Result for the velocity distribution given by Eq. (48—a),

(b) Results by Eq. (48—b),

(c) Results by Eq. (48—c),

(d) Results by Eq. (48—d).

Fig. 13. Prescribed velocity distributions along the wall and calculated forms of the nozzles.

Nozzles with different types of prescribed wall velocity are calculated for g of Eq. (48) as shown in Fig. 13, where the flow is accelerated in early stage (comparatively upstream) for (a) and in late stage (comparatively downstream) for (d). Comparing with the nozzle (a), the contraction of the nozzle (d) is shifted in a downstream section. Since the nozzle (d) has a longer upstream section of near cylindrical form, and therefore, a shorter nozzle is possibly obtained in practice. Since the nozzle (a) has a downstream section with more gentle acceleration, the flow at the nozzle excit is more uniform comparing with the nozzle (d). This form of nozzle may be more suitable for a wind tunnel.

4. 3. Experimental results

In order to verify the present analysis distributions of the wall velocity are measured for the nozzle (a) and (d). These nozzles are installed in the section number 3 of the test equipment shown in Fig. 14, which is connected to the chamber of 260mm ϕ, and the air under atmospheric pressure is sucked into the vacuum tank.

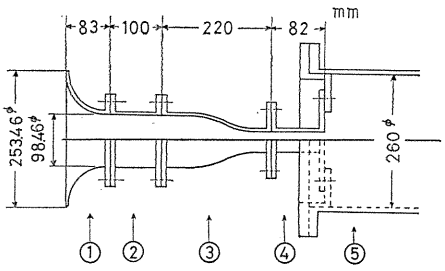

Fig. 14. Installation of the experiment.

Forms of nozzles are determined by adding the calculated displacement thickness to the radius of potential core flow given by the present mothod. Pressure distributions are measured through the pressure holes, which are drilled perpendicularly to the inner surface of the nozzle, and distributions of the wall velocity are obtained as shown in Figs. 15 and 16. Since the present analysis shows an

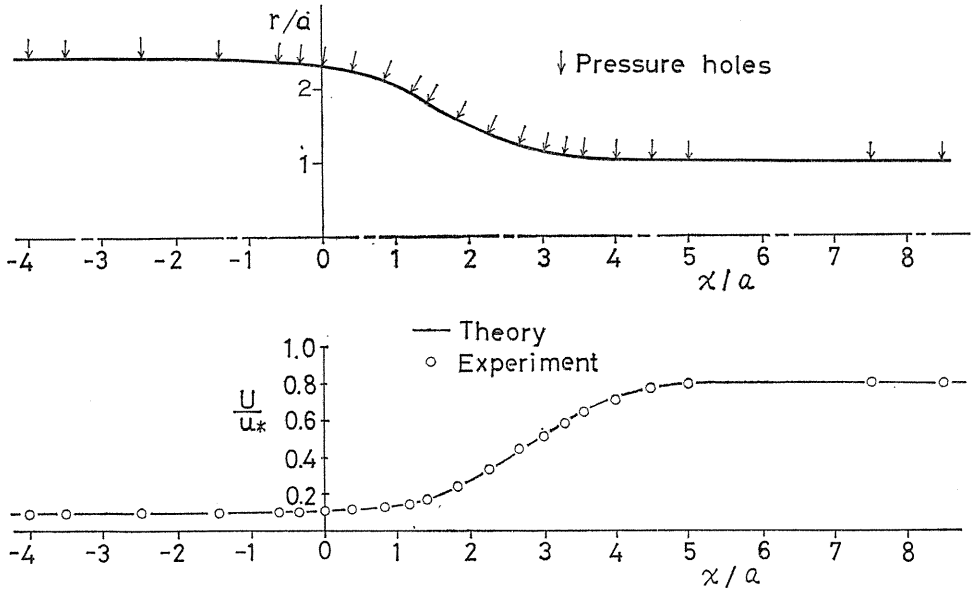

Fig. 15. Velocity distributions of the nozzle A given by $u_1/u_*=0.1$ and $u_2/u_*=0.8$ with Eq. (48—a).

excellent agreement with the measured values, its usefulness may be verified.

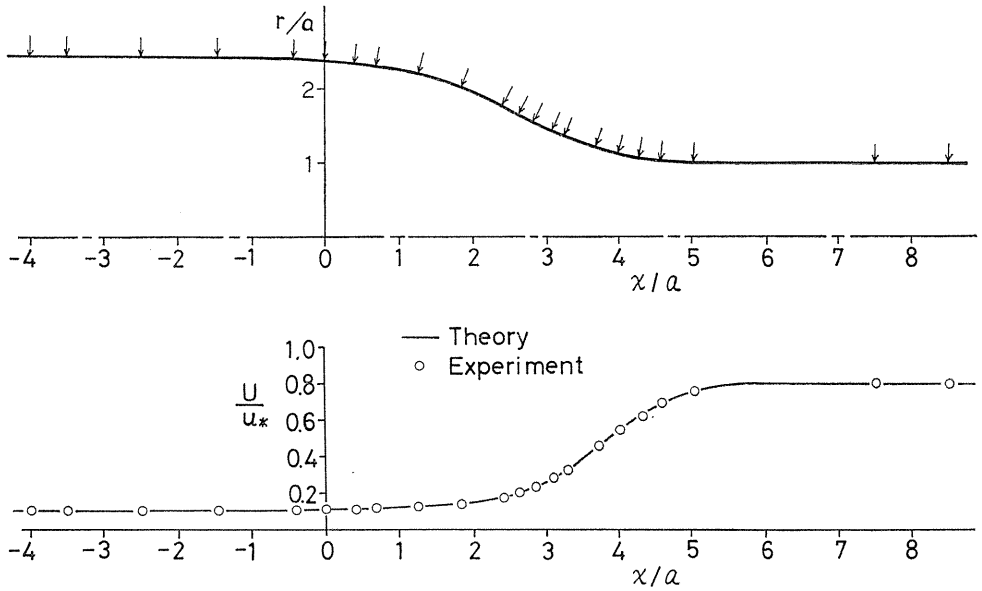

Fig. 16. Velocity distributions of the nozzle D given by $u_1/u_*=0.1$ and $u_2/u_*=0.8$ with Eq. (48—d).

Chapter 5. Calculation of a compressible flow through cascade airfoils

The compressible cascade flow is one of the essential gasdynamic problem in an axial compressor of turbine. The flux analysis method seems to furnish an appropriate means for solving such a highly deformed flow field. In this connection the steady compressible flow through a two-dimensional straight cascade of airfoils are calculated in the present chapter. Though the fundamental concepts are described already in the previous chapters, a brief presentation of fundamental relations is given through a little different way.

5. 1. Fundamental relations

Referring to streamline coordinates the steady two-dimensional flow of an inviscid compressible fluid is goverened by the equation of state:

$$p/\rho=RT, \tag{49}$$

the equation of continuity:

$$\partial(\rho u h_\beta)/\partial\alpha=0, \tag{50}$$

α and β components of equations of motion, respectively:

$$(u/h_\alpha)\cdot\partial u/\partial\alpha=-(1/\rho h_\alpha)\cdot\partial p/\partial\alpha, \tag{51}$$

$$-(u^2/h_\alpha h_\beta)\cdot\partial h_\alpha/\partial\beta=-(1/\rho h_\beta)\cdot\partial p/\partial\beta, \tag{52}$$

and the equation of energy for an ideal fluid:

$$T\frac{u}{h_\alpha}\frac{\partial S}{\partial\alpha}\equiv\frac{u}{h_\alpha}\left[\frac{\partial e}{\partial\alpha}+p\frac{\partial}{\partial\alpha}\left(\frac{1}{\rho}\right)\right]=0, \tag{53}$$

An equation for the entropy S is reduced from Eq. (53).

$$S=S(\psi), \tag{54}$$

where $S(\psi)$ becomes a general constant for an isentropic flow. From Eq. (51)$\times u$+Eq. (53) we have the equation of total energy:

$$(u/h_\alpha)\cdot(\partial/\partial\alpha)[(1/2)u^2+e+(p/\rho)]=0, \tag{55}$$

where the internal energy e can be deformed by the equation of state resulting in $e=c_vT=(p/\rho)/(\gamma-1)$. Integrating Eq. (55) the total energy E is given by

$$E\equiv\frac{u^2}{2}+e+\frac{p}{\rho}=\frac{u^2}{2}+\frac{\gamma}{\gamma-1}\frac{p}{\rho}=E(\psi), \tag{56}$$

where $E(\psi)$ becomes a general constant for an iso-energetic flow.

Eliminating dp/ρ from Eqs. (51) and (52) for an isentropic flow, we have

$$\frac{\partial}{\partial\alpha}\left[\frac{u}{h_\alpha}\frac{\partial(uh_\alpha)}{\partial\beta}\right]=-\frac{\partial}{\partial\alpha}[uh_\beta\zeta]=0, \tag{57}$$

where vorticity $\zeta=-(1/h_\alpha h_\beta)\cdot\partial(uh_\alpha)/\partial\beta$. For the irrotational flow

$$uh_\beta\zeta=(u/h_\alpha)\cdot\partial(uh_\alpha)/\partial\beta=F(\beta)=0, \tag{58}$$

which results in the same expression shown in the previous sections.

$$\partial(uh_\alpha)/\partial\beta=0, \tag{59}$$

or

$$uh_\alpha=F(\alpha)=u_ah_{\alpha a}=u_bh_{\alpha b}. \tag{60}$$

Defining the stream function ψ by $u=(1/\rho h_\beta)\cdot\partial\psi/\partial\beta$, Eq. (50) gives

$$d\psi/d\beta=\rho uh_\beta, \tag{61}$$

which is integrated in

$$\psi=\int\rho uh_\beta d\beta. \tag{62}$$

The succeeding procedure is the same with that described in the previous chapters.

5. 2. Compressible flow through a straight cascade of turbine blades

The flux analysis method is applied to solve the compressible cascade flow of turbine blades by Uchida[9].

5. 2. 1. *Relations between inlet and outlet flows*

The undisturbed inlet flow of w_1 approaches the cascade of turbine blades whose chord length is l and pitch t, and leaves it by the relative velocity w_2 of outlet flow as shown in Fig. 17 (a). Denoting the lift in the direction of cascade line by L and axial and tangential components of velocity by subscript a and t, respectively, the velocity diagram is shown in Fig. 17 (b). The undisturbed flows are governed by the equations of continuity, momentum and energy with the isentropic relation:

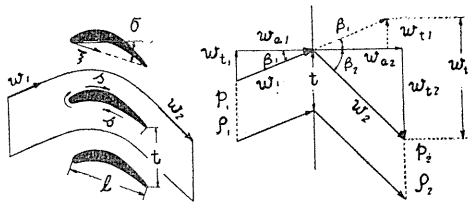

Fig. 17. Nomenclature and velocity diagram of the undisturbed flow (From: Uchida[9] by permission of AIAA).

$$\rho_1 w_{a1} = \rho_2 w_{a2} = (\rho V), \tag{63}$$

$$L = (\rho V) t (w_{t1} + w_{t2}), \tag{64}$$

$$\frac{w_1^2}{2} + \frac{\gamma}{\gamma - 1}\frac{p_1}{\rho_1} = \frac{w_2^2}{2} + \frac{\gamma}{\gamma - 1}\frac{p_2}{\rho_2}, \tag{65}$$

$$p_2/p_1 = (\rho_2/\rho_1)^{\gamma} = (a_2/a_1)^{2\gamma/(\gamma-1)}, \tag{66}$$

where (ρV) is a nomenclature for a mass-flow density common in the inlet and outlet flows. Denoting the velocity and arc length along the blade surface by u_a and s, respectively, the circulation around a blade is given by

$$\Gamma = \oint u_a \mathrm{d}s = t(w_{t1} + w_{t2}). \tag{67}$$

Substituting Eq. (67) into Eq. (64) we have the relation similar to the Kutta-Joukowski theorem:

$$L = (\rho V)\Gamma. \tag{68}$$

In order to get the relationship between the angle of outlet flow β_2 and the circulation $\Gamma/w_{a1}t$, Eq. (65) is deformed by the use of Eqs. (66) and (63) with geometrical relations. Denoting the inlet Mach number by $M_1 (= w_1/a_1)$, we have

$$\tan\beta_2 = \left\{\left[\frac{1 - (w_{a1}/w_{a2})^{\gamma-1}}{M_1^2 \cdot (\gamma-1)/2} + 1\right]\frac{(w_{a1}/w_{a2})^2}{\cos^2\beta_1} - 1\right\}^{1/2}. \tag{69}$$

Transforming Eq. (67), w_{a1}/w_{a2} is given by a function of $\tan\beta_2$:

$$w_{a1}/w_{a2} = \tan\beta_2 / [(\Gamma/w_{a1}t) - \tan\beta_1]. \tag{70}$$

Substituting Eq. (70) into Eq. (69) we have the relation between β_2 and $\Gamma/w_{a1}t$ for a given conditions of β_1 and M_1.

For an incompressible flow the relation is much simplified by putting $w_{a1}=w_{a2}$ in Eq. (66).

$$\tan\beta_2=(\Gamma/w_{a1}t)-\tan\beta_1. \tag{71}$$

5. 2. 2. Calculations of inlet and outlet streamlines

Streamlines in the channel type region bounded by two fixed surfaces of the adjacent blades are easily obtained by the iterative procedure described in the previous chapters.

In the inlet or outlet regions the flow is extending to the infinite distance, where it reaches a uniform state. In the computational procedure it is usually assumed that the flow reaches the uniform state at some definite distance far from the cascade surface.

The procedure to determine the inlet streamline is shown in Fig. 18. Since the flow patterns are extended to the distant section of assumed uniform flow w_1, velocity distributions along the flow normals can be determined by Eq. (60) and the boundary values of $u_a=w_1$ at this distant section. These velocity distributions correct the inlet streamlines resulting in the revised flow patterns, which furnish the corrected velocity distributions. Thus the iterative procedure is continued until the convergent value is obtained as usual.

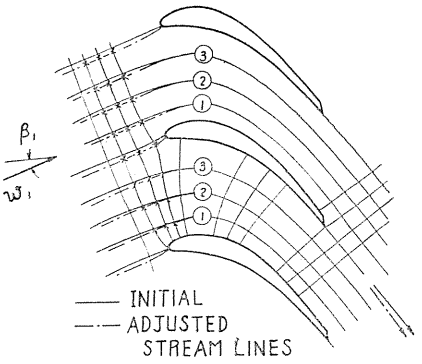

Fig. 18. Adjustment of the inlet streamlines (From: Uchida[9] by permission of AIAA).

The procedure to obtain the outlet streamline is more complicated, since neither the magnitude nor the direction of the outlet uniform flow are known in advance. The calculation is started by assuming the direction of the outlet uniform flow, for example, paralled to the tangent of mean camber line at the trailing edge. Carrying out the procedure for the current step of approximation the outlet streamlines can be determined by the similar way as the inlet streamlines. The convergent values in this step give the solution for the assumed direction of the outlet uniform flow. Calculating the circulation $\Gamma/w_{a1}l$ around a blade surface by Eq. (67) using the process shown in Fig. 19, the direction of outlet uniform flow to be corrected is obtained by β_2 of Eq. (70) or (71).

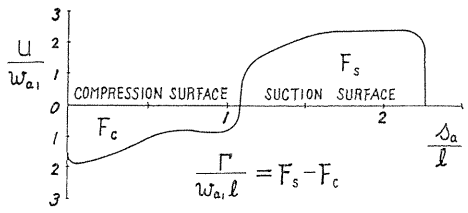

Fig. 19. Velocity distribution along the blade surface to calculate the circulation (From: Uchida[9] by permission of AIAA).

Adjusting the outlet streamlines the succeeding step of iteration is started and the whole procedure is repeated until the convergent values are obtained.

5. 2. 3. Illustrative examples

The accuracy of the present method is examined by comparing with the exact solution of incompressible cascade flow[10], which is obtained by the conformal mapping of the isolated Joukowski profile into the cascade airfoils. Two cases ($\beta_1 = 0$ and $7.72°$) of the cascade flow through these modified Joukowski airfoils are calculated by the flux analysis method as shown in Fig. 20, in which the velocity distributions agree well with those of exact solutions.

The comparison is also made with the measured values on a cascade of turbine blades[11]. Adjusting the movable walls downstream the outlet flow angle in the experiment is determined by the lift coefficient obtained from the pressure distributions on the blade surface. Calculated flow patterns and the velocity distribution along the surface are shown in Fig. 21, in which the surface velocities and the circulation agree well with observed values.

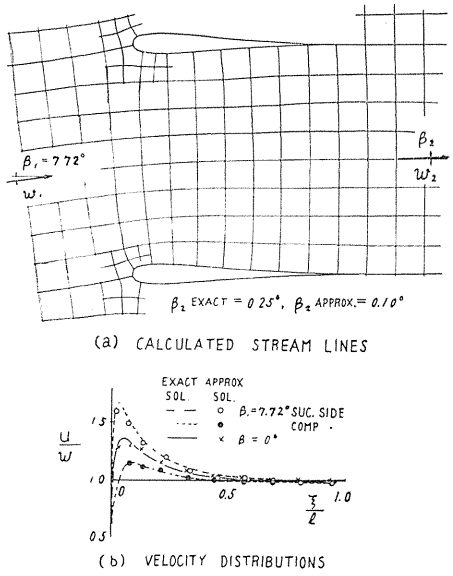

Fig. 20. Incompressible flow through cascade of modified Joukowski airfoils (From: Uchida[9] by permission of AIAA).

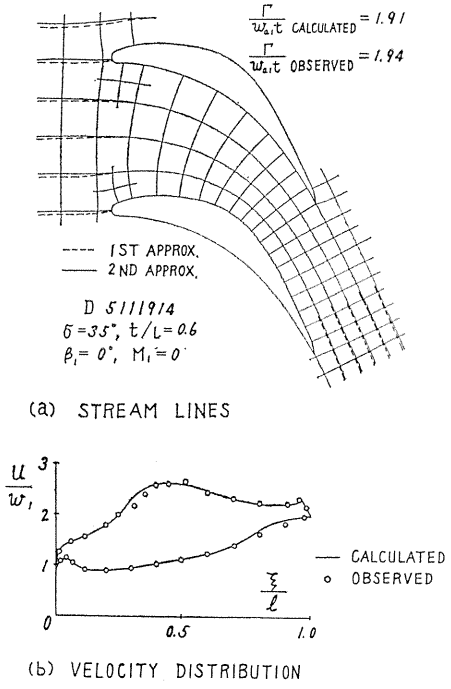

Fig. 21. Incompressible flow through the turbine cascade D5111914 (From: Uchida[9] by permission of AIAA).

Applying the flux analysis method to the cascades of turbine blades Hudimoto[12] and Oswatitsch and Ryhming[13] and Oswatitsch[14] also verify the validity of the present method of analysis.

5. 2. 4. A series of turbine cascade

To study effects of parameters of cascade on the performance a series of

turbine cascade is introduced. The front and rear halves of camber line connected at point Q is deformed from the generalized ellipse:

$$(x/a)^n+(y/b)^n=1, \tag{72}$$

as shown in Fig. 22 (b). The coordinates of basic camber line is given by

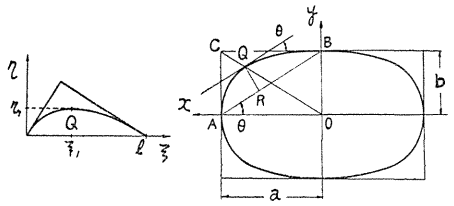

Fig. 22. Generalized elliptic camber (From: Uchida[9] by permission of AIAA).

$$\begin{aligned}\xi/l&=[a(a-x)+by]/(a^2+b^2),\\ \eta/l&=[ay-b(a-x)]/(a^2+b^2),\end{aligned} \tag{73}$$

as shown in Fig. 22 (a). The order of ellipse is selected separately for the front and rear part of camber line. The position and magnitude of the maximum camber are, respectively,

$$\begin{aligned}k&=\xi_1/l=[1-(1-\varepsilon)/2^{1/n}]/(1+\varepsilon^2),\\ f&=\eta_1/l=[2/2^{1/n}-1]\cdot\varepsilon/(1+\varepsilon^2),\end{aligned} \tag{74}$$

where $\varepsilon=b/a$ can be calculated inversely by

$$\varepsilon=[(k+2^{-1/n}-1)/(2^{-1/n}-k)]^{1/2}. \tag{75}$$

The final form of camber line is obtained by elongating the basic camber in the normal direction to the chord line so that the apex angle of basic triangle or the maximum camber reaches the desired value.

The front and rear part of thickness distributions are expressed by polynomials, respectively:

$$\begin{aligned}h/l&=(e/l)[(2g\cdot\xi/l)^{1/2}+g_1(\xi/l)+g_2(\xi/l)^2],\\ h/l&=(e/l)[c+d_1(1-\xi/l)+d_2(1-\xi/l)^2+d_3(1-\xi/l)^3],\end{aligned} \tag{76}$$

Denoting the radius of leading edge circle by r_l, coefficients are determined by the conditions:

$$\begin{aligned}&g(e/l)^2l=r_l;\ h=e/2,\quad dh/d\xi=0 \text{ at } \xi/l=m;\\ &h=ce \text{ and } dh/d\xi=-d_1(e/l) \text{ at } \xi/l=1,\end{aligned} \tag{77}$$

where $2c$ is trailing edge thickness and d_1 is a coefficient for trailing edge angle.

In the following examples $m=0.30$, $g=1.1$, $d_1=1.1$ are chosen.

Superposing the thickness perpendicularly to the camber line the blade profile is obtained as shown in Fig. 23. The arrangement of cascade blade is determined by selecting the setting angle σ of chord line to the turbine axis and by pitch-chord ratio t/l.

This series named IST cascade[9] are described by numbering for camber line, thickness distribution, and arrangement of cascade, respectively, in three lines as follows:

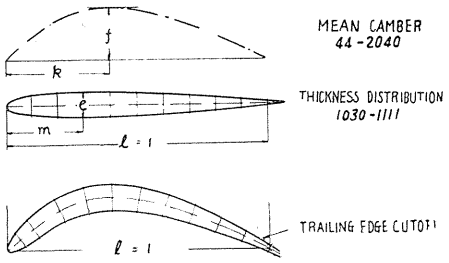

Fig. 23. Parameters for the blade profile (From: Uchida[9] by permission of AIAA).

IST 24−2040
1030−1111
$\sigma=35°$, $t/l=0.6$
$\beta_1=0$, $M_1=0.24$.

The first two numbers behind the sign IST represent the orders of ellipse for the front and rear part of the camber line, respectively, the two numbers next to the hyphen the amount of the maximum camber f and the last two its location k both in percentages of the chord length l. The thickness distribution is expressed by four sets of two numbers representing in order, the maximum thickness e, its location m both in percentage of l, $10g$ and $10d_1$. The thickness of trailing edge is fixed by $c=0.08$. The third and the fourth lines show the values for cascade arrangements and flow conditions.

5. 2. 5. Some results of computation

In order to study effects of parameters on the performance of cascade blades some examples are calculated by the use of graphycal construction of orthogonal streamline coordinates. In these cases a few iterations are sufficient to obtain the convergent values. Among the calculated data some examples of flow patterns and

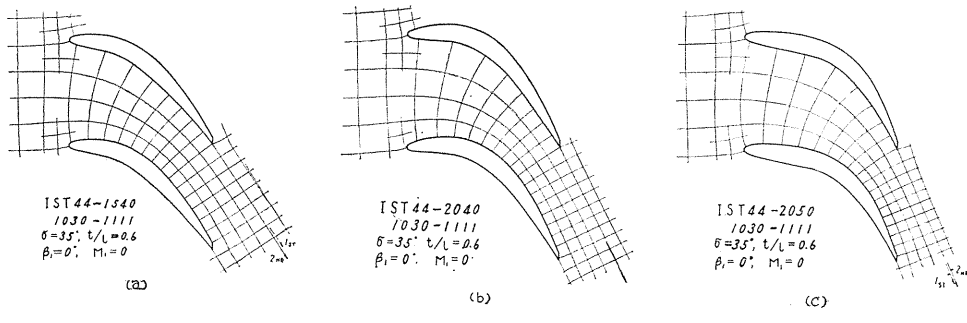

Fig. 24. Flow patterns for various camber lines, (a) $f=0.15$, $k=0.40$, (b) $f=0.20$, $k=0.40$, (c) $f=0.20$, $k=0.50$ (From: Uchida[9] by permission of AIAA).

velocity distributions along the blade surface as well as the variations of circulation are shown in the followings.

Comparisons of flow patterns for various camber lines and those for different pitch chord ratios are shown in Figs. 24 and 25, respectively. Flow patterns for the incompressible flow ($M_1=0$) and those for choking condition ($M_1=0.24$) are compared in Fig. 26.

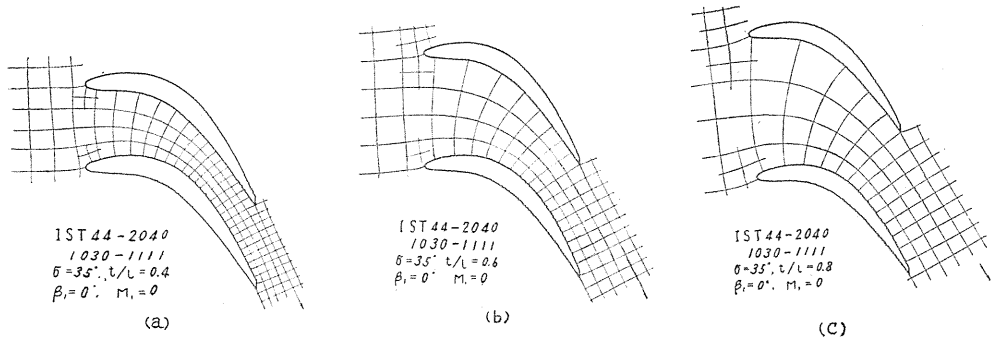

Fig. 25. Flow patterns for various pitch chord ratio, (a) $t/l=0.4$, (b) $t/l=0.6$, (c) $t/l=0.8$ (From: Uchida[9] by permission of AIAA).

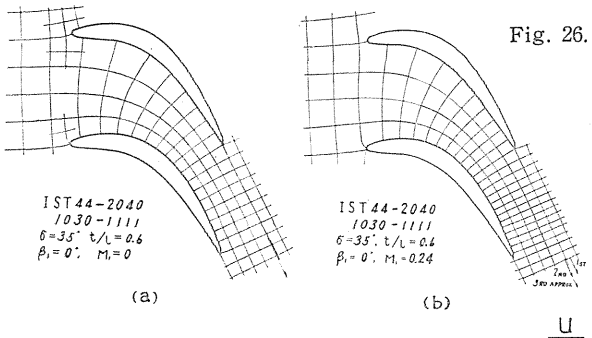

Fig. 26. Flow patterns for different Mach numbers (a) incompressible flow: $M=0$, (b) compressible flow in choking condition: $M=0.24$ (From: Uchida[9] by permission of AIAA).

Effects of the location and the magnitude of maximum camber as well as the order of ellipse are given in Figs. 27, 28 and 29, respectively, in self-explanatory forms. Influences of the maximum thickness and the pitch-chord ratio on performance are shown in Figs. 30 and 31, respectively. Effects of compressibility on the velocity distributions, the circulation and the angle of outlet flow are given in Fig. 32. When the inlet Mach number approaches the

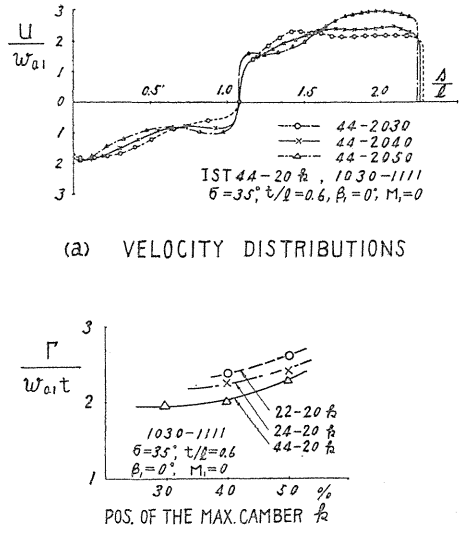

Fig. 27. Effect of the location of maximum camber (From: Uchida[9] by permission of AIAA).

choking condition ($M_1=0.24$), the velocity on the rear part of suction side increases rapidly and finally a narrow region of supersonic flow appears.

The present results seems to demonstrate that the flux analysis method is useful for a quick study on many parameters.

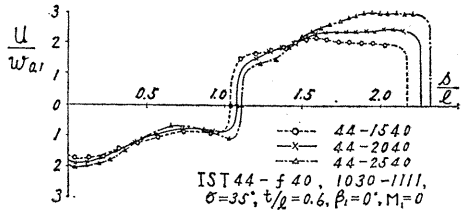

(a) VELOCITY DISTRIBUTIONS

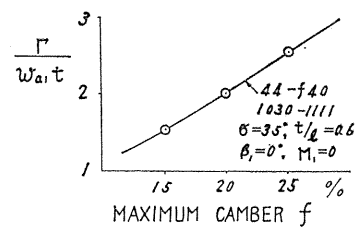

(b) CIRCULATION

Fig. 28. Effect of the magnitude of maximum camber (From: Uchida[9] by permission of AIAA).

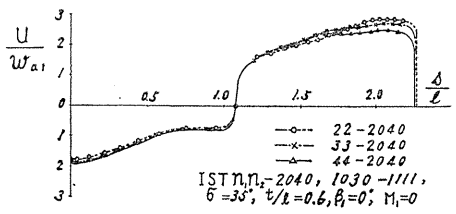

(a) VELOCITY DISTRIBUTIONS

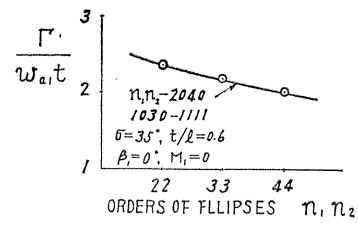

(b) CIRCULATION

Fig. 29. Effect of the orders of generalized elliptic camber (From: Uchida[9] by permission of AIAA).

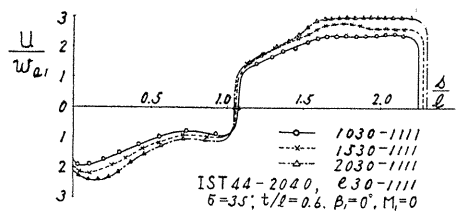

(a) VELOCITY DISTRIBUTIONS

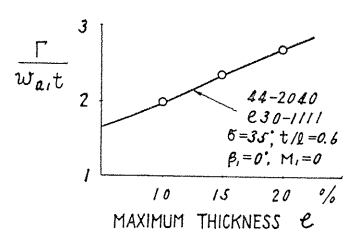

(b) CIRCULATION

Fig. 30. Effect of the maximum thickness (From: Uchida[9] by permission of AIAA).

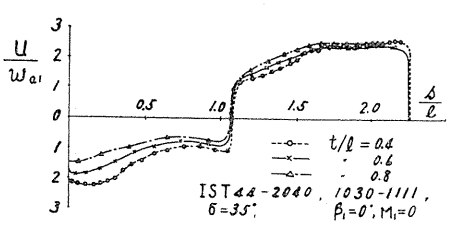

(a) VELOCITY DISTRIBUTIONS

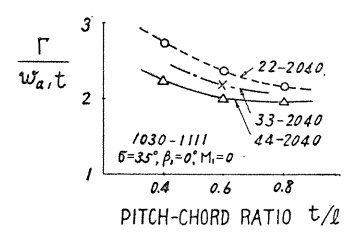

(b) CIRCULATION

Fig. 31. Effect of the pitch chord ratio (From: Uchida[9] by permission of AIAA).

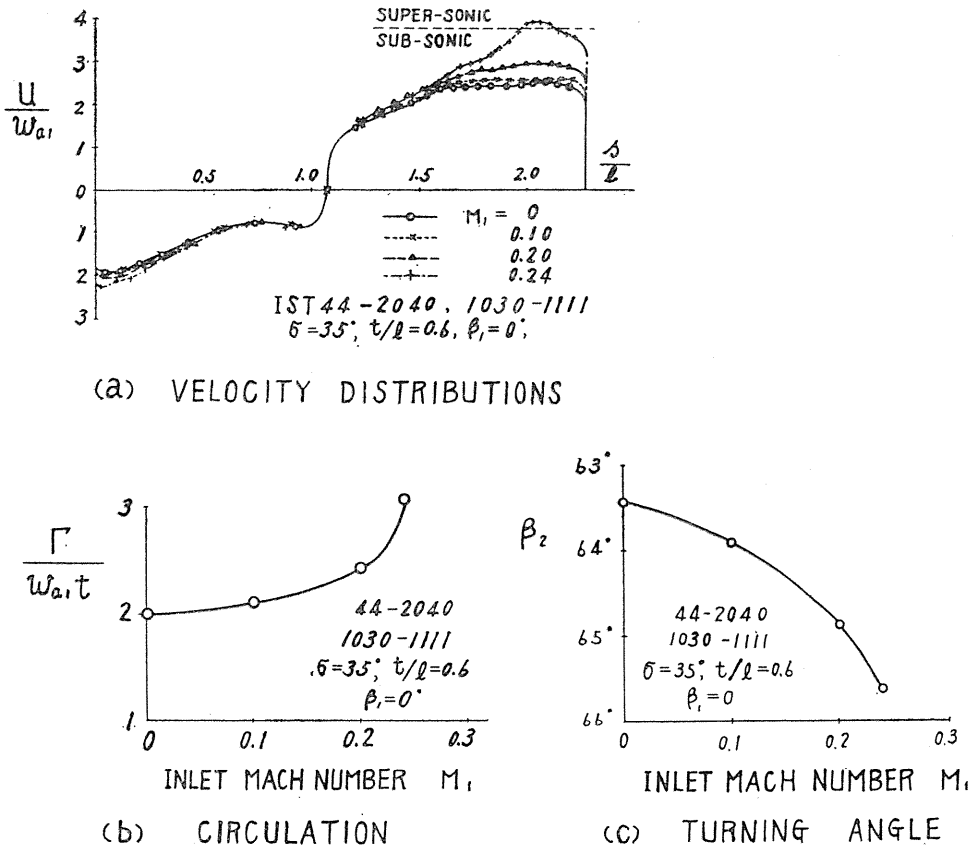

Fig. 32. Effect of the inlet Mach number (From: Uchida[9] by permission of AIAA).

5. 3. Computation on the flow through a compressor cascade airfoils

A computational algorithm for the present method to analyse the subsonic flow through a compressor cascade is studied by Nakamura and Otsuka[15]. The profile of the compressor blade conists of multi-circular arc connected at the maximum height of upper and lower surfaces from the chord line, and has sharp leading-and trailing edges. Assuming the flows are uniform at the sections one chord length upstream and downstream from the front and rear surfaces of cascade, respectively, the computational procedure is performed in the field as shown in Fig. 33. The calculation is started by assuming the zero streamlines passing leading- and trailing edges in the form of straight lines. In succeeding iterations Nakamura and Otsuka corrected the zero streamline by the use of a formura for the stream curvature derived from the equation of motion in the β direction:

$$\frac{1}{R_\alpha}=-\frac{1}{h_\beta}\frac{\partial(u/u_*)}{\partial\beta}\Big/\left(\frac{u}{u_*}\right)=-\frac{\partial(u/u_*)}{\partial n}\Big/\left(\frac{u}{u_*}\right), \tag{78}$$

where $1/R_\alpha$ is the curvature of streamline and u_* velocity of the sonic flow. The velocity gradient $\partial u/\partial n$ is given by the velocity difference between two mesh points D' and E' adjacent to the point A' in both sides, where the value at E' (or E) is

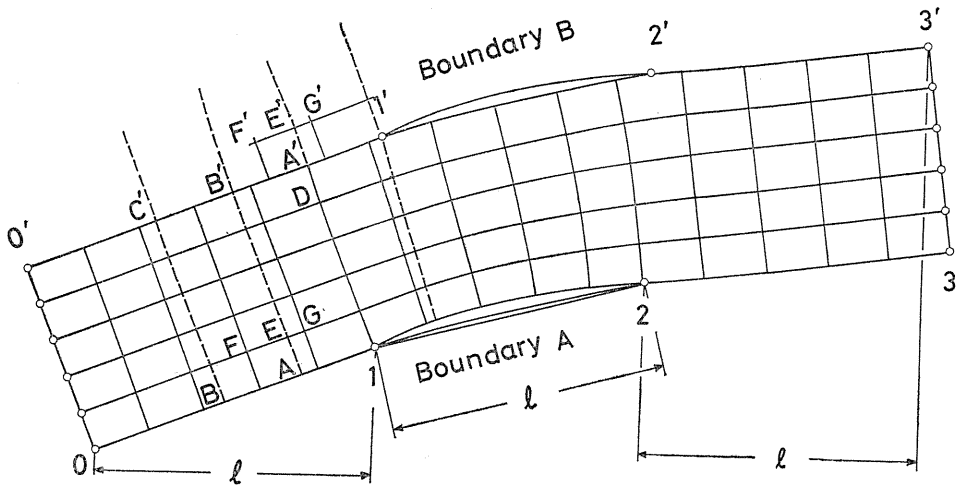

Fig. 33. Streamline coordinates and computational flow field for a compressor cascade (From: Nakamura and Otsuka[15] by permission).

given by interpolating values at F and G.

An alternative method for determining the zero streamline is to select the space of the orthogonal curves as given by folding the orthogonals passing the leading- and trailing edges one after another in the calculating domain as shown by the broken lines in Fig. 33. Advancing the computation forward by equalizing the values at A' and A, B' and B, and so forth, the correction of streamlines is achieved in a general procedure.

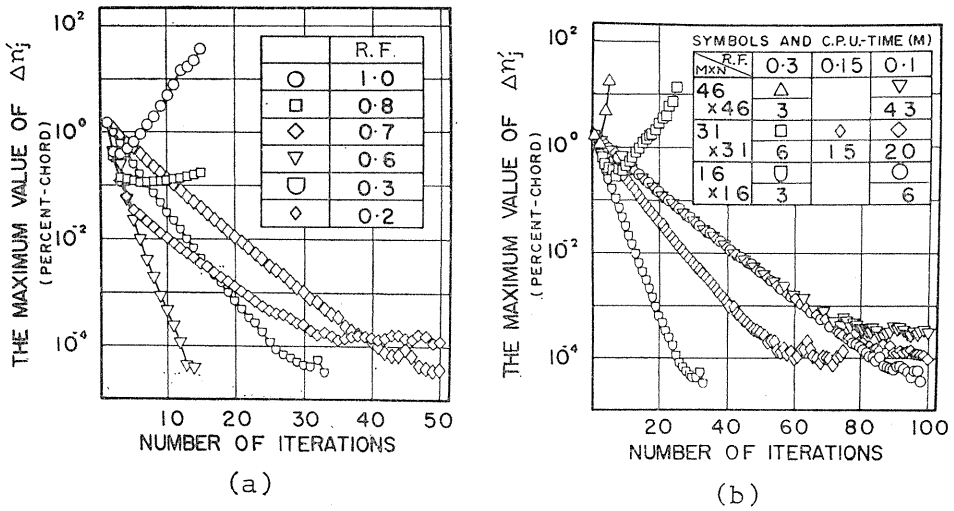

Fig. 34. Convergence of the flux analysis method, (a) Effect of relaxation factor on convergence, (b) Correlative effects of mesh number and relaxation factor on convergence: C.P.U. Time represents the computing time (min.) by FACOM 230-60 (90 Kw), (From: Nakamura and Otsuka[15] by permission).

To accelerate convergence a relaxation factor is introduced. Denoting the correction of mesh points along n designated from the previous iteration by Δn_j and the correction actually applied to the succeeding iteration by $\Delta n'_j$, the relaxation factor is defined by R.F.$=\Delta n'_j/\Delta n_j$. Examining the maximum value of $\Delta n'_j$ in the computing field for every iteration, the effect of relaxation factor on convergence is studied for mesh number $M\times N=16\times 16$ as shown in Fig. 34 (a). It is found that the rapid convergence is obtained by taking R.F.$=0.3\sim 0.6$. The effect of mesh scales on convergence is also studied by comparing the computations with mesh number $M\times N=16\times 16$, 31×31 and 46×46, as shown in Fig. 34 (b). It is found that the proper value of relaxation factor for convergence decreases in finer mesh scales. In these examples the best results is obtained for $M\times N=16\times 16$. For a

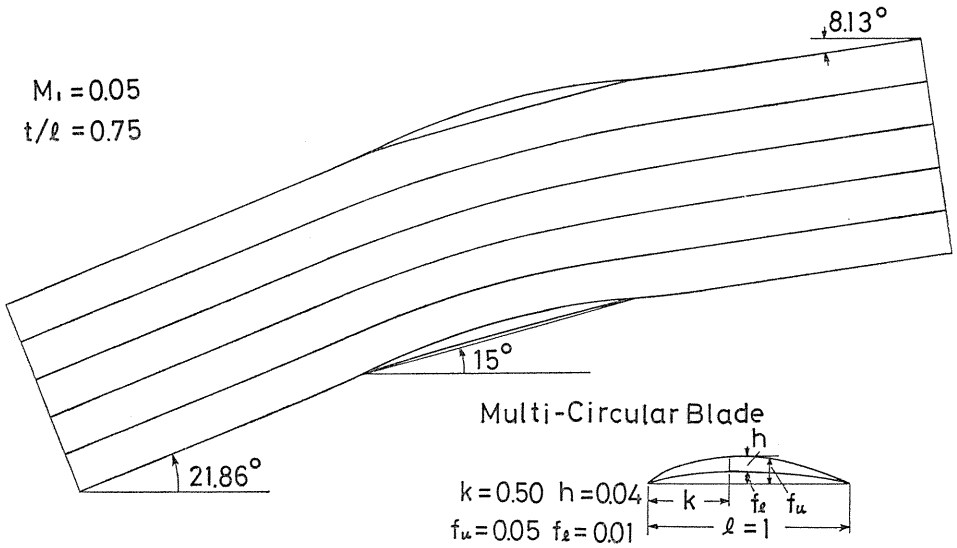

Fig. 35. Streamlines calculated by the flux analysis method comparing with those by the finite difference method which are almost coincident (From: Nakamura and Otsuka[15] by permission).

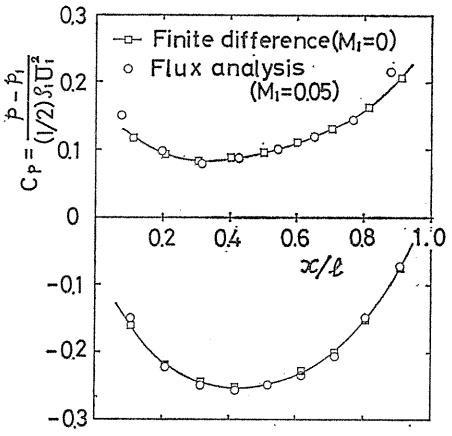

Fig. 36. Pressure distributions along the blade surface (From: Nakamura and Otsuka[15] by permission).

finer mesh scale small disturbances originated from the spline interpolations are amplified resulting in the delay of convergence or dislocation of coordinate meshes.

Some examples are calculated[15] and compared with the results obtained by the finite difference method[16),17]. The calculated streamlines are almost coincident in both methods as shown in Fig. 35. An example of calculated pressure distribution along the blade surface is given in Fig. 36, which shows a good agreement with the values obtained by the finite difference method.

Chapter 6. Calculation of the rotational flow field behind a curved shock wave by the method of flux analysis

The flow behind a curved shock wave or the swirling flow produced by a vortex motion contain distributed vorticities in their flow fields. The present method of flux analysis is a suitable means to calculate the steady rotational flow of an inviscid fluids, since the entropy and the total energy are preserved along the stream-surface. Applying the flux analysis method Uchida and Yasuhara[18] studied the rotational flow field behind a curved shock wave detached from the nose of a blunt body. By the use of the streamline coordinates in the incompressible potential flow an illustrative example is calculated for the supersonic flow around a circular cylinder as shown in Fig. 37. Referring to the original paper[18] the outline of the computational procedure is described in the followings.

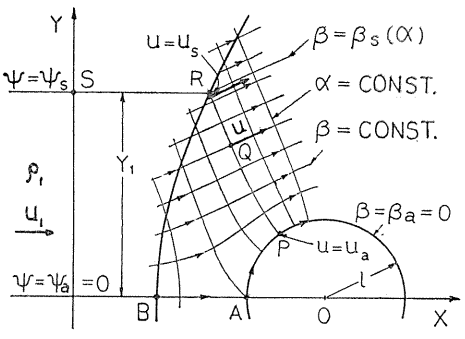

Fig. 37. Flow field of the supersonic flow around a blunt body (From: Uchida and Yasuhara[18] by permission of AIAA).

6. 1. Fundamental relations

6. 1. 1. Fundamental equations for a rotational flow

The steady rotational flow of an inviscid, non-heat-conductive compressible fluid is governed by equation of state:

$$p/\rho=RT, \tag{79}$$

equation of continuity:

$$\partial\rho/\partial t+\mathrm{div}(\rho\boldsymbol{V})=0, \tag{80}$$

equation of motion:

$$D\boldsymbol{V}/Dt=-(1/\rho)\ \mathrm{grad}\ p, \tag{81}$$

equation of energy:

$$De/Dt+p\cdot D(1/\rho)/Dt=T\cdot Ds/Dt, \tag{82}$$

where $e=C_vT=(p/\rho)/(\gamma-1)$ is the internal energy per unit mass of fluid.

Substituting Eq. (79), the equation of energy: Eq. (82), is deformed to

$$(D/Dt)[S-C_v\ln p-C_p\ln(1/\rho)]=0,$$

which is integrated to

$$(p/\rho^\gamma)e^{-S/C_v}=C, \tag{83}$$

where C is a constant parameter for the individual fluid element. When the flow is originated from the uniform source of fluid C becomes a general constant throughout the whole field.

Differentiating Eq. (83) for a steady flow we have

$$\begin{aligned} T\ \mathrm{grad}\ S&=(C_v/R\rho)\ \mathrm{grad}\ p+(C_pp/R)\ \mathrm{grad}\ (1/\rho)\\ &=-(1/\rho)\ \mathrm{grad}\ p+\mathrm{grad}\ (e+p/\rho). \end{aligned} \tag{84}$$

The equation of motion can be changed to a equation of kinetic energy:

$$D(V^2/2)/Dt=-(1/\rho)[Dp/Dt-\partial p/\partial t]. \tag{85}$$

Adding the energy equation (82) to Eq. (85), we have the equation of total energy:

$$DE/Dt=-(1/\rho)(\partial p/\partial t), \tag{86}$$

where the total energy is defined by $E=(1/2)V^2+e+p/\rho$. For a steady flow

$$DE/Dt=0 \tag{87}$$

is obtained from Eq. (86), hence we have

$$E=E(\psi), \tag{88}$$

Since there are no generation or conduction of heat in the present ideal fluid, the entropy is preserved for the individual fluid element:

$$DS/Dt=0. \tag{89}$$

For a steady flow it is given,

$$S=S(\psi). \tag{90}$$

The equation of motion, i. e. Eq. (81), can be deformed to

$$\frac{\partial \boldsymbol{V}}{\partial t}+\mathrm{grad}\frac{V^2}{2}-\boldsymbol{V}\times\mathrm{rot}\ \boldsymbol{V}=-\frac{1}{\rho}\mathrm{grad}\ p. \tag{91}$$

Substituting Eq. (84) for a steady flow Eq. (91) gives the Crocco's equation:

$$\boldsymbol{V}\times\mathrm{rot}\ \boldsymbol{V}=\mathrm{grad}\ E-T\ \mathrm{grad}\ S. \tag{92}$$

When the flow field is two-dimensional or axisymmetric, rot$\boldsymbol{V}$, $\boldsymbol{V}$ and $\boldsymbol{V}\times$rot$\boldsymbol{V}$ are

mutually perpendicular as shown in Fig. 38. Denoting the unit normal to the stream-surface by $\boldsymbol{n}$, we have thus

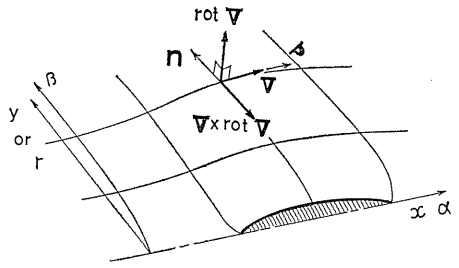

Fig. 38. Relation between velocity and vorticity vector in two-dimensional or axisymmetrical flow.

$$(\boldsymbol{V}\times \mathrm{rot}\ \boldsymbol{V})\cdot\boldsymbol{n}=-V\zeta, \tag{93}$$

where ζ is the vorticity component normal to the xy-plane or the meridian plane (xr-plane). Substituting Eq. (93) into Eq. (92) ζ is obtained[19],

$$\zeta=-\frac{1}{V}\left(\frac{\partial E}{\partial n}-T\frac{\partial S}{\partial n}\right)=-\frac{1}{Vh_\beta}\left(\frac{dE}{d\beta}-T\frac{dS}{d\beta}\right). \tag{94}$$

The equation of continuity for a steady flow:

$$\mathrm{div}(\rho\boldsymbol{V})\equiv\frac{1}{h_\alpha h_\beta r^\delta}\left[\frac{\partial(\rho u h_\beta r^\delta)}{\partial\alpha}+\frac{\partial(\rho v h_\alpha r^\delta)}{\partial\beta}\right]=0, \tag{95}$$

in which $\delta=0$ for two-dimensional and $\delta=1$ for axisymmetric flows, introduces the stream-surface function, which is defined by

$$u=\frac{1}{\rho h_\beta r^\delta}\frac{\partial\psi}{\partial\beta},\quad v=-\frac{1}{\rho h_\alpha r^\delta}\frac{\partial\psi}{\partial\alpha}. \tag{96}$$

Taking the stream-surface coordinates we have

$$u=V=\frac{1}{\rho h_\beta r^\delta}\frac{d\psi}{d\beta},\quad v=0. \tag{97}$$

The equation of continuity can be replaced by this Eq. (97).

Substituting Eq. (97) into Eq. (94) the equation of vorticity originated from the equation of motion is expressed in the following form[18]:

$$\zeta=r^\delta\left[\frac{p}{R}\frac{dS}{d\psi}-\rho\frac{dE}{d\psi}\right]. \tag{98}$$

The vorticity referred to orthogonal curvilinear coordinates:

$$\zeta=\frac{1}{h_\alpha h_\beta}\left[\frac{\partial(vh_\beta)}{\partial\alpha}-\frac{(\partial uh_\alpha)}{\partial\beta}\right], \tag{99}$$

is reduced to

$$\zeta=-(1/h_\alpha h_\beta)[\partial(uh_\alpha)/\partial\beta], \tag{100}$$

for the stream-surface coordinates. Substituting Eq. (100) into Eq. (98) we have

$$-\frac{1}{h_\alpha h_\beta}\frac{\partial(uh_\alpha)}{\partial\beta}=r^\delta\left[\frac{p}{R}\frac{dS}{d\psi}-\rho\frac{dE}{d\psi}\right], \tag{101}$$

which is rearranged by Eq. (97) as follows:

$$\frac{\partial(uh_\alpha)}{\partial\psi}=-\frac{h_\alpha}{u}\left[T\frac{dS}{d\psi}-\frac{dE}{d\psi}\right], \tag{102}$$

or

$$\frac{\partial(uh_\alpha)}{\partial\beta}=-\frac{h_\alpha}{u}\left[T\frac{dS}{d\beta}-\frac{dE}{d\beta}\right]. \tag{103}$$

Since Eq. (103) is originated from Eq. (81), this Eq. (103) can be used in place of the equation of motion.

Representing quantities in the uniform flow, the stagnation and the sonic condition by subscript 1, 0 and $*$, respectively, the total energy can be expressed by

$$E=\frac{1}{2}u^2+\frac{\gamma}{\gamma-1}\frac{p}{\rho}=\frac{1}{2}u_1^2+\frac{\gamma}{\gamma-1}\frac{p_1}{\rho_1}=\frac{\gamma}{\gamma-1}\frac{p_0}{\rho_0}$$

$$=\frac{1}{\gamma-1}a_0^2=\frac{1}{2}\frac{\gamma+1}{\gamma-1}a_*^2=\frac{1}{2}u_{max}^2=\text{const.} \tag{104}$$

By the use of Eq. (83) to-gether with $a=\sqrt{\gamma p/\rho}$, we have the quantities of state:

$$\frac{\rho}{\rho_0}=e^{-\frac{S-S_0}{R}}\left[1-\frac{\gamma-1}{2}\frac{u^2}{a_0^2}\right]^{\frac{1}{\gamma-1}}=e^{-\frac{S-S_0}{R}}\left[1-\frac{\gamma-1}{\gamma+1}\frac{u^2}{a_*^2}\right]^{\frac{1}{\gamma-1}}, \tag{105}$$

$$\frac{p}{p_0}=e^{-\frac{S-S_0}{R}}\left[1-\frac{\gamma-1}{2}\frac{u^2}{a_0^2}\right]^{\frac{\gamma}{\gamma-1}}=e^{-\frac{S-S_0}{R}}\left[1-\frac{\gamma-1}{\gamma+1}\frac{u^2}{a_*^2}\right]^{\frac{\gamma}{\gamma-1}}, \tag{106}$$

$$\frac{T}{T_0}=1-\frac{\gamma-1}{2}\frac{u^2}{a_0^2}=1-\frac{\gamma-1}{\gamma+1}\frac{u^2}{a_*^2}. \tag{107}$$

Fundamental equations (79) through (82) are rearranged to Eqs. (83), (97), (102) or (103), and (104), which can be used as the basic relations for the present analysis.

6. 1. 2. Boundary conditions

Referring to the stream-surface coordinates the body surface is represented by a curve of $\beta=\beta_a=$ constant. The boundary condition along the body surface is given by

$$\psi=\psi_a(=0) \quad \text{at} \quad \beta=\beta_a(=0). \tag{108}$$

In the supersonic flow around a blunt body the uniform flow is abruptly changed through the curved bow shock wave, whose thickness is negligibly small. Regarding

it as a discontinuous surface the small part of a curved shock wave can be replaced by an oblique shock wave tangential to it as shown in Fig. 39. Since the flow conditions immediately behind the shock wave are given relating to its inclination angle σ_1 and the upstream Mach number M_1, the shock relations can be used as the boundary conditions at the surface of shock wave.

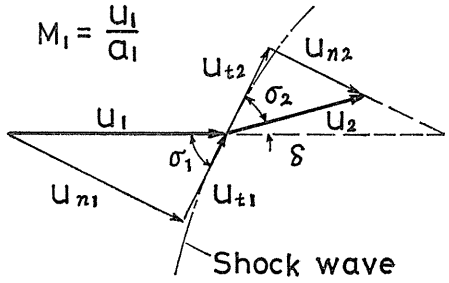

Fig. 39. Velocity diagram at the shock boundary.

Equations of continuity, momentum and energy across the shock wave are given in turn:

$$\rho_2 u_{n2} = \rho_1 u_{n1}, \tag{109}$$

$$\rho_2 u_{n2}^2 + p_2 = \rho_1 u_{n1}^2 + p_1, \tag{110}$$

$$\rho_2 u_{n2} u_{t2} = \rho_1 u_{n1} u_{t1}, \tag{111}$$

$$\frac{1}{2}u_2^2 + \frac{\gamma}{\gamma-1}\frac{p_2}{\rho_2} = \frac{1}{2}u_1^2 + \frac{\gamma}{\gamma-1}\frac{p_1}{\rho_1} = E(\psi). \tag{112}$$

For a given deflection angle δ the shock angle σ_1 can be determined by the relation:

$$\tan\delta = \frac{1}{\tan\sigma_1}\frac{(M_1^2-1)\tan^2\sigma_1 - 1}{\left(1+\frac{\gamma-1}{2}M_1^2\right)\tan^2\sigma_1 + \left(1+\frac{\gamma+1}{2}M_1^2\right)}. \tag{113}$$

The density and pressure ratios are

$$\frac{\rho_1}{\rho_2} = \frac{2}{\gamma+1}\left[\frac{1}{M_1^2\sin^2\sigma_1} + \frac{\gamma-1}{2}\right], \tag{114}$$

$$\frac{p_2}{p_1} = \frac{2\gamma}{\gamma+1}\left[M_1^2\sin^2\sigma_1 - \frac{\gamma-1}{2\gamma}\right]. \tag{115}$$

The increments of entropy is given by the use of Eqs. (114) and (115):

$$e^{\frac{S_2-S_1}{C_v}} = \frac{p_2/p_1}{(\rho_2/\rho_1)^\gamma}, \quad \text{or} \quad e^{\frac{S_2-S_1}{C_p}} = \frac{(p_2/p_1)^{1/\gamma}}{\rho_2/\rho_1}. \tag{116}$$

The form of the shock wave is represented by

$$\beta = \beta_s(\alpha). \tag{117}$$

The boundary conditions at the bow shock wave are expressed by the following four relations in place of Eqs. (109) through (112).

The equations of continuity is satisfied by the integrated from:

$\psi = \psi_s = \rho_1 u_1 y_1$ for two-dimensional flows,

$\psi = \psi_s = \rho_1 u_1 r_1^2/2$ for axisymmetric flows,

$$\text{at}\quad \beta=\beta_s(\alpha). \tag{118}$$

The two-equations of momentum are replaced by the relation between $\sigma_1=\sigma_1(\delta)$ which is given by Eq. (113) and by Eq. (116) for the entropy change.

The equation of total energy is used in its original form. Since the flow is originated from the uniform state upstream, the value of total energy is constant throughout the flow field, i. e. the iso-energetic flow.

The supersonic region between the sonic line and the limiting characteristics is affected by the conditions of boundary through characteristics which are generated ahead of the limiting characteristics. In the present method the general forms of computational procedure are extended to the lower supersonic region around the limiting characteristics, and the boundary conditions there are involved in the general form of conditions along the body surface. Tracing Mach lines the limiting characteristics is determined by taking the one which is tangential to the sonic line in the final step of every iterations.

6. 1. 3. Integration of the fundamental equations

Referring again and integrating the fundamental equations appropriate forms for the present analysis are investigated. The equation of state: Eq. (83), is reduced to

$$p/p_0=(\rho/\rho_0)^{\gamma}e^{\frac{S-S_0}{C_v}}. \tag{119}$$

The substituted equation for continuity: Eq. (97), is integrated to give

$$\psi-\psi_a=\int_{\beta a}^{\beta}\rho u r^{\delta}h_{\beta}\,d\beta=\int_{na}^{n}\rho u r^{\delta}\,dn, \tag{120}$$

where $\psi_a=0$, $\beta_a=0$, $n_a=0$ can be taken. Denoting the reference length by l the non-dimensional form is expressed by

$$\frac{\psi}{\rho_0 a_0 l(l/2)^{\delta}}=\int_0^{\beta}\frac{\rho u}{\rho_0 a_0}\left(2\frac{r}{l}\right)^{\delta}\frac{h_{\beta}}{l}d\beta=\int_0^{n/l}\frac{\rho u}{\rho_0 a_0}\left(2\frac{r}{l}\right)^{\delta}d\left(\frac{n}{l}\right). \tag{121}$$

One of the boundary conditions: Eq. (118), is also satisfied by applying this form of stream-surface function.

The equation of vorticity (102) derived mainly from the equation of motion can be integrated for a designated patterns of iso-energetic flow. Substituting

$$T/T_0=1-[(\gamma-1)/2](u/a_0)^2 \tag{122}$$

into a deformed expression of Eq. (102):

$$\frac{u}{a_0}\frac{\partial}{\partial\psi}\left(\frac{u}{a_0}\right)+\frac{1}{h_{\alpha}}\frac{\partial h_{\alpha}}{\partial\psi}\left(\frac{u}{a_0}\right)^2=-\frac{1}{\gamma}\frac{1}{R}\frac{T}{T_0}\frac{dS}{d\psi},$$

we have

$$\frac{\partial}{\partial\psi}\left(\frac{u}{a_0}\right)^2+\left[\frac{\partial}{\partial\psi}(\ln h_{\alpha}^2)-\frac{d}{d\psi}\left(\frac{S}{C_p}\right)\right]\left(\frac{u}{a_0}\right)^2=-\frac{2}{\gamma-1}\frac{d}{d\psi}\left(\frac{S}{C_p}\right), \tag{123}$$

which is integrated to give

$$\left(\frac{u}{a_0}\right)^2=\frac{1}{h_{\alpha}^2}e^{\frac{S}{C_p}}\left[\int\frac{-2}{\gamma-1}h_{\alpha}^2e^{-\frac{S}{C_p}}\frac{d}{d\psi}\left(\frac{S}{C_p}\right)d\psi+F(\alpha)\right]. \tag{124}$$

The equation of vorticity depending on β is also integrated in the same form with Eq. (124):

$$\left(\frac{u}{a_0}\right)^2=\frac{1}{h_\alpha^2}e^{\frac{S}{C_p}}\left[\int_\beta^{\beta_s}\frac{-2}{\gamma-1}h_\alpha^2 e^{-\frac{S}{C_p}}\frac{d}{d\beta}\left(\frac{S}{C_p}\right)d\beta+F(\alpha)\right], \tag{125}$$

where β_s represents β at the shock wave which is conveniently taken as the outer boundary. The quantities immediately behind the shock wave denoted by subscript s determine

$$F(\alpha)=h_{\alpha s}^2 e^{-\frac{Ss}{C_p}}(u_s/a_0)^2. \tag{126}$$

Substituting Eq. (126) into Eq. (125) we have

$$\left(\frac{u}{a_0}\right)^2=\left(\frac{h_{\alpha s}}{h_\alpha}\right)^2 e^{\frac{S-Ss}{C_p}}\left(\frac{u_s}{a_0}\right)^2$$

$$+\frac{1}{h_\alpha^2}e^{\frac{S}{C_p}}\int_\beta^{\beta_s}\frac{-2}{\gamma-1}h_\alpha^2 e^{-\frac{S}{C_p}}\frac{d}{d\beta}\left(\frac{S}{C_p}\right)d\beta. \tag{127}$$

when the flow patterns and distributions of entropy are assumed, the flow velocity is calculated by Eq. (127) as a function of u_s.

The mass flow density is obtained from the equation of total energy:

$$\frac{\rho u}{\rho_0 a_0}=e^{-\frac{S-S_0}{R}}\left(1-\frac{\gamma-1}{2}\frac{u^2}{a_0^2}\right)^{\frac{1}{\gamma-1}}\frac{u}{a_0}=e^{-\frac{S-S_0}{R}}\left(\frac{\rho u}{\rho_0 a_0}\right)_{\text{isentropic}}. \tag{128}$$

In the present analysis extension parameter h_α and the entropy S are given by assuming the stream-surface coordinates and the form of bow shock wave. The velocity u_s is determined by satisfying the continuity of total mass flow:

$$\frac{\psi_s}{\rho_0 a_0 l(l/2)^\delta}=\int_0^{n_s/l}\frac{\rho u}{\rho_0 a_0}\left(2\frac{r}{l}\right)^\delta d\left(\frac{n}{l}\right). \tag{129}$$

On the midway of iterative procedure ψ_s is taken as

$$\begin{aligned}\psi_s&=H\cdot\rho_1 u_1 y_1 && \text{for two-dimensional flows,}\\ \psi_s&=H\cdot\rho_1 u_1 r_1^2/2 && \text{for axisymmetric flows,}\end{aligned} \tag{130}$$

where the parameter H should be taken as unity from the boundary condition, Eq. (118). In some sections close to the sonic line, however, the attainable maximum value of ψ in the midway of iterations happens to be less than the boundary value, i. e. $H<1$. In such sections the attainable $\psi_{\max}$ is taken for the calculation of Eq. (129). The value of $H=\psi_{\max}/\psi_{\text{boundary}}$ approaches unity with the progress of iterations. The local continuity across the shock wave is satisfied by the successive fulfilment of the continuity of total mass flow from upstream to downstream sections.

6. 2. Computational procedure for the supersonic flow with a detached bow shock wave

The computational procedure of the flux analysis method is started by assuming

the stream-surface coordinates and the form of the detached bow shock wave. The local conditions of the detached shock wave are changed continuously from state of the normal shock wave to Mach wave, and consequently the deflection angle δ has a maximum value δ_{max} as calculated by the theory of oblique shock wave.

Since flow patterns are first assumed in the present procedure the flow angle θ_s behind the assumed shock wave cannot generally coincide with the deflection angle δ. To proceed the iterative computations it is convenient to introduce a constant multiplier K defined by

$$K=\theta_{s\,max}/\delta_{max}=\theta_s/\delta, \tag{131}$$

as shown in Fig. 40. The multiplier K is used to interprete the flow angle into the deflection angle behind the shock wave, which gives the inclination angle of shock wave σ_1 and the entropy jump S_2-S_1 by Eqs. (113) and (116), respectively. In the present calculations all iterations are performed for several values of K, and the results to give $K=1$ is selected for the final solution.

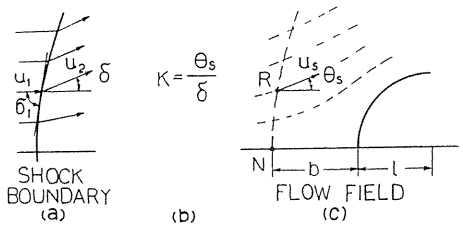

Fig. 40. Conversion of deflection angle by the multiplier K, (a) deflection angle determined by the shock condition, (b) multiplier as a connecting factor, (c) flow direction determined by the procedure of flux calculation (From: Uchida and Yasuhara[18] by permission of AIAA).

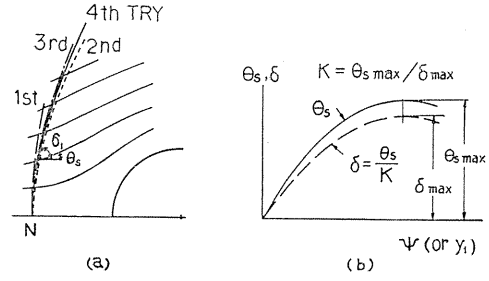

Fig. 41. Formation of the bow shock wave for fixed detachment point and flow patterns (From: Uchida and Yasuhara[18] by permission of AIAA).

Fixing the assumed flow patterns and the detached point N as shown in Fig. 41 (a), the form of bow shock wave is first conveniently assumed to give the distributions of θ_s immediately behind the shock wave and accordingly θ_{smax}. Since the value of multiplier is determined by $K=\theta_{smax}/\delta_{max}$ as shown in Fig. 41(b), the interpreted values of deflection angle $\delta=\theta_s/K$ and the corresponding values of σ_1 are obtained. Then the form of the shock wave is redrawn by the use of the inclination angle σ_1 resulting in the correction of the value K. These processes are repeated until the convergent form of shock wave is obtained and thus the value of K is determined for a fixed location of the detached point N, as shown in Fig. 41(a).

When the form of bow shock wave with a settled value of K is determined for a given form of flow patterns, the distribution of entropy, $S-S_1=f_n(\sigma_1)$, is obtained from the shock condition. Calculating velocities by Eq. (127) and substituting into Eqs. (129) and (130), the boundary value of velocity u_s at the shock wave surface is determined by satisfying the continuity of total mass flow. The

stream-surface coordinates are corrected by the continuity of fractional mass flow. i. e. by Eq. (129), as described in the previous chapters. Starting from the fixed location of detached point N, the form of bow shock wave is revised and the similar calculations are performed to get the second approximation. These procedures are repeated until a convergent value is obtained. Since the result thus obtained is a tentative solution for the assumed location of the detached point N, and generally speaking, K is not unity, then u_s is not yet coincident with the theoretical value u_2 behind the oblique shock wave.

Selecting several locations for the detached point N, similar procedures are repeated and tentative solutions for various values of K are calculated.

If the computations for various locations of detached point N are performed by starting with the identical patterns of initial stream-surface coordinate, the multiplier K will be expressed by a continuous function of the detachment distance b. Interpolating the relation $b=b(K)$ the correct situation of the detached point N can be determined by the value of b to give $K=1$.

The final solution is attained by repeating the computational procedure for this value of b corresponding $K=1$. Since relations for the continuity of mass flow, the inclination angle of shock wave, the flow deflection angle behind it and the conservation of the total energy hold, the boundary conditions at the shock wave are satisfied by this final solution.

6. 3. The supersoic flow around a circular cylinder with detached bow shock wave

Illustrative computations are made for the supersonic flow of $M_1=2$ around a circular cylinder. The iterative procedures are started by referring the flow patterns for the incompressible potential flow around a circular cylinder, which is uniform at the infinity. Considering the deformation of flow patterns in the present iterations other flow patterns, for example, those of a source flow around a circular cylinder from a source point upstream may be more efficient to get the convergent solution.

Selecting the detachment distance $b=0.3$, 0.5, 0.55 and 0.6, several iterations are performed to get the corresponding tentative solutions, where the first through the third iterations are calculated with neglecting the entropy gradients to save the computing time. The variations of multiplier K thus obtained in each iterations are shown in Fig. 42. Interpolating these values the condition: $K=1$ is found to be given by $b/a=0.57$.

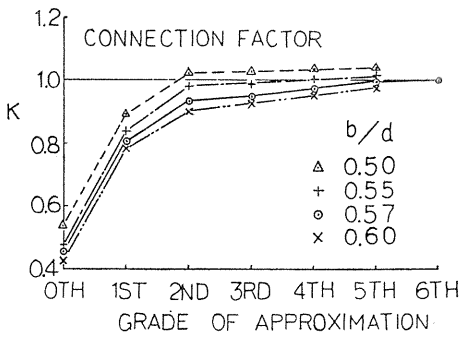

Fig. 42. Multiplier K as the connection factor for various detachment distance (From: Uchida and Yasuhara[18] by permission of AIAA).

The final solution is obtained by accomplishing the computational iterative procedure for $b/a=0.57$. The variations of stream-surface coordinates and the form of detached shock wave in each step of approximations are shown in Fig. 43. Iterations up to the third approximation, which is shown in Fig. 43(a), the second term of Eq. (127) is neglected for the sake of the reduction of computing time.

Distributions of the entropy and its derivative along the stream function is given in Fig. 44. The primary term and the secondary correction term of Eq. (127) for the final solution are shown in Fig. 45. It is found that the magnitude of correciton

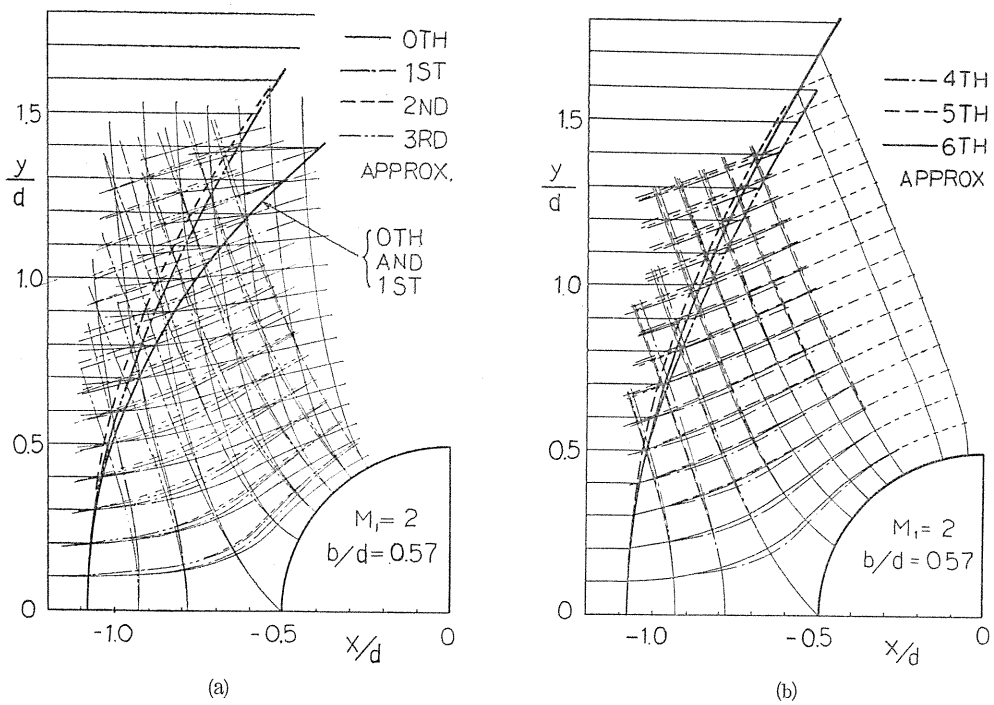

Fig. 43. Progress of iterations for the stream-surface coordinates and the form of detached bow shock wave (From: Uchida and Yasuhara[18] by permission of AIAA).

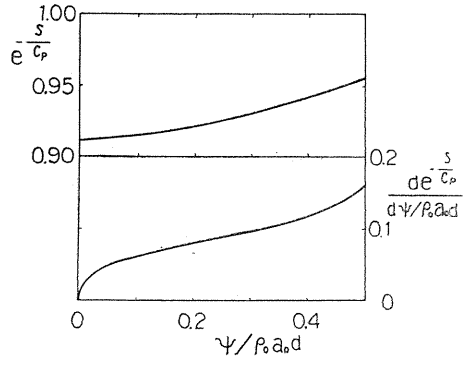

Fig. 44. Distributions of entropy and its derivative by stream-surface function (From: Uchida and Yasuhara[18] by permission of AIAA).

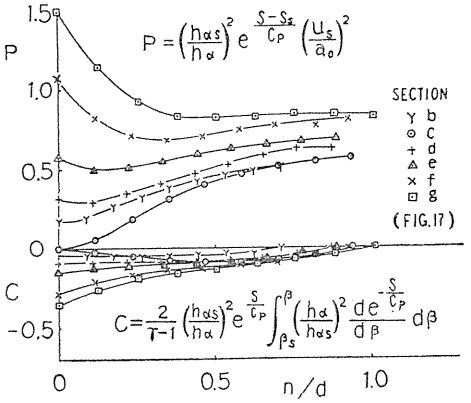

Fig. 45. Comparison of correction term by entropy gradient with primary term in $(u/a_0)^2$, see Eq. (127) (From: Uchida and Yasuhara[18] by permission of AIAA).

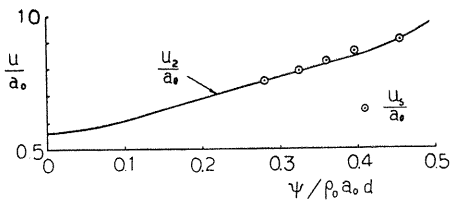

Fig. 46. Comparison of velocity u_s immediately behind the bow shock wave obtained by the present procedure with the theoretical value u_2 from the shock condition (From: Uchida and Yasuhara[18] by permission of AIAA).

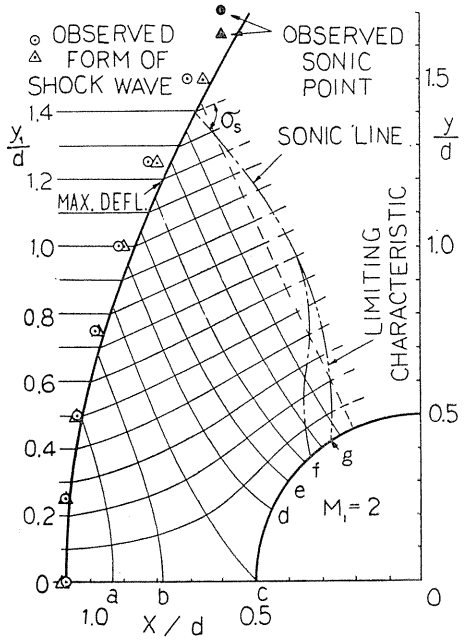

Fig. 47. Flow patterns and the form of bow shock wave (From: Uchida and Yasuhara[18] by permission of AIAA).

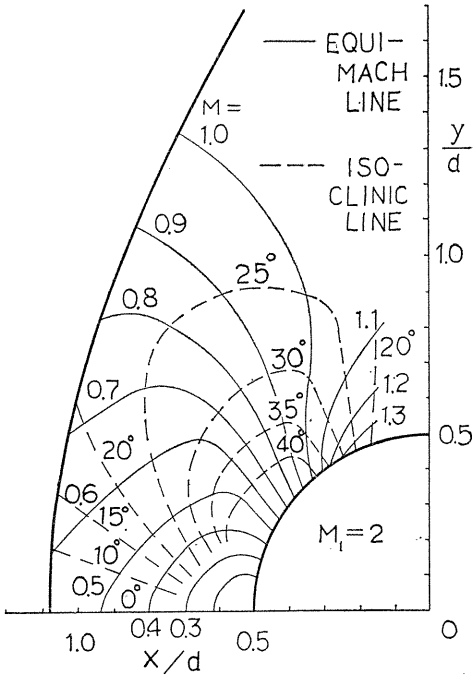

Fig. 48. Equi-Mach line and isoclinic line (From: Uchida and Yasuhara[18] by permission of AIAA).

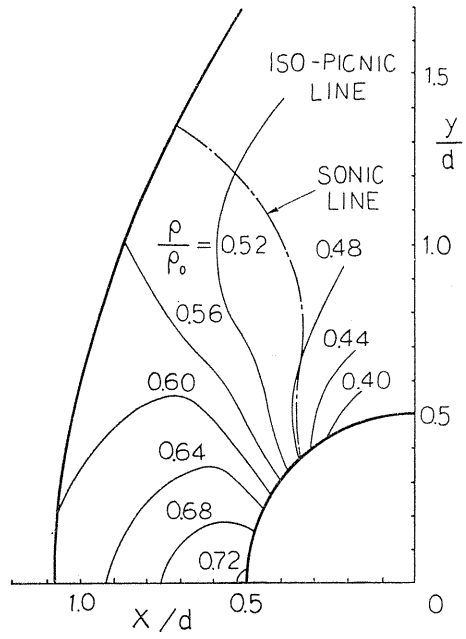

Fig. 49. Isopicnic line (From: Uchida and Yasuhara[18] by permission of AIAA).

term is less than 30% of the primary term in the present example. The velocity u_s immediately behind the shock wave calculated by the present computational procedure agrees well with the velocity u_2 given by the theory of oblique shock wave as shown in Fig. 46. It is verified that the boundary condition at the detached bow shock wave is well satisfied.

The final forms of flow patterns and bow shock wave are shown in Fig. 47. Comparing with the observations the sonic line leans a little forward approaching the shock wave, and consequently the angle σ_s between sonic line and streamline immediatly behind the shock wave is about 71°, which is a little smaller than the theoretical value of 73°34′. The equi-Mach line, isoclinic line are presented in Fig. 48 and isopicnic line in Fig. 49. Streamlines in the hodograph plane are obtained as shown in Fig. 50. Pressure distributions along the surface of the circular cylinder are given in Fig. 51. Comparing with observations by Eula[20], Gowen and Perkins[21] and by Uchida and Yasuhara[18], the present analysis shows a good agreement.

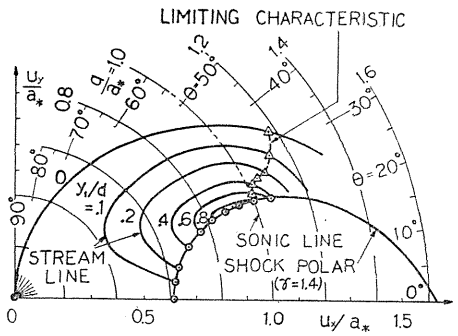

Fig. 50. Streamlines in the hodograph plane (From: Uchida and Yasuhara[18] by permission of AIAA).

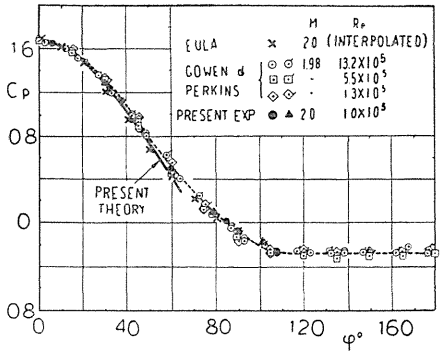

Fig. 51. Pressure distributions along the surface of circular cylinder (From: Uchida and Yasuhara[18] by permission of AIAA).

In the experiment performed by Uchida and Yasuhara a circular cylinder of diameter 10.02mm is set in the suction wind tunnel[18], detaching 5 mm each from the both side walls to avoid the interference from the boundary layer developed on the tunnel wall. The used equipment is shown in Fig. 52, in which a multi-nozzle is installed to generate the supersonic flows. Pressure distributions along the surface and the form of the bow shock wave are measured as shown in the previous figures.

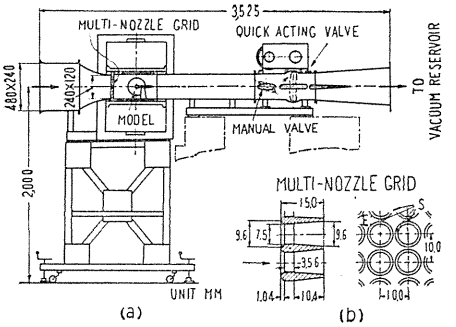

Fig. 52. Equipment for the experiment (a) High-speed wind tunnel of suction type, (b) Multi-nozzle grid (From: Uchida and Yasuhara[18] by permission of AIAA).

Chapter 7. Computations on the Swirling Flow through a Circular Pipe of Arbitrary Form[22]

The swirling flow through a diffuser pipe is decelerated highly in the axial region, and generating a stagnation point on the axis the vortex breakdown is finally occured. Several approaches for the initiataion of vortex breakdown are described in comprehensive reviews by Hall[23,24], Sarpkaya[25,26] and Leibovich[27]. Sarpkaya[26] observed the deformations of swirling flow through a slightly diffusing pipe. The detail of structure of the swirling flow with vortex breakdown is obtained by Uchida et al.[28] and Faler and Leibovich[29].

In the present chapter the initial deformations of the swirling flow in a circular pipe of arbitrary form are calculated by the use of flux analysis method, and the effect of pressure gradient on the steep deceleration in the axial region is examined.

7. 1. Fundamental relations

The axisymmetrical steady swirling flow is analyzed for an inviscid barotropic fluid. An axisymmetrical system of orthogonal curvilinear coordinates: (α,β,θ) is introduced as shown in Fig. 53 (See Appendix C). Extension parameters are expressed by $h_\alpha=\partial s/\partial\alpha$, $h_\beta=\partial n/\partial\beta$ and $h_\theta=r$, where r is the radial distance from the axis. The α, β and θ components of velocity are represented by u, v and w, respectively. For an axisymmetrical steady flow the Euler derivative of a scalar quantity is expressed by

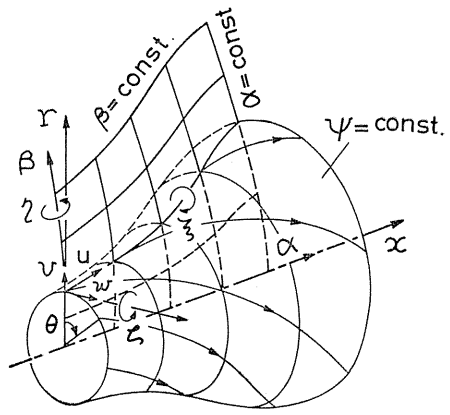

Fig. 53. Orthogonal curvilinear coordinates for the axisymmetric flow.

$$D/Dt=(u/h_\alpha)(\partial/\partial\alpha)+(v/h_\beta)(\partial/\partial_\beta). \tag{132}$$

In order to analyze the nature of a barotropic fluid the perfect gas, whose state is governed by the equation of state:

$$p/\rho=RT, \tag{133}$$

is first considered. Denoting the internal energy by $e=C_vT=(p/\rho)/(\gamma-1)$, the energy equation for an inviscid, non heat conducting gas is given by

$$T\frac{DS}{Dt}\equiv\frac{De}{Dt}+p\frac{D}{Dt}\left(\frac{1}{\rho}\right)=0, \tag{134}$$

in which the entropy S is fixed to the individual fluid element. For a steady flow we have

$$S=S(\psi), \tag{135}$$

where ψ represents the stream surface function. Substituting Eq. (133) the equation of energy can be deformed to

$$DA/Dt \equiv (D/Dt)[(p/\rho^{\tau})e^{-S/C_v}]=0. \tag{136}$$

This equation expresses that the function $A \equiv (p/\rho^{\tau})\exp(-S/C_v)$ is fixed to the individual fluid element. For a steady flow A is expressed by

$$A=A(\psi). \tag{137}$$

Introducing a function $H \equiv A\exp(S/C_v)$ we have

$$p/\rho^{\tau}=Ae^{S/C_v}=H(\psi). \tag{138}$$

When the entropy is given by a function of pressure, the gas becomes a barotropic fluid. An incompressible fluid, whoes equation of state is substituted by

$$\rho=\text{constant}, \tag{139}$$

is a special case of the barotropic fluid.

Fundamental equations for the axisymmetric flow referred to the orthogonal curvilinear coordinates (α,β,θ) are derived in Appendix C. From the equation of continuity:

$$(\rho urh_{\beta})_{\alpha}+(\rho vrh_{\alpha})_{\beta}=0, \tag{140}$$

the stream surface function defined by

$$\rho ur=\psi_{\beta}/h_{\beta}, \quad \rho vr=-\psi_{\alpha}/h_{\alpha}, \tag{141}$$

is introduced. Referring to the stream-surface coordinates, in which $\beta=$constant coincides with the stream-surface, u becomes the meridian component of velocity, since $v=0$. The Euler derivative is simplified to

$$D/Dt=(u/h_{\alpha})(\partial/\partial\alpha). \tag{142}$$

Since $\partial\psi/\partial\alpha=0$, the equation of continuity is simply

$$\rho urh_{\beta}=d\psi/d\beta. \tag{143}$$

Integrated form of continuity is given by

$$\psi-\psi_a=\int_{\beta a}\rho urh_{\beta}d\beta=\int_{na}\rho urdn, \tag{144}$$

where subscript a represents the quantity at a boundary.

Introducing the α, β and θ components of vorticity denoted by ξ, η and ζ, respectively, the equations of motion for a barotropic fluid free of external forces are

$$h_{\alpha}^{-1}(V^2/2)_{\alpha}+w\eta=-h_{\alpha}^{-1}(\int dp/\rho)_{\alpha}, \tag{145}$$

$$h_\beta^{-1}(V^2/2)_\beta - w\xi + u\zeta = -h_\beta^{-1}\left(\int dp/\rho\right)_\beta, \tag{146}$$

$$u\eta = 0, \tag{147}$$

where $V=\sqrt{u^2+w^2}$ and

$$\xi = \frac{(wr)_\beta}{rh_\beta}, \quad \eta = -\frac{(wr)_\alpha}{rh_\alpha}, \quad \zeta = -\frac{(uh_\alpha)_\beta}{h_\alpha h_\beta}. \tag{148}$$

Since Eq. (147) gives

$$\eta = -(wr)_\alpha/rh_\alpha = 0, \tag{149}$$

the Euler derivative of the circulation function $K\equiv wr$ vanishes to give $DK/Dt=0$, and we have

$$wr \equiv K = K(\phi). \tag{150}$$

Substituting Eq. (147) into Eq. (145) the Euler derivative of the total energy defined by $E=V^2/2+\int(dp/\rho)$ also vanishes to give $DE/Dt=0$, and we have

$$V^2/2 + \int(dp/\rho) \equiv E = E(\phi). \tag{151}$$

For a compressible flow the enthalpy can be integrated along a stream-surface by the use of Eq. (138) as follows:

$$\int \frac{dp}{\rho} = \frac{\gamma}{\gamma-1}\rho^{\gamma-1}H(\phi) = \frac{\gamma}{\gamma-1}\frac{p}{\rho}. \tag{152}$$

The density is given by

$$\rho = \left[\frac{\gamma-1}{\gamma}\frac{E}{H}\left(1-\frac{u^2+w^2}{2E}\right)\right]^{\frac{1}{\gamma-1}}. \tag{153}$$

The density and the velocity of sound at the sonic state along the individual stream-surface are given by

$$\rho_*(\phi) = \left(\frac{2}{\gamma+1}\frac{\gamma-1}{\gamma}\frac{E}{H}\right)^{\frac{1}{\gamma-1}}, \quad a_*(\phi) = \left(2\frac{\gamma-1}{\gamma+1}E\right)^{\frac{1}{2}}, \tag{154}$$

the density is expressed by

$$\frac{\rho}{\rho^*} = \left[\frac{\gamma+1}{2} - \frac{\gamma-1}{2}\frac{u^2+w^2}{a_*^2}\right]^{\frac{1}{\gamma-1}}. \tag{155}$$

Eq. (146) can be transformed to

$$u\zeta = -(1/h_\beta)(d\phi/d\beta)[E' + KK'/r^2], \tag{156}$$

where prime stands for $d/d\phi$. Substituting Eq. (143) we have

$$-(uh_\alpha)_\beta/h_\alpha h_\beta \equiv \zeta = -\rho r[E' - KK'/r^2]. \tag{157}$$

Transformation of variables from β to ψ yields

$$(u/h_\alpha)(uh_\alpha)_\psi = E' - KK'/r^2, \tag{158}$$

or

$$[(uh_\alpha)^2]_\psi = 2h_\alpha^2[E' - KK'/r^2]. \tag{159}$$

Integrating Eq. (159) with respect to ψ we obtain

$$u^2h_\alpha^2 = u_a^2h_{\alpha a}^2 + \int_{\psi_a}^{\psi} 2h_\alpha^2(E' - KK'/r^2)\,d\psi, \tag{160}$$

and hence,

$$u = \frac{h_{\alpha a}}{h_\alpha}\left[u_a^2 + \int_{\psi_a}^{\psi} 2\left(\frac{h_\alpha}{h_{\alpha a}}\right)^2\left(E' - \frac{KK'}{r^2}\right)d\psi\right]^{1/2}, \tag{161}$$

where subscript a represents conditions at the boundaries a or b shown in Fig. 54.

The boundary conditions are expressed, for example, by

$$\begin{gathered}\psi=\psi_a \text{ at } \beta=\beta_a\,;\ \psi=\psi_b \text{ at } \beta=\beta_b,\\ (\partial/\partial\alpha)(u,\ \rho,\ p,\ T)=0 \text{ at } \alpha=\alpha_c \text{ and } \alpha=\alpha_d,\end{gathered} \tag{162}$$

where the boundaries a to d are shown in Fig. 54.

7. 2. *Computational procedure of the flux analysis method applied to the swirling flow through a pipe*

Flowing down through a circular pipe the basic swirling flow upstream suffers deformations by the change of pipe radius. Designating the distributions of velocity components along the radius the basic swirling flow is given by that with uniform structure in the axial direction. Distributions of total energy $E(\psi)$, circulation function $K(\psi)$, and of the function $H(\psi)$ for a compressible flow, are given by specifying the basic swirling flow.

The procedure is started by assuming appropriate forms of stream-surface in the meridian plane employing, for example, point rows dividing the pipe radius in equal parts. Values of $\psi_j(j=1, 2, \ldots N)$ corresponding to those in the basic swirling flow are assigned.

Dividing the curve of a boundary a into small elements as $\widehat{CD}$ in Fig. 54, orthognal coordinates are drawn from points C, D and from their middle point A, by the use of McNally's method[6]. Arc lengths of meridional stream-surface cut by two orthogonals such as $\delta s_a=\widehat{CD}$, $\delta s=\widehat{EF}$ and $\delta s_b=\widehat{GH}$, and arc length of the middle orthogonal $n_j=\widehat{AJ}$ are calculated. Replacing the extension parameters by finite differences we have approximately

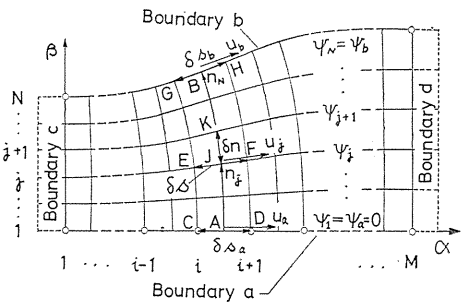

Fig. 54. Flow in the meridian plane referred to the stream-surface coordinates.

$$\frac{h_\alpha}{h_{\alpha a}}=\frac{\partial s/\partial\alpha}{(\partial s/\partial\alpha)_a}\doteqdot\frac{\delta s/\delta\alpha}{\delta s_a/\delta\alpha}=\frac{\delta s}{\delta s_a}. \tag{163}$$

The velocity u_j at the middle mesh point can be calculated in terms of the boundary value of velocity u_a (or u_b) by

$$u_j=\frac{\delta s_a}{\delta s}\left[u_a^2+\int_{\phi_a}^{\phi_j}2\left(\frac{\delta s}{\delta s_a}\right)^2\left(E'-\frac{KK'}{r^2}\right)d\phi\right]^{1/2}, \tag{164}$$

where the subscript a is replaced by b in case of referring values at the boundary b. The azimuthal component of velocity is obtained by

$$w_j=K(\phi_j)/r_j, \tag{165}$$

where r_j is the radial distance of the middle mesh point from the axis. The density ρ_j required for the compressible flow is given by Eqs. (153) or (155).

Values of stream-surface function are calculated by Eq. (144), and hence the total mass flux is given by

$$\phi_b-\phi_a=\int_{n_a}^{n_b}\rho urdn, \tag{166}$$

where $n_a=0$ is taken for the sake of simplicity. Since the total mass flux $\phi_b-\phi_a$ is fixed, the boundary value of velocity u_a (or u_b) is determined from Eq. (166).

Using this boundary value we have distributions of stream-surface function along the relevant section of constant α, such as $\widehat{AJB}$ in Fig. 2. Since the fraction of mass flow is calculated by

$$\phi_j-\phi_a=\int_0^{n'_j}\rho urdn, \tag{167}$$

corresponding arc length n'_j is obtained inversely from Eq. (167) by using an appropriate interpolation. Marking the arc length n'_j on $\widehat{AJB}$ the revised position of mesh point J', can be determined. Similar calculations along all of the middle orthogonals provide the revised point rows for stream-surfaces to be corrected as shown in Fig. 55. Applying the spline interpolations to these revised point rows the renewed approximation of the coordinates of orthogonal mesh points can be obtained.

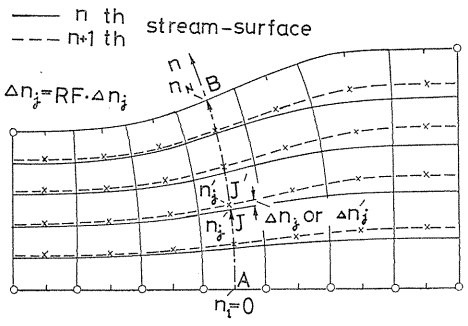

Fig. 55. Correction of stream-surfaces.

Substituting the new values of δs into Eqs. (164) and (166), the boundary value of u is corrected again, and the computation of Eq. (167) gives inversely the second correction of the stream-surface points. The orthogonal mesh points are thus refined. Repeating these iterations the solution is regarded to converge, when the correction of stream-surface defined by $\Delta n_j=n'_j-n_j$ becomes less than a designated small value, i. e. $|\Delta n_j|/a<\varepsilon$.

On convergence final values of velocity components are calculated by Eqs. (164) and (165). The density and pressure for a compressible flow are obtained by Eqs. (153) or (155) and by Eq. (138), respectively, and the pressure for an incompressible flow is calculated by

$$p/\rho=E(\psi)-(1/2)(u^2+w^2). \tag{168}$$

7. 3. Convergence of the procedure

The convergence and accuracy of the present method are now examined on comparing the results with a known exact solution. When the basic swirling flow of radius a has an axially uniform velocity U and a constant angular velocity Ω, the inviscid swirling flow of an incompressible fluid has a general solution given by Long[30], Chow[31] and others. Studying the inverse problem with prescribed velocity distribution along the axis, Uchida, Nakamura and Taniguchi[32] have also obtained an exact solution. The strength of swirl in these flows is represented by the inverse Rossby number defined by $R_0^{-1}=2\Omega a/U$.

One of the simplest solutions of the inverse problem is the swirling flow with a prescribed velocity of sinusoidal distribution along the axis:

$$u_a/U=1+D\cos(2\pi x/L). \tag{169}$$

The exact solution of the wall radius r_b of this pipe is calculated from

$$\left(\frac{r_b}{a}\right)^2+\left[\frac{2}{\sqrt{R_0^{-2}-\kappa^2}}\left(\frac{r_b}{a}\right)\cdot J_1\left(\sqrt{R_0^{-2}-\kappa^2}\,\frac{r_b}{a}\right)\right]\cdot D\cos(2\pi x/L)=1, \tag{170}$$

where $\kappa=2\pi a/L$ is the non-dimensional wave number. Taking $D=0.8$, $L/a=6\pi$, $\kappa=1/3$ and $R_0^{-1}=2.5$ the form of the pipe is calculated, and the present method of flux analysis is applied to solve the swirling flow in this pipe. Comparing the final value of velocity distribution along the axis with the prescribed one initially by Eq. (169), the accuracy of the present method is estimated.

The rate of convergence of the calculation is examined with the stream-surface

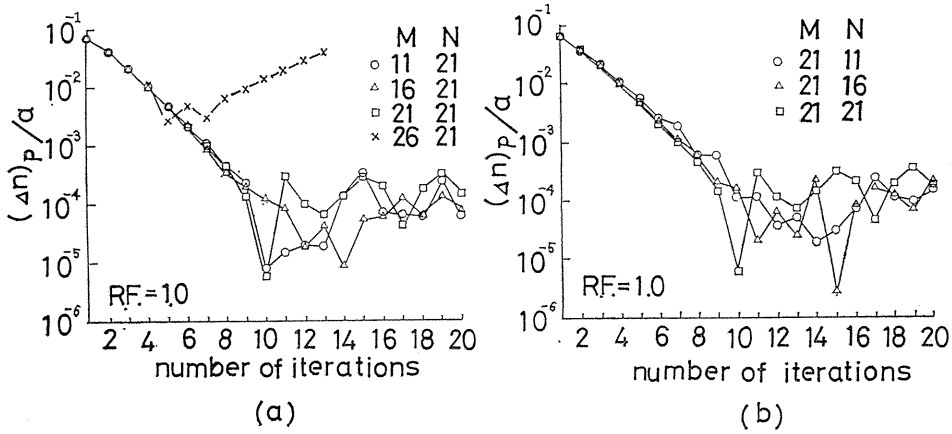

Fig. 56. Convergence of the flux analysis method, (a) Effect of longitudinal mesh numbers, (b) Effect of lateral mesh numbers.

correction $\Delta n/a$ at the middle point P of the boundary d, which is specified by $i=M$, $j=(N+1)/2$ for odd N or $(N/2)+1$ for even N. Effects of mesh numbers M and N are investigated as shown in Figs. 56 (a) and (b), respectively. The accuracies may depend mainly on the arc length δs. Since the present orthogonals consist of linear segments which are normal to the interpolated curves of stream-surfaces as a mean, fluctuations in δs become relatively large for a fine mesh, resulting in the divergent solution as shown in the case of $M=26$ and $N=21$ in Fig. 56(a). The

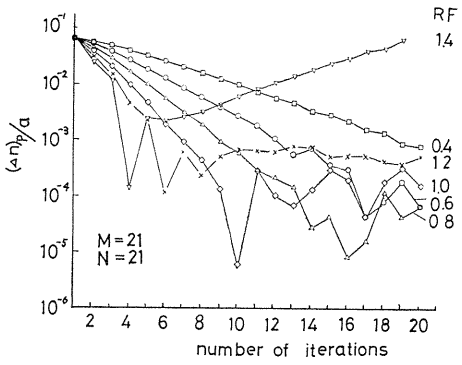

Fig. 57. Effect of relaxation factors on convergence.

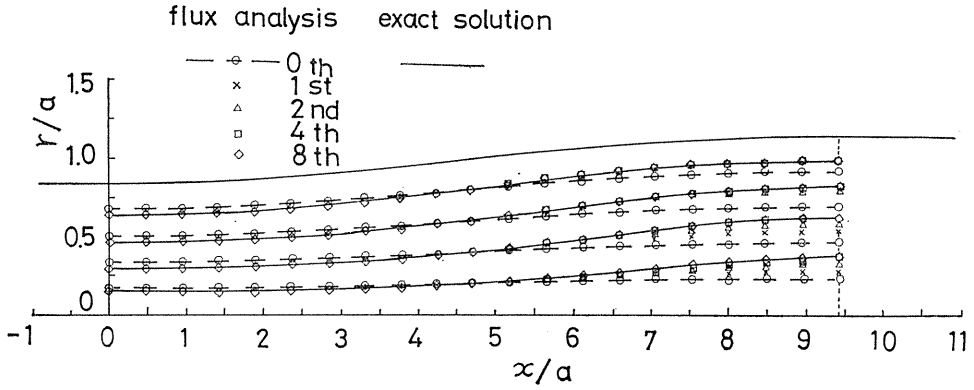

Fig. 58. Convergence and accuracy of the stream-surface comparing with the exact solution.

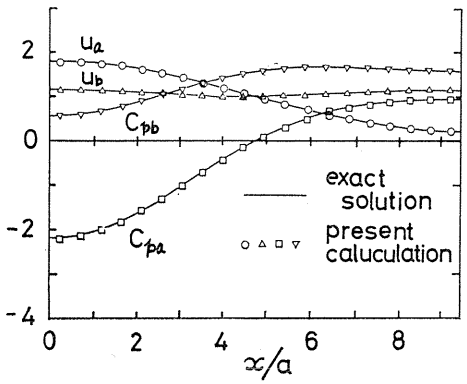

Fig. 59. Distributions of velocity and pressure compared with the exact solution.

oscillations in other cases, which finnally tend to converge, are also due to the same source.

To accelerate convergence the relaxation factor defined by $\Delta n'=\text{R.F.}\times\Delta n$, where $\Delta n'$ is the arc length to carry out the stream-surface correction for the succeeding iteration, is introduced. Examining the effect of relaxation factor on the convergence, it is found that R.F.$=0.6\sim0.8$ produces good results as shown in Fig. 57.

Flow patterns, distributions of meridian component of velocity and pressure coefficient along the axis and the wall, in which $C_p=(p-p_R)/(\rho U^2/2)$ is

referred to the wall pressure p_R in the basic flow, are given in Figs. 58 and 59. It is noticed that the present analysis shows an excellent agreement with the exact solution.

7. 4. Swirling flow in a diffusing pipe

The swirling flow of an incompressible fluid through a diffusing pipe is studied for various forms of the basic swirling flow. Introducing a pipe diffusing from a uniform radius a to another radius b with the sinusoidal contour of axial length l as shown in Fig. 60, the present computation is performed for an example of the pipe with $b/a=1.5$ and $l/a=10$.

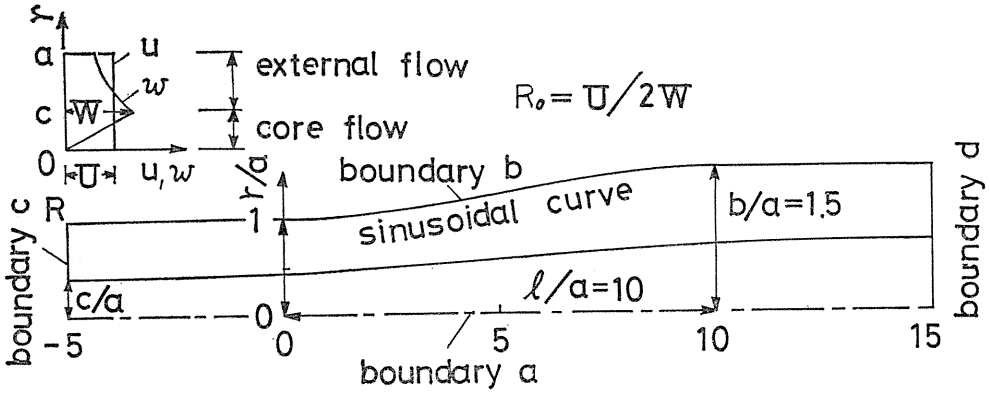

Fig. 60. Swirling flow in a diffusing pipe.

A swirling flow based on a single vortex with a uniform axial velocity U and a constant angular velocity Ω is first considered. The effect of the strength of swirl is studied for the basic flows of $R_0^{-1}=0$, 0.8 and 1.2, where the inverse Rossby number is defined by $R_0^{-1}=2\Omega a/U$. Distributions of velocity components, circulation function and of total energy referred to the value at the wall E_R in the basic swirling flow is given in Fig. 61.

Applying the boundary condition expressed by Eq. (162) the flow is computed

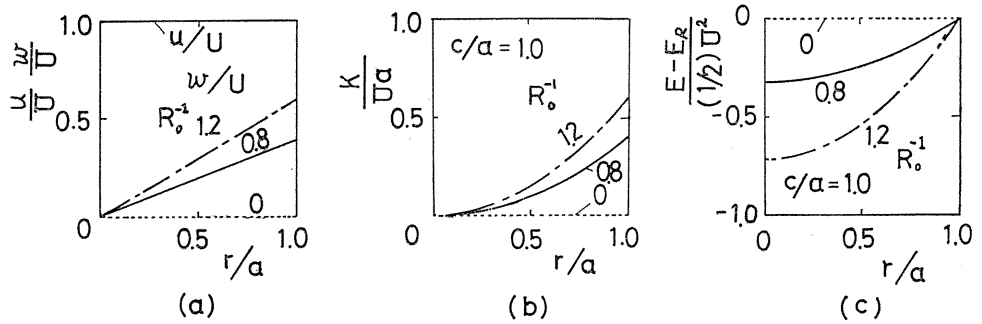

Fig. 61. Characteristics of the single vortices, (a) Velocity components, (b) Circulation function, (c) Total energy.

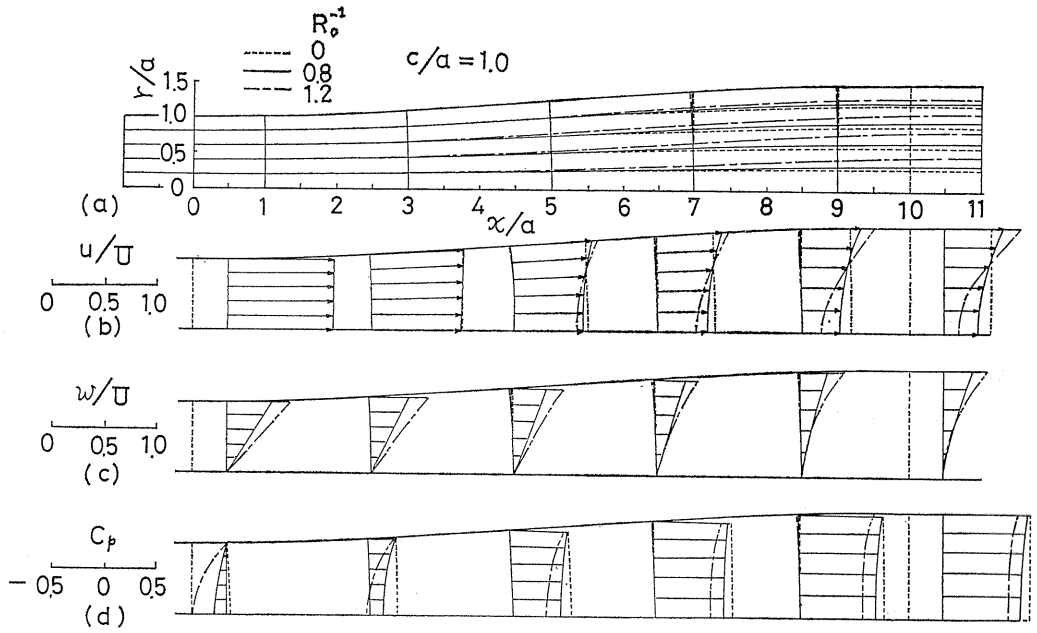

Fig. 62. Deformations of single vortices, (a) Flow patterns, (b) Meridian velocity, (c) Azimuthal velocity, (d) Pressure coefficient.

by the flux analysis method referring to the boundary value at the boundary b. Flow patterns, velocity components and pressure coefficients defined by $C_p=(p-p_R)/(\rho U^2/2)$ are obtained as shown in Fig. 62.

The swell of each stream-surface downstream caused by the expansion of pipe radius increases the pressure as well decreases the azimuthal velocity component, resulting in a pressure distribution across the stream more uniform in the downstream sections as shown in Fig. 62. Since the total energy is less in the axial region, the deceleration becomes more pronounced along the axis. This suggests the occurrence of a stagnation point on increasing the strength of swirl R_0^{-1}.

The basic swirling flow of a compound vortex consisting of a vortex core of

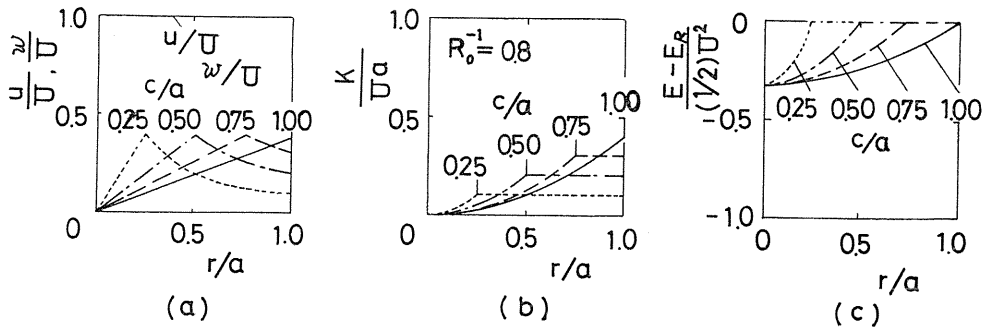

Fig. 63. Characteristics of compound vortices, (a) Velocity components, (b) Circulation function, (c) Total energy.

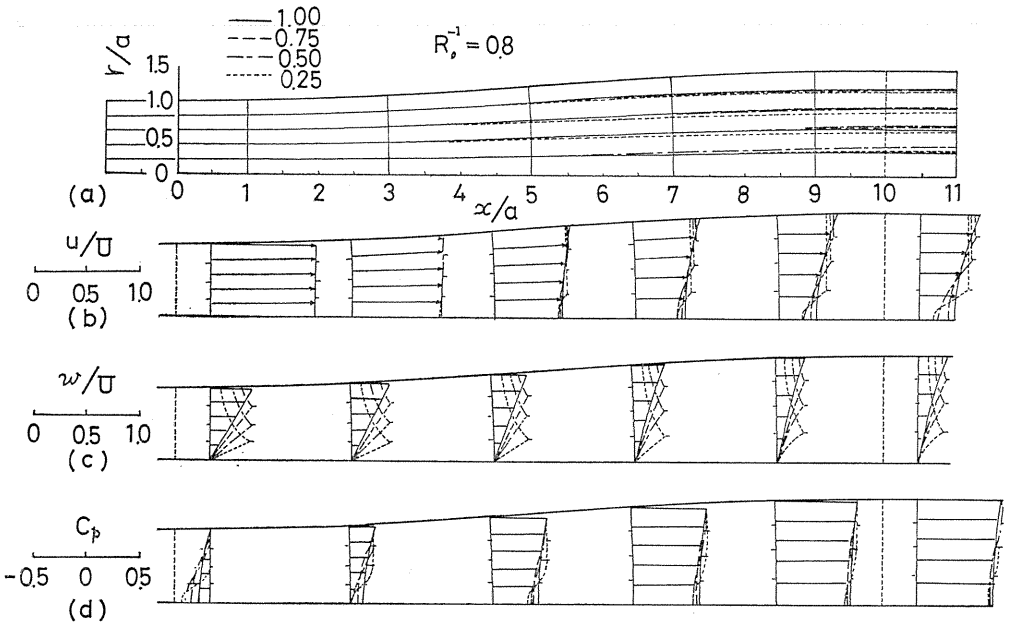

Fig. 64. Deformations of compound vortices, (a) Flow patterns, (b) Meridian velocity, (c) Azimuthal velocity, (d) Pressure coefficient.

solid rotation and of the circulating external flow without vorticity is now studied for the second example. Denoting the radius of the vortex core by c and the azimuthal velocity component at the core boundary by W, the strength of swirl is represented by $R_0^{-1}=2\Omega c/U=2W/U$. Taking several values of c/a for a fixed strength of $R_0^{-1}=0.8$, distributions of velocity, circulation function and total energy in the basic flow are shown in Fig. 63 as functions of r/a.

The compound swirling flows for $c/a=1.00$, 0.75, 0.50 and 0.25 with a fixed value of $R_0^{-1}=0.8$ are computed by applying the boundary condition (162). Flow patterns, distributions of velocity components and pressure coefficient are given in Fig. 64. Integrations across the stream are calculated separately in the core and in the outer region, these being connected at the dividing stream-surface of the core-flow boundary shown by the short line in Fig. 64.

The decrease of azimuthal velocity caused by the swell of stream-surface makes the pressure distribution more uniform in downstream sections. Since the pressure increases downstream generally by the expansion of pipe radius the adverse pressure gradient becomes large in the axial region. For a small value of R_0^{-1} as in the present case, however, effects of the swirl in various c/a are not significant as seen in the distribution of C_p along the wall, which takes almost the same value for four cases considered.

Since the level of total energy is low in the core region, less kinetic energy remains downstream than in the external region, resulting in the higher deceleration along the axis. The fraction of sectional area of the core is least in the case of $c/a=0.25$, and hence the whole flow suffers little effect from the swell of core boundary. Since the external flow is mainly governed by the increase in area of pipe section resulting in the comparatively higher adverse pressure gradient along

the core stream-surface. The impressed pressure gradient produces, therefore, the greatest swelling ratio of core radius in the case of $c/a=0.25$, as seen in Fig. 64. In this consequence the lowest velocity along the axis downstream is obtained in $c/a=0.25$ as shown in Fig. 64, which suggusts the earlier occurrence of a stagnation point, i. e. the vortex breakdown.

Chapter 8. Supplementary and Concluding Remarks

8. 1. Supplementary remarks

Analytical solutions of flow phenomena referred to streamline coordinates are obtained as briefly mentioned in the followings. Applying boundary layer approximations to the equation of viscous flow referred to streamline coordinates similar solutions of curved mixing layer (or half jet) have been obtained by Uchida and Suzuki[33] for a turbulent mixing and by Uchida, Kuwabara and Kishi[34] for a laminar mixing. Since in these analysis Gauss' equation of orthogonarity is solved simultaneously to give the streamline coordinates, no iterative procedure is needed. The effect of curvature in a mixing layer is first obtained by Uchida and Suzuki[32]. The same idea is applied to solve the similar solution for a turbulent curved jet by Murano and Uchida[35].

The Crocco type particular solutions for the energy equation of compressible boundary layer referred to the streamline coordinates are also obtained by Uchida and Kuwabara[36] for a laminar flow and by Uchida and Kuwabara[37] for a turbulent flow. Using this relation Kuwabara[38] has given an approximate solution for the curved laminar mixing layer of a compressible fluid.

8. 2. Concluding remarks

The fundamental idea of the theory of streamline analysis method or of flux analysis method is to solve the flow field by referring to the orthogonal curvilinear coordinates. Developing the computational procedure solutions for several types of flow are presented.

The merit of the present method is to proceed the analysis following closely to the structure of physical patterns of flow. The weak point of this method at the present stage is in the finite difference approximation of the arc segment which may limit the accuracy of the present computations. The recent study by Ishii[39] may suggest a new direction for the divelopment of these sorts of analysis.

Acknowledgement

Dedicating the present paper to late Prof. Sandi Kawada the author expresses sincere thanks for the ever-lasting encouragement. The author acknowledges excellent collaborations of Prof. M. Yasuhara, Drs. K. Kuwabara and Y. Nakamura, and of Mr. K. Tsuboi and others. His thanks are also due to Dr. K. Kuwabara and Mrs. Futsukaichi for their warm helps in the preparation of the present paper. The author gratefully acknowledges the financial support of a Grant-in-Aid for Scientific Research given along the course of the present investigation.

The author greatly appreciates the courtesy of the American Institute of Aeronautics and Astronautics (AIAA) for the permission to reproduce some figures.

Appendices

Appendix A

Fundamental Relations of Fluid Dynamics Referred to the Generalized Orthogonal Curvilinear Coordinates with Twist of Axes

1. Fundamental relations of coordinates

A generalized system of orthogonal curvilinear coordinates suitable for the description of swirling flows is constructed by coordinate axes, α, β and γ, being twisted around themselves. The strength of twist is represented by the rate of twist angle per unit length of α, β and γ axes, which are denoted by φ_1, φ_2 and φ_3, respectively. The angles of twist of α, β and γ axes at points A, B and C in Fig. A1 are, therefore, given by

$$\delta\theta_{11}=\varphi_1 h_\alpha \delta\alpha,\ \delta\theta_{22}=\varphi_2 h_\beta \delta\beta,\ \delta\theta_{33}=\varphi_3 h_\gamma \delta\gamma. \tag{A1}$$

Fundamental relations of coordinates and of fluid dynamics are studied in the followings. If we take $\varphi_1=\varphi_2=\varphi_3=0$, it is found that those equations result in the fundamental relations referred to the ordinary system of orthogonal curvilinear coordinates without twist of axes.

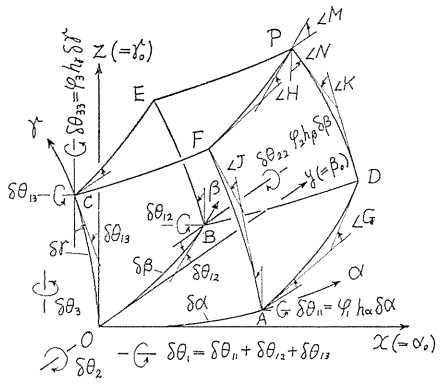

Fig. A1. Angles of rotation of coordinate axes (around x axis).

1. 1. Conditions of orthogonality

In order to study the orthogonality of coordinate axes, angles of rotation of individual side around x axis is calculated. Introducing extension parameters of α, β and γ axes denoted by h_α, h_β and h_γ, respectively, angles of rotation around x axis written in Fig. A1 are given by

$$\delta\theta_{12}=-\frac{1}{h_\gamma}\frac{\partial h_\beta}{\partial\gamma}\delta\beta,\quad \angle G=-\frac{1}{h_\gamma}\frac{\partial h_\beta}{\partial\gamma}\delta\beta-\frac{\partial}{\partial\alpha}\left(\frac{1}{h_\gamma}\frac{\partial h_\beta}{\partial\gamma}\right)\delta\beta\delta\alpha,$$

$$\angle H=-\frac{1}{h_\gamma}\frac{\partial h_\beta}{\partial\gamma}\delta\beta-\frac{\partial}{\partial\alpha}\left(\frac{1}{h_\gamma}\frac{\partial h_\beta}{\partial\gamma}\right)\delta\beta\delta\alpha-\frac{\partial}{\partial\gamma}\left(\frac{1}{h_\gamma}\frac{\partial h_\beta}{\partial\gamma}\right)\delta\beta\delta\gamma,$$

$$\delta\theta_{13}=\frac{1}{h_\beta}\frac{\partial h_\tau}{\partial\beta}\delta\gamma,\quad \angle J=\frac{1}{h_\beta}\frac{\partial h_\tau}{\partial\beta}\delta\gamma+\frac{\partial}{\partial\alpha}\left(\frac{1}{h_\beta}\frac{\partial h_\tau}{\partial\beta}\right)\delta\gamma\delta\alpha, \tag{A2}$$

$$\angle K=\frac{1}{h_\beta}\frac{\partial h_\tau}{\partial\beta}\delta\gamma+\frac{\partial}{\partial\alpha}\left(\frac{1}{h_\beta}\frac{\partial h_\tau}{\partial\beta}\right)\delta\gamma\delta\alpha+\frac{\partial}{\partial\beta}\left(\frac{1}{h_\beta}\frac{\partial h_\tau}{\partial\beta}\right)\delta\gamma\delta\beta.$$

The angle of twist around x axis of the side BD from B to D, of the side CF from C to F, and that of the side EP from E to P are, respectively,

$$\varphi_1 h_\alpha\delta\alpha+\frac{\partial(\varphi_1 h_\alpha)}{\partial\beta}\delta\alpha\delta\beta,\quad \varphi_1 h_\alpha\delta\alpha+\frac{\partial(\varphi_1 h_\alpha)}{h\gamma}\delta\alpha\delta\gamma,$$

$$\varphi_1 h_\alpha\delta\alpha+\frac{\partial(\varphi_1 h_\alpha)}{\partial\beta}\delta\alpha\delta\beta+\frac{\partial(\varphi_1 h_\alpha)}{\partial\gamma}\delta\alpha\delta\gamma. \tag{A3}$$

The angle of rotation of AD from y direction at the point D is calculated by $\delta\theta_{11}+\angle G$, and that of DP from z direction at the point D is given by $\delta\theta_{12}+\varphi_1 h_\alpha\delta\alpha+[\partial(\varphi_1 h_\alpha)/\partial\beta]\delta\alpha\delta\beta$.

Equalizing these angles of rotation the orthogonality of AD and DP at D is satisfied. Substituting Eqs. (A1) and (A2) into

$$\delta\theta_{11}+\angle G=\delta\theta_{12}+\left[\varphi_1 h_\alpha\delta\alpha+\frac{\partial(\varphi_1 h_\alpha)}{\partial\beta}\delta\alpha\delta\beta\right],$$

we have

$$\frac{\partial(\varphi_1 h_\alpha)}{\partial\beta}=-\frac{\partial}{\partial\alpha}\left(\frac{1}{h_\tau}\frac{\partial h_\beta}{\partial\gamma}\right).$$

From the similar relation:

$$\delta\theta_{11}+\angle J=\delta\theta_{13}+\left[\varphi_1 h_\alpha\delta\alpha+\frac{\partial(\varphi_1 h_\alpha)}{\partial\gamma}\delta\alpha\delta\gamma\right],$$

the orthogonality of AF and EP is satisfied by

$$\frac{\partial(\varphi_1 h_\alpha)}{\partial\gamma}=\frac{\partial}{\partial\alpha}\left(\frac{1}{h_\beta}\frac{\partial h_\tau}{\partial\beta}\right).$$

The angle of rotation of BE from z direction at the point E is calculated by $\delta\theta_{12}+\delta\theta_{13}+[\partial(\delta\theta_{13})/\partial\beta]\delta\beta$ and that of CE from y direction at the point E is given by $\delta\theta_{13}+\delta\theta_{12}+[\partial(\delta\theta_{12})/\partial\gamma]\delta\gamma$. Equalizing these angles of rotation the orthogonality of BE and CE at E is satisfied by

$$\frac{\partial}{\partial\beta}\left(\frac{1}{h_\beta}\frac{\partial h_\tau}{\partial\beta}\right)=-\frac{\partial}{\partial\gamma}\left(\frac{1}{h_\tau}\frac{\partial h_\beta}{\partial\gamma}\right). \tag{A4}$$

The angle of rotation of FP from y direction at the point P is calculated by $\angle M=\delta\theta_{11}+\angle J+\angle H$, and that of DP from z direction at the point P is given by $\angle N=\delta\theta_{11}+\angle G+\angle K$. Equalizing these angles, i.e. $\angle M=\angle N$, it is found that the orthogonality of FP and DP at P is satisfied by Eq. (A4).

Studying other components of angles of rotation around y and z axes we have the following form of conditions. These orthogonality equations consist of the

Gauss' orthogonality conditions:

$$\frac{\partial}{\partial\beta}\left(\frac{1}{h_\beta}\frac{\partial h_\gamma}{\partial\beta}\right)+\frac{\partial}{\partial\gamma}\left(\frac{1}{h_\gamma}\frac{\partial h_\beta}{\partial\gamma}\right)=0,\quad \frac{\partial}{\partial\gamma}\left(\frac{1}{h_\gamma}\frac{\partial h_\alpha}{\partial\gamma}\right)+\frac{\partial}{\partial\alpha}\left(\frac{1}{h_\alpha}\frac{\partial h_\gamma}{\partial\alpha}\right)=0,$$

$$\frac{\partial}{\partial\alpha}\left(\frac{1}{h_\alpha}\frac{\partial h_\beta}{\partial\alpha}\right)+\frac{\partial}{\partial\beta}\left(\frac{1}{h_\beta}\frac{\partial h_\alpha}{\partial\beta}\right)=0, \tag{A5}$$

and orthogonality conditions for twist of axes:

$$\frac{\partial}{\partial\beta}(\varphi_1 h_\alpha)=-\frac{\partial}{\partial\alpha}\left(\frac{1}{h_\gamma}\frac{\partial h_\beta}{\partial\gamma}\right),\quad \frac{\partial}{\partial\gamma}(\varphi_1 h_\alpha)=\frac{\partial}{\partial\alpha}\left(\frac{1}{h_\beta}\frac{\partial h_\gamma}{\partial\beta}\right),$$

$$\frac{\partial}{\partial\alpha}(\varphi_2 h_\beta)=-\frac{\partial}{\partial\beta}\left(\frac{1}{h_\alpha}\frac{\partial h_\gamma}{\partial\alpha}\right),\quad \frac{\partial}{\partial\alpha}(\varphi_2 h_\beta)=\frac{\partial}{\partial\beta}\left(\frac{1}{h_\gamma}\frac{\partial h_\alpha}{\partial\gamma}\right), \tag{A6}$$

$$\frac{\partial}{\partial\alpha}(\varphi_3 h_\gamma)=-\frac{\partial}{\partial\gamma}\left(\frac{1}{h_\beta}\frac{\partial h_\alpha}{\partial_\beta}\right),\quad \frac{\partial}{\partial\beta}(\varphi_3 h_\gamma)=\frac{\partial}{\partial\gamma}\left(\frac{1}{h_\alpha}\frac{\partial h_\beta}{\partial\alpha}\right).$$

The strength of twist represented by φ_1, φ_2 and φ_3 should satisfy the constraint condition given by Eq. (A6). It is found that Eq. (A6) reduces also

$$\frac{\partial}{\partial\alpha}\left[\frac{\partial}{\partial\beta}\left(\frac{1}{h_\beta}\frac{\partial h_\gamma}{\partial\beta}\right)+\frac{\partial}{\partial\gamma}\left(\frac{1}{h_\gamma}\frac{\partial h_\beta}{\partial\gamma}\right)\right]=0,$$

$$\frac{\partial}{\partial\beta}\left[\frac{\partial}{\partial\gamma}\left(\frac{1}{h_\gamma}\frac{\partial h_\alpha}{\partial\gamma}\right)+\frac{\partial}{\partial\alpha}\left(\frac{1}{h_\alpha}\frac{\partial h_\gamma}{\partial\alpha}\right)\right]=0, \tag{A7}$$

$$\frac{\partial}{\partial\gamma}\left[\frac{\partial}{\partial\alpha}\left(\frac{1}{h_\alpha}\frac{\partial h_\beta}{\partial\alpha}\right)+\frac{\partial}{\partial\beta}\left(\frac{1}{h_\beta}\frac{\partial h_\alpha}{\partial\beta}\right)\right]=0,$$

which are the differentials of Gauss' conditions.

1. 2. Differentials of vector

The sum of rotational angle of coordinate due to $\delta\alpha$, $\delta\beta$ and $\delta\gamma$ around x, y and z axes are given by

$$\delta\theta_1=\varphi_1 h_\alpha\delta\alpha-\frac{1}{h_\gamma}\frac{\partial h_\beta}{\partial\gamma}\delta\beta+\frac{1}{h_\beta}\frac{\partial h_\gamma}{\partial\beta}\delta\gamma,$$

$$\delta\theta_2=\frac{1}{h_\gamma}\frac{\partial h_\alpha}{\partial\gamma}\delta\alpha+\varphi_2 h_\beta\delta\beta-\frac{1}{h_\alpha}\frac{\partial h_\gamma}{\partial\alpha}\delta\gamma, \tag{A8}$$

$$\delta\theta_3=-\frac{1}{h_\beta}\frac{\partial h_\alpha}{\partial\beta}\delta\alpha+\frac{1}{h_\alpha}\frac{\partial h_\beta}{\partial\alpha}\delta\beta+\varphi_3 h_\gamma\delta\gamma.$$

Denoting α, β and γ components of a vector V by u, v and w, respectively, a small spacial increment of u is expressed by

$$\delta u=du-v\delta\theta_3+w\delta\theta_2$$

$$=\left[\frac{\partial u}{\partial\alpha}\delta\alpha+\frac{\partial u}{\partial\beta}\delta\beta+\frac{\partial u}{\partial\gamma}\delta\gamma\right]-v\left[-\frac{1}{h_\beta}\frac{\partial h_\alpha}{\partial\beta}\delta\alpha+\frac{1}{h_\alpha}\frac{\partial h_\beta}{\partial\alpha}\delta\beta\right.$$

$$\left.+\varphi_3 h_\gamma\delta\gamma\right]+w\left[\frac{1}{h_\gamma}\frac{\partial h_\alpha}{\partial\gamma}\delta\alpha+\varphi_2 h_\beta\delta\beta-\frac{1}{h_\alpha}\frac{\partial h_\gamma}{\partial\alpha}\delta\gamma\right]. \tag{A9}$$

Since the x, y and z axes are fixed to the initial directions of α, β and γ axes, respectively, it is also given

$$\delta u=\frac{\partial u}{\partial x}h_\alpha\delta\alpha+\frac{\partial u}{\partial y}h_\beta\delta\beta+\frac{\partial u}{\partial z}h_\gamma\partial\gamma. \tag{A10}$$

Comparing Eq. (A9) with Eq. (A10) we have differentials of vector components as follows:

$$\frac{\partial u}{\partial x}=\frac{1}{h_\alpha}\frac{\partial u}{\partial\alpha}+\frac{v}{h_\alpha h_\beta}\frac{\partial h_\alpha}{\partial\beta}+\frac{w}{h_\gamma h_\alpha}\frac{\partial h_\alpha}{\partial\gamma},\quad \frac{\partial u}{\partial y}=\frac{1}{h_\beta}\frac{\partial u}{\partial\beta}-\frac{v}{h_\alpha h_\beta}\frac{\partial h_\beta}{\partial\alpha}+w\varphi_2,$$

$$\frac{\partial u}{\partial z}=\frac{1}{h_\gamma}\frac{\partial u}{\partial\gamma}-v\varphi_3-\frac{w}{h_\gamma h_\alpha}\frac{\partial h_\gamma}{\partial\alpha};\quad \frac{\partial v}{\partial x}=\frac{1}{h_\alpha}\frac{\partial v}{\partial\alpha}-w\varphi_1-\frac{u}{h_\alpha h_\beta}\frac{\partial h_\alpha}{\partial\beta},$$

$$\frac{\partial v}{\partial y}=\frac{1}{h_\beta}\frac{\partial v}{\partial\beta}+\frac{w}{h_\beta h_\gamma}\frac{\partial h_\beta}{\partial\gamma}+\frac{u}{h_\alpha h_\beta}\frac{\partial h_\beta}{\partial\alpha},\quad \frac{\partial v}{\partial z}=\frac{1}{h_\gamma}\frac{\partial v}{\partial\gamma}-\frac{w}{h_\beta h_\gamma}\frac{\partial h_\gamma}{\partial\beta}+u\varphi_3;$$

$$\frac{\partial w}{\partial x}=\frac{1}{h_\alpha}\frac{\partial w}{\partial\alpha}-\frac{u}{h_\gamma h_\alpha}\frac{\partial h_\alpha}{\partial\gamma}+v\varphi_1,\quad \frac{\partial w}{\partial y}=\frac{1}{h_\beta}\frac{\partial w}{\partial\beta}-u\varphi_2-\frac{v}{h_\beta h_\gamma}\frac{\partial h_\beta}{\partial\gamma},$$

$$\frac{\partial w}{\partial z}=\frac{1}{h_\gamma}\frac{\partial w}{\partial\gamma}+\frac{u}{h_\gamma h_\alpha}\frac{\partial h_\gamma}{\partial\alpha}+\frac{v}{h_\beta h_\gamma}\frac{\partial h_\gamma}{\partial\beta}. \tag{A11}$$

1. 3. The Euler derivative

The Euler derivative of a vector $\boldsymbol{A}$ $(A_\alpha, A_\beta, A_\gamma)$ is given by

$$\frac{DA_\alpha}{Dt}=\frac{\partial A_\alpha}{\partial t}+u\frac{\partial A_\alpha}{\partial x}+v\frac{\partial A_\gamma}{\partial y}+w\frac{\partial A_\alpha}{\partial z}$$

$$=\frac{\partial A_\alpha}{\partial t}+\frac{u}{h_\alpha}\frac{\partial A_\alpha}{\partial\alpha}+\frac{v}{h_\beta}\frac{\partial A_\alpha}{\partial\beta}+\frac{w}{h_\gamma}\frac{\partial A_\alpha}{\partial\gamma}-A_\beta\left[\frac{v}{h_\alpha h_\beta}\frac{\partial h_\beta}{\partial\alpha}\right.$$

$$\left.-\frac{u}{h_\alpha h_\beta}\frac{\partial h_\alpha}{\partial\beta}+w\varphi_3\right]+A_\gamma\left[\frac{u}{h_\gamma h_\alpha}\frac{\partial h_\alpha}{\partial\gamma}-\frac{w}{h_\gamma h_\alpha}\frac{\partial h_\gamma}{\partial\alpha}+v\varphi_2\right],$$

$$\text{etc.,} \tag{A12}$$

while the Euler differential of a scalar θ is simply given by

$$\frac{D\theta}{Dt}=\frac{\partial\theta}{\partial t}+\frac{u}{h_\alpha}\frac{\partial\theta}{\partial\alpha}+\frac{v}{h_\beta}\frac{\partial\theta}{\partial\beta}+\frac{w}{h_\gamma}\frac{\partial\theta}{\partial\gamma}. \tag{A13}$$

2. Fundamental relations on the infinitesimal fluid element

2. 1. The strain of fluid element

The rate of elongation and shearing strain of a moving fluid element per unit time are expressed by

$$e_{\alpha\alpha}=\frac{\partial u}{\partial x}=\frac{1}{h_\alpha}\frac{\partial u}{\partial\alpha}+\frac{v}{h_\alpha h_\beta}\frac{\partial h_\alpha}{\partial\beta}+\frac{w}{h_\alpha h_\gamma}\frac{\partial h_\alpha}{\partial\gamma},$$

$$e_{\beta\beta}=\frac{\partial v}{\partial y}=\frac{1}{h_\beta}\frac{\partial v}{\partial\beta}+\frac{w}{h_\beta h_\gamma}\frac{\partial h_\beta}{\partial\gamma}+\frac{u}{h_\beta h_\alpha}\frac{\partial h_\beta}{\partial\alpha}, \tag{A14}$$

$$e_{\gamma\gamma}=\frac{\partial w}{\partial z}=\frac{1}{h_\gamma}\frac{\partial w}{\partial\gamma}+\frac{u}{h_\gamma h_\alpha}\frac{\partial h_\gamma}{\partial\alpha}+\frac{v}{h_\gamma h_\beta}\frac{\partial h_\gamma}{\partial\beta};$$

and

$$e_{\beta\gamma}=\frac{\partial w}{\partial y}+\frac{\partial v}{\partial z}=\frac{h_\gamma}{h_\beta}\frac{\partial}{\partial\beta}\left(\frac{w}{h_\gamma}\right)+\frac{h_\beta}{h_\gamma}\frac{\partial}{\partial\gamma}\left(\frac{v}{h_\beta}\right)+u(\varphi_3-\varphi_2)=e_{\gamma\beta},$$

$$e_{\gamma\alpha}=\frac{\partial u}{\partial z}+\frac{\partial w}{\partial x}=\frac{h_\alpha}{h_\gamma}\frac{\partial}{\partial\gamma}\left(\frac{u}{h_\alpha}\right)+\frac{h_\gamma}{h_\alpha}\frac{\partial}{\partial\alpha}\left(\frac{w}{h_\gamma}\right)+v(\varphi_1-\varphi_3)=e_{\alpha\gamma}, \tag{A15}$$

$$e_{\alpha\beta}=\frac{\partial v}{\partial x}+\frac{\partial u}{\partial y}=\frac{h_\beta}{h_\gamma}\frac{\partial}{\partial\alpha}\left(\frac{v}{h_\beta}\right)+\frac{h_\alpha}{h_\beta}\frac{\partial}{\partial\beta}\left(\frac{u}{h_\alpha}\right)+w(\varphi_2-\varphi_1)=e_{\beta\alpha}.$$

It is noted that the shearing strain contains terms of twist of coordinates.

The rate of expansion of volume is given by

$$\begin{aligned}\mathrm{div}\,V&=\frac{\partial u}{\partial x}+\frac{\partial v}{\partial y}+\frac{\partial w}{\partial z}\\&=\frac{1}{h_\alpha h_\beta h_\gamma}\left[\frac{\partial(uh_\beta h_\gamma)}{\partial\alpha}+\frac{\partial(vh_\gamma h_\alpha)}{\partial\beta}+\frac{\partial(wh_\alpha h_\beta)}{\partial\gamma}\right].\end{aligned} \tag{A16}$$

Components of vorticity vector $\zeta=rot\ V$ denoted by ξ, η and ζ are obtained from Eq. (A11) as follows:

$$\xi=\frac{1}{h_\beta h_\gamma}\left[\frac{\partial(wh_\gamma)}{\partial_\beta}-\frac{\partial(vh_\beta)}{\partial\gamma}\right]-u(\varphi_2+\varphi_3),$$

$$\eta=\frac{1}{h_\gamma h_\alpha}\left[\frac{\partial(uh_\alpha)}{\partial\gamma}-\frac{\partial(wh_\gamma)}{\partial\alpha}\right]-v(\varphi_3+\varphi_1), \tag{A17}$$

$$\zeta=\frac{1}{h_\alpha h_\beta}\left[\frac{\partial(vh_\beta)}{\partial\alpha}-\frac{\partial(uh_\alpha)}{\partial\beta}\right]-w(\varphi_1+\varphi_2).$$

The vorticity vector is solenoidal, i.e. $div\zeta=0$. Substituting the the similar terms with those in Eq. (A11) into

$$\mathrm{div}\,\zeta=\partial\xi/\partial x+\partial\eta/\partial y+\partial\zeta/\partial z,$$

we have

$$\text{div}\,\zeta=\frac{1}{h_\alpha h_\beta h_\gamma}\left[\frac{\partial(\xi h_\beta h_\gamma)}{\partial\alpha}+\frac{\partial(\eta h_\gamma h_\alpha)}{\partial\beta}+\frac{\partial(\zeta h_\alpha h_\beta)}{\partial\gamma}\right]$$

$$=\frac{1}{h_\alpha h_\beta h_\gamma}\left\{\frac{\partial}{\partial\alpha}\left[-u(\varphi_2+\varphi_3)h_\beta h_\gamma\right]+\frac{\partial}{\partial\beta}\left[-v(\varphi_3+\varphi_1)h_\gamma h_\alpha\right]\right.$$

$$\left.+\frac{\partial}{\partial\gamma}\left[-w(\varphi_1+\varphi_2)h_\alpha h_\beta\right]\right\}=0. \tag{A18}$$

Since $-u\varphi_2 h_\beta\delta\beta=\Delta w$, $u\varphi_3 h_\gamma\delta\gamma=\Delta v$, etc., are velocity components and $-u(\varphi_2+\varphi_3)h_\beta h_\gamma\delta\beta\delta\gamma=\Gamma_\alpha$, etc., represent circulations appeared by the twist of coordinate axes as shown in Fig. A2, therefore, Eq. (A18) expresses the law representing that the virtual production of vorticity should not be existed in the space of twisted coordinates.

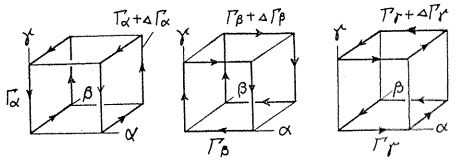

Fig. A2. Each term of div ζ.

2. 2. The relation between stress and strain

The Stokes' law between stress and strain for a Newtonian fluid is expressed by the same formulae with the ordinary case, but it is noticed that the shearing stress contains terms due to the twist of coordinate axes.

It is given

$$\begin{aligned}
&\sigma_{\alpha\alpha}=-p+\tau_{\alpha\alpha},\quad \sigma_{\beta\beta}=-p+\tau_{\beta\beta},\quad \sigma_{\gamma\gamma}=-p+\tau_{\gamma\gamma};\\
&\tau_{\alpha\alpha}=\lambda\,\text{div}\,\boldsymbol{V}+2\mu e_{\alpha\alpha},\quad \tau_{\beta\gamma}=\mu e_{\beta\gamma}=\mu e_{\gamma\beta}=\tau_{\gamma\beta},\\
&\tau_{\beta\beta}=\lambda\,\text{div}\,\boldsymbol{V}+2\mu e_{\beta\beta},\quad \tau_{\gamma\alpha}=\mu e_{\gamma\alpha}=\mu e_{\alpha\gamma}=\tau_{\alpha\gamma},\\
&\tau_{\gamma\gamma}=\lambda\,\text{div}\,\boldsymbol{V}+2\mu e_{\gamma\gamma},\quad \tau_{\alpha\beta}=\mu e_{\alpha\beta}=\mu e_{\beta\alpha}=\tau_{\beta\alpha}.
\end{aligned} \tag{A19}$$

2. 3. Dissipation function

The dissipation function denoted by Φ is also expressed by the same form with the ordinary case.

$$\begin{aligned}
\Phi&=\tau_{\alpha\alpha}e_{\alpha\alpha}+\tau_{\beta\beta}e_{\beta\beta}+\tau_{\gamma\gamma}e_{\gamma\gamma}+\tau_{\alpha\beta}e_{\alpha\beta}+\tau_{\beta\gamma}e_{\beta\gamma}+\tau_{\gamma\alpha}e_{\gamma\alpha}\\
&=\lambda\text{div}^2\boldsymbol{V}+\mu\left[2e_{\alpha\alpha}^2+2e_{\beta\beta}^2+2e_{\gamma\gamma}^2+e_{\alpha\beta}^2+e_{\beta\gamma}^2+e_{\gamma\alpha}^2\right].
\end{aligned} \tag{A20}$$

It is noted that the shearing stress and strain contain terms due to the twist of coordinates as shown in Eq, (A15).

3. Fundamental equations for the flow of a viscous fluid

3. 1. Equation of state

Two types of idealized fluids are considered. One of them is a thermodynamically perfect gas governed by the equation of states:

$$p/\rho=RT, \tag{A21}$$

where R is the gas constant per unit mass.

Another one is an incompressible fluid, as it were a perfect liquid, governed by the equation of state:

$$\rho=\text{constant}. \tag{A22}$$

This condition represents that the density of a perfect liquid does not change with other quantities of state as p or T.

3. 2. Equation of continuity

Referring to the orthogonal curvilinear coordinates the equation of continuity:

$$D\rho/Dt+\rho \text{ div } \boldsymbol{V}=0, \tag{A23}$$

is expressed by

$$\frac{\partial\rho}{\partial t}+\frac{1}{h_\alpha h_\beta h_\gamma}\left[\frac{\partial(\rho u h_\beta h_\gamma)}{\partial\alpha}+\frac{\partial(\rho v h_\gamma h_\alpha)}{\partial\beta}+\frac{\partial(\rho w h_\alpha h_\beta)}{\partial\gamma}\right]=0. \tag{A24}$$

3. 3. Equations of motion

The components of acceleration are given by

$$\frac{Du}{Dt}=\frac{\partial u}{\partial t}+\frac{u}{h_\alpha}\frac{\partial u}{\partial\alpha}+\frac{v}{h_\beta}\frac{\partial u}{\partial\beta}+\frac{w}{h_\gamma}\frac{\partial u}{\partial\gamma}$$

$$-v\left[\frac{v}{h_\alpha h_\beta}\frac{\partial h_\beta}{\partial\alpha}-\frac{u}{h_\alpha h_\beta}\frac{\partial h_\alpha}{\partial\beta}+w\varphi_3\right]+w\left[\frac{u}{h_\gamma h_\alpha}\frac{\partial h_\alpha}{\partial\gamma}-\frac{w}{h_\gamma h_\alpha}\frac{\partial h_\gamma}{\partial\alpha}+v\varphi_2\right], \tag{A25}$$

and by its cyclic changes of variables. The components of equation of motion are expressed by

$$\frac{Du}{Dt}=X-\frac{1}{\rho}\frac{1}{h_\alpha}\frac{\partial p}{\partial\alpha}$$

$$+\frac{1}{\rho}\frac{1}{h_\alpha h_\beta h_\gamma}\left[\frac{\partial(\tau_{\alpha\alpha}h_\beta h_\gamma)}{\partial\alpha}+\tau_{\alpha\beta}h_\gamma\frac{\partial h_\alpha}{\partial\beta}+\tau_{\alpha\gamma}h_\beta\frac{\partial h_\alpha}{\partial\gamma}\right.$$

$$+\frac{\partial(\tau_{\beta\alpha}h_\gamma h_\alpha)}{\partial\beta}-\tau_{\beta\beta}h_\gamma\frac{\partial h_\beta}{\partial\alpha}+\tau_{\beta\gamma}h_\alpha h_\beta h_\gamma\varphi_2$$

$$\left.+\frac{\partial(\tau_{\gamma\alpha}h_\alpha h_\beta)}{\partial\gamma}-\tau_{\gamma\beta}h_\alpha h_\beta h_\gamma\varphi_3-\tau_{\gamma\gamma}h_\beta\frac{\partial h_\gamma}{\partial\alpha}\right], \tag{A26}$$

and by its cyclic changes of variables.

Multiplying velocity components u, v and w to the x, y and z components of equations of motion, respectively, the summation gives the transfer equation of kinetic energy:

$$\frac{D}{Dt}\left(\frac{u^2+v^2+w^2}{2}\right)=u\frac{Du}{Dt}+v\frac{Dv}{Dt}+w\frac{Dw}{Dt}$$

$$=(uX+vY+wZ)-\frac{1}{\rho}\left(\frac{u}{h_\alpha}\frac{\partial p}{\partial x}+\frac{v}{h_\beta}\frac{\partial p}{\partial y}+\frac{w}{h_\gamma}\frac{\partial p}{\partial z}\right)+\phi, \qquad (A27)$$

where ϕ represents the work per unit time done by viscous forces for the translational motion of fluid element.

3. 4. Equation of energy

Introducing the internal energy per unit mass denoted by e, the first law of thermodynamics for the unit mass of fluid element is given by

$$\frac{De}{Dt}+p\frac{D}{Dt}\left(\frac{1}{\rho}\right)=\frac{1}{\rho}\left[H+\Phi\right], \qquad (A28)$$

where denoting the heat concuctivity by k

$$H=\frac{1}{h_\alpha h_\beta h_\gamma}\left[\frac{\partial}{\partial\alpha}\left(k\frac{h_\beta h_\gamma}{h_\alpha}\frac{\partial T}{\partial\alpha}\right)+\frac{\partial}{\partial\beta}\left(k\frac{h_\gamma h_\alpha}{h_\beta}\frac{\partial T}{\partial\beta}\right)+\frac{\partial}{\partial\gamma}\left(k\frac{h_\alpha h_\beta}{h_\gamma}\frac{\partial T}{\partial\gamma}\right)\right], \qquad (A29)$$

represents heat energy transmitted to the unit volume of fluid per unit time by heat conduction. The dissipation function represents heat energy produced by friction in the unit volume per unit time which is given by the work per unit time done by viscous forces for the pure deformation of fluid element. The effect of twist of coordinates is contained in terms of shearing stress and strain in Eq. (A20).

Denoting the total energy per unit mass by E, the equation for the total energy is obtained by adding Eq. (A27) and Eq. (A28). When the body force has a potential of single value denoted by Ω, we have

$$\frac{DE}{Dt}-\frac{\partial\Omega}{\partial t}-\frac{1}{\rho}\frac{\partial p}{\partial t}=\frac{1}{\rho}\left[H+\Phi+\Psi\right], \qquad (A30)$$

where $\Phi+\Psi$ represents the total work done by viscous force to the unit volume of fluid element per unit time. It is given by

$$\Phi+\Psi=\left[1/(h_\alpha h_\beta h_\gamma)\right]$$

$$\times\left(\frac{\partial(u\tau_{\alpha\alpha}h_\beta h_\gamma)}{\partial\alpha}+\frac{\partial(u\tau_{\beta\alpha}h_\gamma h_\alpha)}{\partial\beta}+\frac{\partial(u\tau_{\gamma\alpha}h_\alpha h_\beta)}{\partial\gamma}\right.$$

$$+\frac{\partial(v\tau_{\alpha\beta}h_\beta h_\gamma)}{\partial\alpha}+\frac{\partial(v\tau_{\beta\beta}h_\gamma h_\alpha)}{\partial\beta}+\frac{\partial(v\tau_{\gamma\beta}h_\alpha h_\beta)}{\partial\gamma}$$

$$\left.+\frac{\partial(w\tau_{\alpha\gamma}h_\beta h_\gamma)}{\partial\alpha}+\frac{\partial(w\tau_{\beta\gamma}h_\gamma h_\alpha)}{\partial\beta}+\frac{\partial(w\tau_{\gamma\gamma}h_\alpha h_\beta)}{\partial\gamma}\right). \qquad (A31)$$

In a particular case of steady flow of inviscid, non-heat-conductive fluid it is easily found that the total energy per unit mass of individual fluid element is conserved.

4. *Streamline coordinates*

4. 1. *Fundamental equations*

In some analyses streamline coordinates are conveniently used, since the fundamental equations are greatly simplified.

Fundamental equations referred to streamline coordinates, in which the α-axis is taken along the streamline, are obtaied by substituting $u=V$ and $v=w=0$ into the previous equations.

4. 2. *Streamline coordinates for a simple swirling flow*

As an example of orthogonal curvilinear coordinates with twist, streamline coordinates for a simple swirling flow is considered. Rotating with a constant angular velocity ω around the x-axis, the fluid flows along it with axial velocity $v_x=v_x(r)$. Taking the α-axis along the streamline, the β-axis along the cylindrical stream surface and γ-axis normal to it, the present coordinate system is shown in Fig. A3 together with the cylindrical coordinates: x, r, θ. Denoting the swirling angle on a cylindrical surface of radius r by Λ, geometrical relations shown in Fig. A4 lead $\delta s \sin\Lambda\cos\Lambda=r\tan\delta\theta_{11}$, $\delta h\cos\Lambda\sin\Lambda=-r\tan\delta\theta_{22}$. We have, therefore, the rate of twist angle as follows:

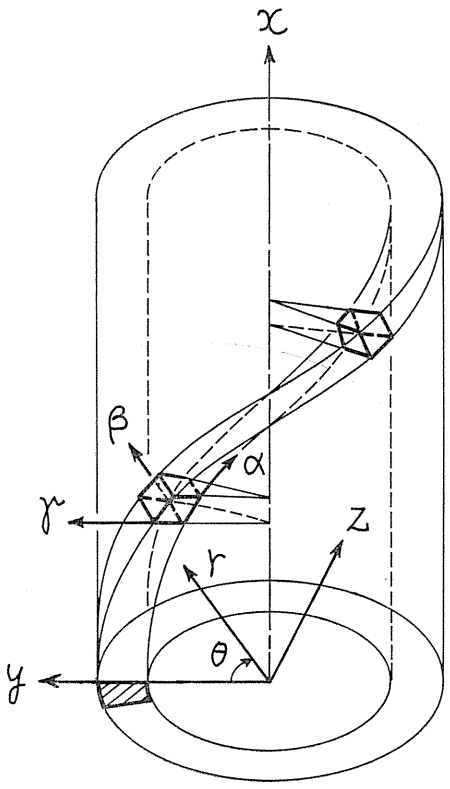

Fig. A3. Stream tube of a simple swirling flow.

$$\varphi_1=\lim_{\delta s\to 0}\frac{\delta\theta_{11}}{\delta s}=\frac{\sin\Lambda\cos\Lambda}{r},\quad \varphi_2=\lim_{\delta h\to 0}\frac{\delta\theta_{22}}{\delta h}=-\frac{\cos\Lambda\sin\Lambda}{r}. \tag{A32}$$

Since $\sin\Lambda=\omega r/V$, where V is flow speed, we have

$$\varphi_1=(\omega/V)\cos\Lambda,\quad \varphi_2=-(\omega/V)\cos\Lambda. \tag{A33}$$

Using $\Lambda=\tan^{-1}(\omega r/v_x)$, φ_3 is given by

$$\varphi_3=\lim_{\delta n\to 0}\frac{\delta\theta_{33}}{\delta n}=-\frac{\partial\Lambda}{\partial n}=-\frac{\partial\Lambda}{dr}=-\frac{\omega}{V}\cos\Lambda+\frac{1}{V}\frac{dv_x}{dr}\sin\Lambda. \tag{A34}$$

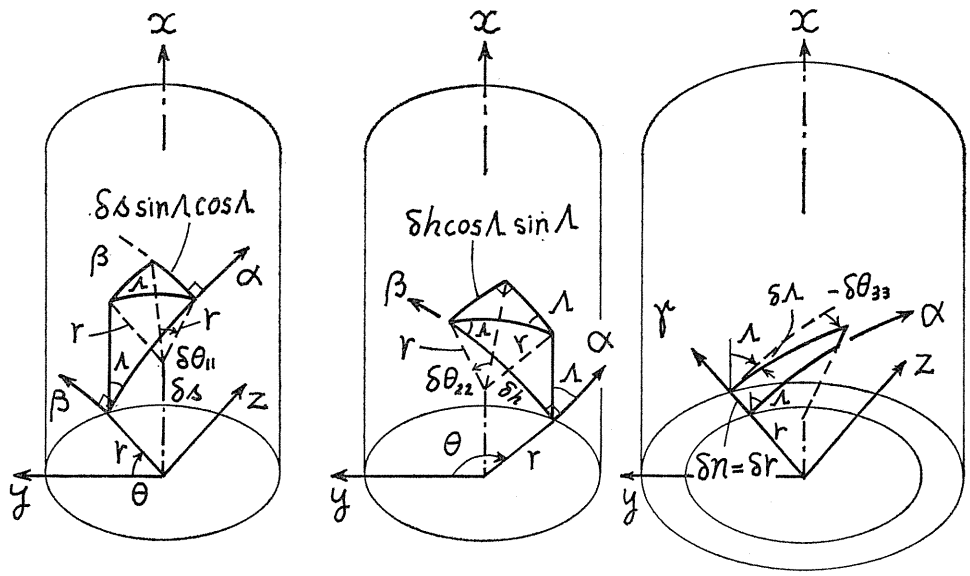

Fig. A4. Twist angle of coordinate axes.

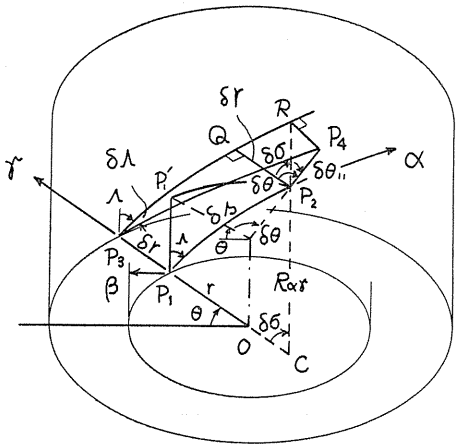

Fig. A5. The curvature $1/R_{\alpha r}=(1/h_\alpha h_r)\cdot(\partial h_\alpha/\partial r)$.

The curvature of α-axis in the $\alpha\gamma$-plane, which is denoted by $1/R_{\alpha r}$ is introduced as shown in Fig. A5, where arcs P_1P_2 and P_3P_4 represent the part of streamlines on the cylindrical surface of radius r and $r+\delta r$, respectivery. Taking the normal P_4R down to the surface $P_3P_1P_2$ from the point P, the included angle $\delta\sigma$ between RP_2 and P_3P_1 at the point of intersection C is calculated from $\widehat{QR}^2=\widehat{QP}_4{}^2-\widehat{P_4R}^2$

i.e. from

$$(\delta r\cdot\tan\delta\sigma)^2=(\delta r\cdot\delta\theta)^2-(\delta r\cdot\tan\delta\theta_{11})^2,$$

as follows:

$$\tan\delta\sigma=\sqrt{(\delta\theta)^2-\tan^2\delta\theta_{11}}\,.$$

We have, therefore,

$$\frac{1}{R_{\alpha r}}=\lim_{\delta s\to 0}\frac{\delta\sigma}{\delta s}=\sqrt{\lim_{\delta s\to 0}\left(\frac{\delta\theta}{\delta s}\right)^2-\lim_{\delta s\to 0}\left(\frac{\delta\theta_{11}}{\delta s}\right)^2}\,. \tag{A35}$$

Using $r\delta\theta=\delta s\sin\Lambda$, it is given

$$\lim_{\delta s\to 0}(\delta\theta/\delta s)=(\sin\Lambda)/r,$$

and

$$\lim_{\delta s\to 0}(\delta\theta_{11}/\delta s)=\varphi_1=(\sin\Lambda\cos\Lambda)/r.$$

Hence, We obtain the curvature

$$1/R_{\alpha\beta}=(\sin^2\Lambda)/r. \tag{A36}$$

Since the form of streamline is not changed in the direction of β-axis, the curvature of streamline in $\alpha\beta$-plane is zero as represented by

$$1/R_{\alpha\beta}=0. \tag{A37}$$

In order to confirm the previous expressions referred to the generalized orthogonal curvilinear coordinates with twist, formulations of vorticity is investigated. Substituting $u=V$, $v=w=0$ into Eq. (A17), we have expressions of vorticity components:

$$\xi=-V(\varphi_2+\varphi_3),\quad \eta=\frac{1}{h_\gamma h_\alpha}\frac{\partial(Vh_\alpha)}{\partial\gamma},\quad \zeta=\frac{1}{h_\alpha h_\beta}\frac{\partial(Vh_\alpha)}{\partial\beta}. \tag{A38}$$

For the concerning simple vortex flow it is given

$$\frac{1}{h_\alpha}\frac{\partial V}{\partial\gamma}=\frac{\partial V}{\partial n}=\frac{dV}{dr}=\frac{d}{dr}\sqrt{v_x^2+\omega^2r^2}=\omega\sin\Lambda+\frac{dv_x}{dr}\cos\Lambda,$$

$$\frac{V}{h_\gamma h_\alpha}\frac{\partial h_\alpha}{\partial\gamma}=\frac{V}{R_{\alpha\gamma}}=V\frac{\sin^2\Lambda}{r}=w\sin\Lambda,\quad \frac{1}{h_\beta}\frac{\partial V}{\partial\beta}=0.$$

Substituting these ralations into Eq. (A38) we have vorticity components:

$$\begin{aligned}\xi&=2\omega\cos\Lambda-(dv_x/dr)\sin\Lambda,\\ \eta&=2\omega\sin\Lambda+(dv_x/dr)\cos\Lambda,\\ \zeta&=0.\end{aligned} \tag{A39}$$

The vorticity components referred to the cylindrical coordinates shown in Fig. A6 is given by

$$\zeta_x=2\omega,\quad \zeta_r=0,\quad \zeta_\theta=-dv_x/dr. \tag{A40}$$

Then the x, y and z components of vorticity are given by

$$\zeta_x=2\omega,\quad \zeta_y=(dv_x/dr)\sin\theta,\quad \zeta_z=-(dv_x/dr)\cos\theta. \tag{A41}$$

Direction cosines of the unit vector $\boldsymbol{s}$, $\boldsymbol{h}$, and $\boldsymbol{n}$ along α, β and γ axes, respectively, are

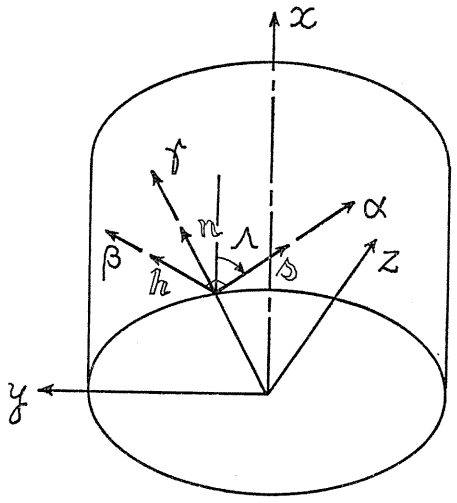

Fig. A6. Relation between each coordinate axes.

$$\boldsymbol{s}\ (\cos\Lambda,\quad -\sin\Lambda\sin\theta,\quad \sin\Lambda\cos\theta),$$

$$\boldsymbol{h}\ (\sin\Lambda,\quad \cos\Lambda\sin\theta,\quad -\cos\Lambda\cos\theta),$$

$$\boldsymbol{n}\ (0,\quad \cos\theta,\quad \sin\theta).$$

The α, β and γ components of vorticity are, therefore, calculated by

$$\begin{aligned}\zeta_\alpha &= 2\omega\cos\Lambda-(dv_x/dr)\sin\Lambda,\\ \zeta_\beta &= 2\omega\sin\Lambda+(dv_x/dr)\cos\Lambda,\\ \zeta_\gamma &= 0,\end{aligned}\qquad (A42)$$

which are the identical expressions with Eq. (A39). Even though the discussion with a particular example the propriety of the formulae for vorticity components given by Eq. (A17) is confirmed.

The present coordinate system has a spiral symmetry, and therefore, the constraint condition:

$$\operatorname{div}\zeta=\frac{1}{h_\alpha h_\beta h_\gamma}\frac{\partial}{\partial\alpha}[-V(\varphi_2+\varphi_3)h_\beta h_\gamma]=0,\qquad (A43)$$

is essentially satisfied.

5. Concluding remarks

A generalized system of orthogonal curvilinear coordinates with twist of axes, which is suitable to describe swirling flows in a turbo-machine, etc. is investigated.

The financial support by a grant in Aid for Scientific Research to the present part of study is highly appreciated.

Appendix B

Fundamental Relations of Fluid Dynamics Referred to Orthogonal Curvilinear Coordinates with no Twist of Axes

Fundamental equations for the flow of a compressible or incompressible fluid referred to orthogonal curvilinear coordinates without twist of axes can be easily deduced from the preceding discussions. They are formulated in the followings.

1. Fundamental relation of coordinates

1. 1. Gauss' condition of orthogonality

$$\frac{\partial}{\partial\beta}\left(\frac{1}{h_\beta}\frac{\partial h_\gamma}{\partial\beta}\right)+\frac{\partial}{\partial\gamma}\left(\frac{1}{h_\gamma}\frac{\partial h_\beta}{\partial\gamma}\right)=0,\quad \frac{\partial}{\partial\gamma}\left(\frac{1}{h_\gamma}\frac{\partial h_\alpha}{\partial\gamma}\right)+\frac{\partial}{\partial\alpha}\left(\frac{1}{h_\alpha}\frac{\partial h_\gamma}{\partial\alpha}\right)=0,$$

$$\frac{\partial}{\partial\alpha}\left(\frac{1}{h_\alpha}\frac{\partial h_\beta}{\partial\alpha}\right)+\frac{\partial}{\partial\beta}\left(\frac{1}{h_\beta}\frac{\partial h_\alpha}{\partial\beta}\right)=0. \tag{B1}$$

1. 2. Differentials of vector

$$\frac{\partial u}{\partial x}=\frac{1}{h_\alpha}\frac{\partial u}{\partial\alpha}+\frac{v}{h_\alpha h_\beta}\frac{\partial h_\alpha}{\partial\beta}+\frac{w}{h_\gamma h_\alpha}\frac{\partial h_\alpha}{\partial\gamma},$$

$$\frac{\partial u}{\partial y}=\frac{1}{h_\beta}\frac{\partial u}{\partial\beta}-\frac{v}{h_\alpha h_\beta}\frac{\partial h_\beta}{\partial\alpha},\quad \frac{\partial u}{\partial z}=\frac{1}{h_\gamma}\frac{\partial u}{\partial\gamma}-\frac{w}{h_\gamma h_\alpha}\frac{\partial h_\gamma}{\partial\alpha},$$

$$\frac{\partial v}{\partial y}=\frac{1}{h_\beta}\frac{\partial v}{\partial\beta}+\frac{w}{h_\beta h_\gamma}\frac{\partial h_\beta}{\partial\gamma}+\frac{u}{h_\alpha h_\beta}\frac{\partial h_\beta}{\partial\alpha},$$

$$\frac{\partial v}{\partial z}=\frac{1}{h_\gamma}\frac{\partial v}{\partial\gamma}-\frac{w}{h_\beta h_\gamma}\frac{\partial h_\gamma}{\partial\beta},\quad \frac{\partial v}{\partial x}=\frac{1}{h_\alpha}\frac{\partial v}{\partial\alpha}-\frac{u}{h_\alpha h_\beta}\frac{\partial h_\alpha}{\partial\beta}, \tag{B2}$$

$$\frac{\partial w}{\partial z}=\frac{1}{h_\gamma}\frac{\partial w}{\partial\gamma}+\frac{u}{h_\gamma h_\alpha}\frac{\partial h_\gamma}{\partial\alpha}+\frac{u}{h_\beta h_\gamma}\frac{\partial h_\gamma}{\partial\beta},$$

$$\frac{\partial w}{\partial x}=\frac{1}{h_\alpha}\frac{\partial w}{\partial\alpha}-\frac{u}{h_\gamma h_\alpha}\frac{\partial h_\alpha}{\partial\gamma},\quad \frac{\partial w}{\partial y}=\frac{1}{h_\beta}\frac{\partial w}{\partial\beta}-\frac{v}{h_\beta h_\gamma}\frac{\partial h_\beta}{\partial\gamma}.$$

1. 3. The Euler derivative

The Euler derivative for a vector $A(A_\alpha, A_\beta, A_\gamma)$ and for a scalar ρ are, respectively,

$$\frac{DA_\alpha}{Dt}=\frac{\partial A_\alpha}{\partial t}+\frac{u}{h_\alpha}\frac{\partial A_\alpha}{\partial\alpha}+\frac{v}{h_\beta}\frac{\partial A_\alpha}{\partial\beta}+\frac{w}{h_\gamma}\frac{\partial A_\alpha}{\partial\gamma}$$

$$-A_\beta\left[\frac{v}{h_\alpha h_\beta}\frac{\partial h_\beta}{\partial\alpha}-\frac{u}{h_\alpha h_\beta}\frac{\partial h_\alpha}{\partial\beta}\right]+A_\gamma\left[\frac{u}{h_\gamma h_\alpha}\frac{\partial h_\alpha}{\partial\gamma}-\frac{w}{h_\gamma h_\alpha}\frac{\partial h_\gamma}{\partial\alpha}\right],$$

$$\frac{DA_\beta}{Dt}=\frac{\partial A_\beta}{\partial t}+\frac{u}{h_\alpha}\frac{\partial A_\beta}{\partial\alpha}+\frac{v}{h_\beta}\frac{\partial A_\beta}{\partial\beta}+\frac{w}{h_\gamma}\frac{\partial A_\beta}{\partial\gamma}$$

$$-A_\tau\left[\frac{w}{h_\beta h_\tau}\frac{\partial h_\tau}{\partial\beta}-\frac{v}{h_\beta h_\tau}\frac{\partial h_\beta}{\partial\gamma}\right]+A_\alpha\left[\frac{v}{h_\alpha h_\beta}\frac{\partial h_\beta}{\partial\alpha}-\frac{u}{h_\alpha h_\beta}\frac{\partial h_\alpha}{\partial\beta}\right], \tag{B3}$$

$$\frac{DA_\tau}{Dt}=\frac{\partial A_\tau}{\partial t}+\frac{u}{h_\alpha}\frac{\partial A_\tau}{\partial\alpha}+\frac{v}{h_\beta}\frac{\partial A_\tau}{\partial\beta}+\frac{w}{h_\tau}\frac{\partial A_\tau}{\partial\gamma}$$

$$-A_\alpha\left[\frac{u}{h_\tau h_\alpha}\frac{\partial h_\alpha}{\partial\gamma}-\frac{w}{h_\tau h_\alpha}\frac{\partial h_\tau}{\partial\alpha}\right]+A_\beta\left[\frac{w}{h_\beta h_\tau}\frac{\partial h_\tau}{\partial\beta}-\frac{v}{h_\beta h_\tau}\frac{\partial h_\beta}{\partial\gamma}\right],$$

$$\frac{D\rho}{Dt}=\frac{\partial\rho}{\partial t}+\frac{u}{h_\alpha}\frac{\partial\rho}{\partial\alpha}+\frac{v}{h_\beta}\frac{\partial\rho}{\partial\beta}+\frac{w}{h_\tau}\frac{\partial\rho}{\partial\gamma}. \tag{B4}$$

2. Fundamental relation on the infinitesimal fluid element

2. 1. The strain of fluid element

The strains are given by

$$\begin{aligned}
e_{\alpha\alpha}&=\frac{1}{h_\alpha}\frac{\partial u}{\partial\alpha}+\frac{v}{h_\alpha h_\beta}\frac{\partial h_\alpha}{\partial\beta}+\frac{w}{h_\tau h_\alpha}\frac{\partial h_\alpha}{\partial\gamma},\\
e_{\beta\beta}&=\frac{1}{h_\beta}\frac{\partial v}{\partial\beta}+\frac{w}{h_\beta h_\tau}\frac{\partial h_\beta}{\partial\gamma}+\frac{u}{h_\alpha h_\beta}\frac{\partial h_\beta}{\partial\alpha},\\
e_{\tau\tau}&=\frac{1}{h_\tau}\frac{\partial w}{\partial\gamma}+\frac{u}{h_\tau h_\alpha}\frac{\partial h_\tau}{\partial\alpha}+\frac{v}{h_\beta h_\tau}\frac{\partial h_\tau}{\partial\beta};\\
e_{\beta\tau}&=\frac{h_\tau}{h_\beta}\frac{\partial}{\partial\beta}\left(\frac{w}{h_\tau}\right)+\frac{h_\beta}{h_\tau}\frac{\partial}{\partial\gamma}\left(\frac{v}{h_\beta}\right)=e_{\tau\beta},\\
e_{\tau\alpha}&=\frac{h_\alpha}{h_\tau}\frac{\partial}{\partial\gamma}\left(\frac{u}{h_\alpha}\right)+\frac{h_\tau}{h_\alpha}\frac{\partial}{\partial\alpha}\left(\frac{w}{h_\tau}\right)=e_{\alpha\tau},\\
e_{\alpha\beta}&=\frac{h_\beta}{h_\alpha}\frac{\partial}{\partial\alpha}\left(\frac{v}{h_\beta}\right)+\frac{h_\alpha}{h_\beta}\frac{\partial}{\partial\beta}\left(\frac{u}{h_\alpha}\right)=e_{\beta\alpha}.
\end{aligned} \tag{B5}$$

The rate of expansion of fluid element

$$\begin{aligned}
\mathrm{div}\,\boldsymbol{V}&=e_{\alpha\alpha}+e_{\beta\beta}+e_{\tau\tau}\\
&=\frac{1}{h_\alpha h_\beta h_\tau}\left[\frac{\partial(uh_\beta h_\tau)}{\partial\alpha}+\frac{\partial(vh_\tau h_\alpha)}{\partial\beta}+\frac{\partial(wh_\alpha h_\beta)}{\partial\gamma}\right].
\end{aligned} \tag{B6}$$

The vorticity components are given by

$$\xi=\frac{1}{h_\beta h_\tau}\left[\frac{\partial(wh_\tau)}{\partial\beta}-\frac{\partial(vh_\beta)}{\partial\gamma}\right],\quad \eta=\frac{1}{h_\tau h_\alpha}\left[\frac{\partial(uh_\alpha)}{\partial\gamma}-\frac{\partial(wh_\tau)}{\partial\alpha}\right],$$

$$\zeta=\frac{1}{h_\alpha h_\beta}\left[\frac{\partial(vh_\beta)}{\partial\alpha}-\frac{\partial(uh_\alpha)}{\partial\beta}\right], \tag{B7}$$

and $div\boldsymbol{\zeta}=0$ are automatically satisfied.

2. 2. The relation between stress and strain

The stokes' law for the Newtonian fluid reduces

$$\begin{aligned}
&\sigma_{\alpha\alpha}=-p+\tau_{\alpha\alpha},\quad \sigma_{\beta\beta}=-p+\tau_{\beta\beta},\quad \sigma_{\gamma\gamma}=-p+\tau_{\gamma\gamma};\\
&\tau_{\alpha\alpha}=\lambda\ \mathrm{div}\ V+2\mu e_{\alpha\alpha};\ \tau_{\beta\gamma}=\mu e_{\beta\gamma}=\mu e_{\gamma\beta}=\tau_{\gamma\beta},\\
&\tau_{\beta\beta}=\lambda\ \mathrm{div}\ V+2\mu e_{\beta\beta};\ \tau_{\gamma\alpha}=\mu e_{\gamma\alpha}=\mu e_{\alpha\gamma}=\tau_{\alpha\gamma},\\
&\tau_{\gamma\gamma}=\lambda\ \mathrm{div}\ V+2\mu e_{\gamma\gamma};\ \tau_{\alpha\beta}=\mu e_{\alpha\beta}=\mu e_{\beta\alpha}=\tau_{\beta\alpha}.
\end{aligned}\tag{B8}$$

2. 3. Dissipation function

$$\Phi=\tau_{\alpha\alpha}e_{\alpha\alpha}+\tau_{\beta\beta}e_{\beta\beta}+\tau_{\gamma\gamma}e_{\gamma\gamma}+\tau_{\alpha\beta}e_{\alpha\beta}+\tau_{\beta\gamma}e_{\beta\gamma}+\tau_{\gamma\alpha}e_{\gamma\alpha}.\tag{B9}$$

3. Fundamental equations for the flow of a viscous fluid

3. 1. Equation of state

The equation of state for a perfect gas is

$$p/\rho=RT.\tag{B10}$$

The equation of state for an incompressible fluid is expressed by

$$\rho=\text{constant}.\tag{B11}$$

3. 2. Equation of continuity

$$D\rho/Dt+\rho\ \mathrm{div}\ V=0,\tag{B12}$$

or

$$\frac{\partial\rho}{\partial t}+\frac{1}{h_\alpha h_\beta h_\gamma}\left[\frac{\partial(\rho u h_\beta h_\gamma)}{\partial\alpha}+\frac{\partial(\rho v h_\gamma h_\alpha)}{\partial\beta}+\frac{\partial(w h_\alpha h_\beta)}{\partial\gamma}\right]=0.\tag{B13}$$

3. 3. Equations of motion

$$\begin{aligned}
&\frac{\partial u}{\partial t}+\frac{u}{h_\alpha}\frac{\partial u}{\partial\alpha}+\frac{v}{h_\beta}\frac{\partial u}{\partial\beta}+\frac{w}{h_\gamma}\frac{\partial u}{\partial\gamma}\\
&\quad-v\left(\frac{v}{h_\beta h_\alpha}\frac{\partial h_\beta}{\partial\alpha}-\frac{u}{h_\alpha h_\beta}\frac{\partial h_\alpha}{\partial\beta}\right)+w\left(\frac{u}{h_\alpha h_\gamma}\frac{\partial h_\alpha}{\partial\gamma}-\frac{w}{h_\gamma h_\alpha}\frac{\partial h_\gamma}{\partial\alpha}\right)\\
&=X-\frac{1}{\rho}\frac{1}{h_\alpha}\frac{\partial p}{\partial\alpha}+\frac{1}{\rho}\frac{1}{h_\alpha h_\beta h_\gamma}\left[\frac{\partial(\tau_{\alpha\alpha}h_\beta h_\gamma)}{\partial\alpha}+\tau_{\alpha\beta}h_\gamma\frac{\partial h_\alpha}{\partial\beta}+\tau_{\alpha\gamma}h_\beta\frac{\partial h_\alpha}{\partial\gamma}\right.\\
&\qquad\left.+\frac{\partial(\tau_{\beta\alpha}h_\gamma h_\alpha)}{\partial\beta}-\tau_{\beta\beta}h_\gamma\frac{\partial h_\beta}{\partial\alpha}+\frac{\partial(\tau_{\gamma\alpha}h_\alpha h_\beta)}{\partial\gamma}-\tau_{\gamma\gamma}h_\beta\frac{\partial h_\gamma}{\partial\alpha}\right],\\
&\frac{\partial v}{\partial t}+\frac{u}{h_\alpha}\frac{\partial v}{\partial\alpha}+\frac{v}{h_\beta}\frac{\partial v}{\partial\beta}+\frac{w}{h_\gamma}\frac{\partial v}{\partial\gamma}
\end{aligned}$$

$$-w\left(\frac{w}{h_\gamma h_\beta}\frac{\partial h_\gamma}{\partial \beta}-\frac{v}{h_\beta h_\gamma}\frac{\partial h_\beta}{\partial \gamma}\right)+u\left(\frac{v}{h_\beta h_\alpha}\frac{\partial h_\beta}{\partial \alpha}-\frac{u}{h_\alpha h_\beta}\frac{\partial h_\alpha}{\partial \beta}\right)$$

$$=Y-\frac{1}{\rho}\frac{1}{h_\beta}\frac{\partial p}{\partial \beta}+\frac{1}{\rho}\frac{1}{h_\alpha h_\beta h_\gamma}\left[\frac{\partial(\tau_{\alpha\beta}h_\beta h_\gamma)}{\partial \alpha}-\tau_{\alpha\alpha}h_\gamma\frac{\partial h_\alpha}{\partial \beta}\right. \tag{B14}$$

$$\left.+\frac{\partial(\tau_{\beta\beta}h_\gamma h_\alpha)}{\partial \beta}+\tau_{\beta\gamma}h_\alpha\frac{\partial h_\beta}{\partial \gamma}+\tau_{\beta\alpha}h_\gamma\frac{\partial h_\beta}{\partial \alpha}+\frac{\partial(\tau_{\gamma\beta}h_\alpha h_\beta)}{\partial \gamma}-\tau_{\gamma\gamma}h_\alpha\frac{\partial h_\gamma}{\partial \beta}\right],$$

$$\frac{\partial w}{\partial t}+\frac{u}{h_\alpha}\frac{\partial w}{\partial \alpha}+\frac{v}{h_\beta}\frac{\partial w}{\partial \beta}+\frac{w}{h_\gamma}\frac{\partial w}{\partial \gamma}$$

$$-u\left(\frac{u}{h_\alpha h_\gamma}\frac{\partial h_\alpha}{\partial \gamma}-\frac{w}{h_\gamma h_\alpha}\frac{\partial h_\gamma}{\partial \alpha}\right)+v\left(\frac{w}{h_\gamma h_\beta}\frac{\partial h_\gamma}{\partial \beta}-\frac{v}{h_\beta h_\gamma}\frac{\partial h_\beta}{\partial \gamma}\right)$$

$$=Z-\frac{1}{\rho}\frac{1}{h_\gamma}\frac{\partial p}{\partial \gamma}+\frac{1}{\rho}\frac{1}{h_\alpha h_\beta h_\gamma}\left[\frac{\partial(\tau_{\alpha\gamma}h_\beta h_\gamma)}{\partial \alpha}-\tau_{\alpha\alpha}h_\beta\frac{\partial h_\alpha}{\partial \gamma}\right.$$

$$\left.+\frac{\partial(\tau_{\beta\gamma}h_\gamma h_\alpha)}{\partial \beta}-\tau_{\beta\beta}h_\alpha\frac{\partial h_\beta}{\partial \gamma}+\frac{\partial(\tau_{\gamma\gamma}h_\alpha h_\beta)}{\partial \gamma}+\tau_{\gamma\alpha}h_\beta\frac{\partial h_\gamma}{\partial \alpha}+\tau_{\gamma\beta}h_\alpha\frac{\partial h_\gamma}{\partial \beta}\right].$$

Multiplying u, v and w to α, β and γ components of Eq. (B14), respectively, the summation gives the transfer equation of kinetic energy:

$$\frac{D}{Dt}\left(\frac{u^2+v^2+w^2}{2}\right)=(Xu+Yv+Zw)$$

$$-\frac{1}{\rho}\left(\frac{u}{h_\alpha}\frac{\partial p}{\partial \alpha}+\frac{v}{h_\beta}\frac{\partial p}{\partial \beta}+\frac{w}{h_\gamma}\frac{\partial p}{\partial \gamma}\right)+\frac{1}{\rho}\Psi, \tag{B15}$$

where Ψ is the work done by the force acting on the unit volume of fluid element in translational motion per unit time. In a concise form it is given

$$\Psi=\left(\frac{\partial \tau_{\alpha\alpha}}{\partial x}+\frac{\partial \tau_{\beta\alpha}}{\partial y}+\frac{\partial \tau_{\gamma\alpha}}{\partial z}\right)u$$

$$+\left(\frac{\partial \tau_{\alpha\beta}}{\partial x}+\frac{\partial \tau_{\beta\beta}}{\partial y}+\frac{\partial \tau_{\gamma\beta}}{\partial z}\right)v+\left(\frac{\partial \tau_{\alpha\gamma}}{\partial x}+\frac{\partial \tau_{\beta\gamma}}{\partial y}+\frac{\partial \tau_{\gamma\gamma}}{\partial z}\right)w. \tag{B16}$$

When the external force has a single valued potential Ω, we have

$$\frac{D}{Dt}\left(\frac{u^2+v^2+w^2}{2}\right)+\frac{1}{\rho}\left(\frac{Dp}{Dt}-\frac{\partial p}{\partial t}\right)+\left(\frac{D\Omega}{Dt}-\frac{\partial \Omega}{\partial t}\right)=\frac{1}{\rho}\Psi. \tag{B17}$$

3. 4. Equation of energy

The first law of thermodynamics is formulated by

$$\frac{De}{Dt}+p\frac{D}{Dt}\left(\frac{1}{\rho}\right)=\frac{1}{\rho}[H+\Phi], \tag{B18}$$

where

$$H=\frac{1}{h_\alpha h_\beta h_\tau}\left[\frac{\partial}{\partial\alpha}\left(k\frac{h_\beta h_\tau}{h_\alpha}\frac{\partial T}{\partial\alpha}\right)+\frac{\partial}{\partial\beta}\left(k\frac{h_\tau h_\alpha}{h_\beta}\frac{\partial T}{\partial\beta}\right)+\frac{\partial}{\partial\gamma}\left(k\frac{h_\alpha h_\beta}{h_\tau}\frac{\partial T}{\partial\gamma}\right)\right]. \tag{B19}$$

Addition of Eqs. (B17) and (B18) gives the tranfer equation of the total energy defined by $E=(u^2+v^2+w^2)/2+e+(p/\rho)+\Omega$:

$$\frac{DE}{Dt}=\frac{1}{\rho}\frac{\partial p}{\partial t}+\frac{\partial\Omega}{\partial t}+\frac{1}{\rho}[H+\Phi+\Psi]. \tag{B20}$$

For a steady flow it is simply

$$\frac{DE}{Dt}=\frac{1}{\rho}[H+\Phi+\Psi], \tag{B21}$$

where

$$\begin{aligned}\Phi+\Psi=&[1/h_\alpha h_\beta h_\tau]\\&\times\left[\frac{\partial(u\tau_{\alpha\alpha}h_\beta h_\tau)}{\partial\alpha}+\frac{\partial(u\tau_{\beta\alpha}h_\tau h_\alpha)}{\partial\beta}+\frac{\partial(u\tau_{\tau\alpha}h_\alpha h_\beta)}{\partial\gamma}\right.\\&+\frac{\partial(v\tau_{\beta\beta}h_\tau h_\alpha)}{\partial\beta}+\frac{\partial(v\tau_{\tau\beta}h_\alpha h_\beta)}{\partial\gamma}+\frac{\partial(v\tau_{\alpha\beta}h_\beta h_\tau)}{\partial\alpha}\\&\left.+\frac{\partial(w\tau_{\tau\tau}h_\alpha h_\beta)}{\partial\gamma}+\frac{\partial(w\tau_{\alpha\tau}h_\beta h_\tau)}{\partial\alpha}+\frac{\partial(w\tau_{\beta\tau}h_\tau h_\alpha)}{\partial\beta}\right].\end{aligned} \tag{B22}$$

It is noticed that $\Phi+\Psi$ represents the work done by adjacent stresses to the unit volume of fluid element per unit time.

Appendix C

Fundamental Relations of Fluid Dynamics for a Viscous Fluid Referred to an Axisymmetric System of Orthogonal Curvilinear Coordinates without Twist of Axes

Referring to the axisymmetric system of orthogonal curvilinear coordinates as shown in Fig. C1, fundamental equations suitable for the analysis of a flow along the axis are obtained by taking

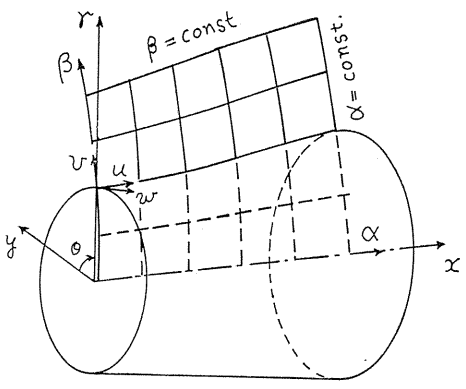

Fig. C1. Orthogonal curvilinear coordinates with axial symmetry.

$$\gamma=\theta \qquad h_\gamma=r, \tag{C1}$$

where r is the radial distance from the axis.

1. Fundamental relation of coordinates

1. 1. Condition of orthogonality

$$\frac{\partial}{\partial\alpha}\left(\frac{1}{h_\alpha}\frac{\partial h_\beta}{\partial\alpha}\right)+\frac{\partial}{\partial\beta}\left(\frac{1}{h_\beta}\frac{\partial h_\alpha}{\partial\beta}\right)=0. \tag{C2}$$

Other components of Gauss' condition are automatically satisfied.

1. 2. Differentials of vector

$$\begin{aligned}
&\frac{\partial u}{\partial x}=\frac{1}{h_\alpha}\frac{\partial u}{\partial\alpha}+\frac{v}{h_\alpha h_\beta}\frac{\partial h_\alpha}{\partial\beta}, \quad \frac{\partial u}{\partial y}=\frac{1}{h_\beta}\frac{\partial u}{\partial\beta}-\frac{v}{h_\alpha h_\beta}\frac{\partial h_\beta}{\partial\alpha},\\
&\frac{\partial u}{\partial z}=\frac{1}{r}\frac{\partial u}{\partial\theta}-\frac{w}{rh_\alpha}\frac{\partial r}{\partial\alpha} \;;\; \frac{\partial v}{\partial y}=\frac{1}{h_\beta}\frac{\partial v}{\partial\beta}+\frac{v}{h_\alpha h_\beta}\frac{\partial h_\beta}{\partial\alpha},\\
&\frac{\partial v}{\partial z}=\frac{1}{r}\frac{\partial v}{\partial\theta}-\frac{w}{rh_\beta}\frac{\partial r}{\partial\beta}, \quad \frac{\partial v}{\partial x}=\frac{1}{h_\alpha}\frac{\partial v}{\partial\alpha}-\frac{u}{h_\alpha h_\beta}\frac{\partial h_\alpha}{\partial\beta} \;;\\
&\frac{\partial w}{\partial z}=\frac{1}{r}\frac{\partial w}{\partial\theta}+\frac{u}{rh_\alpha}\frac{\partial r}{\partial\alpha}+\frac{v}{rh_\beta}\frac{\partial r}{\partial\beta}, \quad \frac{\partial w}{\partial x}=\frac{1}{h_\alpha}\frac{\partial w}{\partial\alpha}, \quad \frac{\partial w}{\partial y}=\frac{1}{h_\beta}\frac{\partial w}{\partial\beta}.
\end{aligned} \tag{C3}$$

1. 3. The Euler derivative

The Euler derivatives of a vector $A(A_\alpha,A_\beta,A_\theta)$ are given by

$$\begin{aligned}
\frac{DA_\alpha}{Dt}=&\frac{\partial A_\alpha}{\partial t}+\frac{u}{h_\alpha}\frac{\partial A_\alpha}{\partial\alpha}+\frac{v}{h_\beta}\frac{\partial A_\alpha}{\partial\beta}+\frac{w}{r}\frac{\partial A_\alpha}{\partial\theta}\\
&-A_\beta\left(\frac{v}{h_\alpha h_\beta}\frac{\partial h_\beta}{\partial\alpha}-\frac{u}{h_\alpha h_\beta}\frac{\partial h_\alpha}{\partial\beta}+A_\gamma\left(-\frac{w}{rh_\alpha}\frac{\partial r}{\partial\alpha}\right),\right.\\
\frac{DA_\beta}{Dt}=&\frac{\partial A_\beta}{\partial t}+\frac{u}{h_\alpha}\frac{\partial A_\beta}{\partial\alpha}+\frac{v}{h_\beta}\frac{\partial A_\beta}{\partial\beta}+\frac{w}{r}\frac{\partial A_\beta}{\partial\theta}\\
&-A_\theta\left(\frac{w}{rh_\beta}\frac{\partial r}{\partial\beta}\right)+A_\alpha\left(\frac{v}{h_\alpha h_\beta}\frac{\partial h_\beta}{\partial\alpha}-\frac{u}{h_\alpha h_\beta}\frac{\partial h_\alpha}{\partial\beta}\right.,\\
\frac{DA_\theta}{Dt}=&\frac{\partial A_\theta}{\partial t}+\frac{u}{h_\alpha}\frac{\partial A_\theta}{\partial\alpha}+\frac{v}{h_\beta}\frac{\partial A_\theta}{\partial\beta}+\frac{w}{r}\frac{\partial A_\theta}{\partial\theta}\\
&-A_\alpha\left(-\frac{w}{rh_\alpha}\frac{\partial r}{\partial\alpha}\right)+A_\theta\left(\frac{w}{rh_\beta}\frac{\partial r}{\partial\beta}\right).
\end{aligned} \tag{C4}$$

The Euler derivative of a scalar ρ is simply

$$\frac{D\rho}{Dt}=\frac{\partial\rho}{\partial t}+\frac{u}{h_\alpha}\frac{\partial\rho}{\partial\alpha}+\frac{v}{h_\beta}\frac{\partial\rho}{\partial\beta}+\frac{w}{r}\frac{\partial\rho}{\partial\theta}. \tag{C5}$$

2. Fundamental relations on the infinitesimal fluid element

2. 1. The strain of a fluid element

$$e_{\alpha\alpha}=\frac{1}{h_\alpha}\frac{\partial u}{\partial\alpha}+\frac{v}{h_\alpha h_\beta}\frac{\partial h_\alpha}{\partial\beta},\quad e_{\beta\beta}=\frac{1}{h_\beta}\frac{\partial v}{\partial\beta}+\frac{u}{h_\alpha h_\beta}\frac{\partial h_\beta}{\partial\alpha},$$

$$e_{\theta\theta}=\frac{1}{r}\frac{\partial w}{\partial\theta}+\frac{u}{rh_\alpha}\frac{\partial r}{\partial\alpha}+\frac{v}{rh_\beta}\frac{\partial r}{\partial\beta};$$

$$e_{\beta\theta}=\frac{r}{h_\beta}\frac{\partial}{\partial\beta}\left(\frac{w}{r}\right)+\frac{1}{r}\frac{\partial v}{\partial\theta},\quad e_{\theta\alpha}=\frac{1}{r}\frac{\partial u}{\partial\theta}+\frac{r}{h_\alpha}\frac{\partial}{\partial\alpha}\left(\frac{w}{r}\right),\tag{C6}$$

$$e_{\alpha\beta}=\frac{h_\beta}{h_\alpha}\frac{\partial}{\partial\alpha}\left(\frac{v}{h_\beta}\right)+\frac{h_\alpha}{h_\beta}\frac{\partial}{\partial\beta}\left(\frac{u}{h_\alpha}\right).$$

The rate of expansion of fluid volume is

$$\text{div } V=\frac{1}{h_\alpha h_\beta r}\left[\frac{\partial(urh_\beta)}{\partial\alpha}+\frac{\partial(vrh_\alpha)}{\partial\beta}+h_\alpha h_\beta\frac{\partial w}{\partial\theta}\right].\tag{C7}$$

The α, β and θ components of vorticity are

$$\xi=\frac{1}{h_\beta r}\frac{\partial(wr)}{\partial\beta}-\frac{1}{r}\frac{\partial v}{\partial\theta},\quad \eta=\frac{1}{r}\frac{\partial u}{\partial\theta}-\frac{1}{h_\alpha r}\frac{\partial(wr)}{\partial\alpha},$$

$$\zeta=\frac{1}{h_\alpha h_\beta}\left[\frac{\partial(vh_\beta)}{\partial\alpha}-\frac{\partial(uh_\alpha)}{\partial\beta}\right],\tag{C8}$$

where $div\,\zeta=0$ are automatically satisfied.

2. 2. The relation between stress and strain

The Stokes law reduces to

$$\begin{aligned}
&\sigma_{\alpha\alpha}=-p+\tau_{\alpha\alpha},\quad \sigma_{\beta\beta}=-p+\tau_{\beta\beta},\quad \sigma_{\theta\theta}=-p+\tau_{\theta\theta};\\
&\tau_{\alpha\alpha}=\lambda\,\text{div}\,V+2\mu e_{\alpha\alpha},\quad \tau_{\beta\theta}=\mu e_{\beta\theta}=\mu e_{\theta\beta}=\tau_{\theta\beta},\\
&\tau_{\beta\beta}=\lambda\,\text{div}\,V+2\mu e_{\beta\beta},\quad \tau_{\theta\alpha}=\mu e_{\theta\alpha}=\mu e_{\alpha\theta}=\tau_{\alpha\theta},\\
&\tau_{\theta\theta}=\lambda\,\text{div}\,V+2\mu e_{\theta\theta},\quad \tau_{\alpha\beta}=\mu e_{\alpha\beta}=\mu e_{\beta\alpha}=\tau_{\beta\alpha}.
\end{aligned}\tag{C9}$$

2. 3. Dissipation function

$$\Phi=\tau_{\alpha\alpha}e_{\alpha\alpha}+\tau_{\beta\beta}e_{\beta\beta}+\tau_{\theta\theta}e_{\theta\theta}+\tau_{\alpha\beta}e_{\alpha\beta}+\tau_{\beta\theta}e_{\beta\theta}+\tau_{\theta\alpha}e_{\theta\alpha}.\tag{C10}$$

3. Fundamental equations for the flow of a viscous fluid

3. 1. Equation of state

The equation of state for a perfect gas is given by

$$p/\rho=RT,\tag{C11}$$

and that for an incompressible fluid is

$$\rho=\text{constant.} \tag{C 12}$$

3. 2. Equation of continuity

$$D\rho/Dt+\rho\,\mathrm{div}\,\boldsymbol{V}=0, \tag{C 13}$$

gives

$$\frac{\partial\rho}{\partial t}+\frac{1}{h_\alpha h_\beta r}\left[\frac{\partial(\rho u r h_\beta)}{\partial\alpha}+\frac{\partial(\rho v r h_\alpha)}{\partial\beta}+h_\alpha h_\beta\frac{\partial(\rho w)}{\partial\theta}\right]=0. \tag{C 14}$$

3. 3. Equations of motion

$$\begin{aligned}
&\frac{\partial u}{\partial t}+\frac{u}{h_\alpha}\frac{\partial u}{\partial\alpha}+\frac{v}{h_\beta}\frac{\partial u}{\partial\beta}+\frac{w}{r}\frac{\partial u}{\partial\theta}\\
&\quad-v\left(\frac{v}{h_\alpha h_\beta}\frac{\partial h_\beta}{\partial\alpha}-\frac{u}{h_\alpha h_\beta}\frac{\partial h_\alpha}{\partial\beta}\right)+w\left(-\frac{w}{r h_\alpha}\frac{\partial r}{\partial\alpha}\right)\\
&=X-\frac{1}{\rho}\frac{1}{h_\alpha}\frac{\partial p}{\partial\alpha}+\frac{1}{\rho}\frac{1}{h_\alpha h_\beta r}\left[\frac{\partial(\tau_{\alpha\alpha}r h_\beta)}{\partial\alpha}+\tau_{\alpha\beta}r\frac{\partial h_\alpha}{\partial\beta}\right.\\
&\quad\left.+\frac{\partial(\tau_{\beta\alpha}r h_\alpha)}{\partial\beta}-\tau_{\beta\beta}r\frac{\partial h_\beta}{\partial\alpha}+\frac{\partial(\tau_{\theta\alpha}h_\alpha h_\beta)}{\partial\theta}-\tau_{\theta\theta}h_\beta\frac{\partial r}{\partial\alpha}\right],\\
&\frac{\partial v}{\partial t}+\frac{u}{h_\alpha}\frac{\partial v}{\partial\alpha}+\frac{v}{h_\beta}\frac{\partial v}{\partial\beta}+\frac{w}{r}\frac{\partial v}{\partial\theta}\\
&\quad-w\left(\frac{w}{r h_\beta}\frac{\partial r}{\partial\beta}\right)+u\left(\frac{v}{h_\alpha h_\beta}\frac{\partial h_\beta}{\partial\alpha}-\frac{u}{h_\alpha h_\beta}\frac{\partial h_\alpha}{\partial\beta}\right)\\
&=Y-\frac{1}{\rho}\frac{1}{h_\beta}\frac{\partial p}{\partial\beta}+\frac{1}{\rho}\frac{1}{h_\alpha h_\beta r}\left[\frac{\partial(\tau_{\alpha\beta}h_\beta r)}{\partial\alpha}-\tau_{\alpha\alpha}r\frac{\partial h_\alpha}{\partial\beta}\right.\\
&\quad\left.+\frac{\partial(\tau_{\beta\beta}r h_\alpha)}{\partial\beta}+\tau_{\beta\alpha}r\frac{\partial h_\beta}{\partial\alpha}+\frac{\partial(\tau_{\theta\beta}h_\alpha h_\beta)}{\partial\theta}-\tau_{\theta\theta}h_\alpha\frac{\partial r}{\partial\beta}\right],\\
&\frac{\partial w}{\partial t}+\frac{u}{h_\alpha}\frac{\partial w}{\partial\alpha}+\frac{v}{h_\beta}\frac{\partial w}{\partial\beta}+\frac{w}{r}\frac{\partial w}{\partial\theta}+u\frac{w}{r h_\alpha}\frac{\partial r}{\partial\alpha}+v\frac{w}{r h_\beta}\frac{\partial r}{\partial\beta}\\
&\quad=Z-\frac{1}{\rho}\frac{1}{r}\frac{\partial p}{\partial\theta}+\frac{1}{\rho}\frac{1}{h_\alpha h_\beta r}\left[\frac{\partial(\tau_{\alpha\theta}h_\beta r)}{\partial\alpha}+\frac{\partial(\tau_{\beta\beta}r h_\alpha)}{\partial\beta}\right.\\
&\quad\left.+h_\alpha h_\beta\frac{\partial\tau_{\theta\theta}}{\partial\theta}+\tau_{\theta\alpha}h_\beta\frac{\partial r}{\partial\alpha}+\tau_{\theta\beta}h_\alpha\frac{\partial r}{\partial\beta}\right].
\end{aligned} \tag{C 15}$$

The transfer equation of kinetic energy is

$$\frac{D}{Dt}\left(\frac{u^2+v^2+w^2}{2}\right)=(Xu+Yv+Zw)$$

$$-\frac{1}{\rho}\left(\frac{u}{h_\alpha}\frac{\partial p}{\partial\alpha}+\frac{v}{h_\beta}\frac{\partial p}{\partial\beta}+\frac{w}{r}\frac{\partial p}{\partial\theta}\right)+\frac{1}{\rho}\Psi, \qquad (C16)$$

where Ψ represents the work done by adjacent fluid for the translational motion of the concerning fluid element. It is reduced from

$$\Psi=\left(\frac{\partial\tau_{\alpha\alpha}}{\partial x}+\frac{\partial\tau_{\beta\alpha}}{\partial y}+\frac{\partial\tau_{\theta\alpha}}{\partial z}\right)u+\left(\frac{\partial\tau_{\alpha\beta}}{\partial x}+\frac{\partial\tau_{\beta\beta}}{\partial y}+\frac{\partial\tau_{\theta\beta}}{\partial z}\right)v$$

$$+\left(\frac{\partial\tau_{\alpha\theta}}{\partial x}+\frac{\partial\tau_{\beta\theta}}{\partial y}+\frac{\partial\tau_{\theta\theta}}{\partial z}\right)w. \qquad (C17)$$

3. 4. Energy equation

The first law of thermodynamics is expressed by

$$\frac{De}{Dt}+p\frac{D}{Dt}\left(\frac{1}{\rho}\right)=\frac{1}{\rho}(H+\Phi), \qquad (C18)$$

where

$$H=\frac{1}{h_\alpha h_\beta r}\left[\frac{\partial}{\partial\alpha}\left(k\frac{h_\beta r}{h_\alpha}\frac{\partial T}{\partial\alpha}\right)+\frac{\partial}{\partial\beta}\left(k\frac{h_\alpha r}{h_\beta}\frac{\partial T}{\partial\beta}\right)+\frac{\partial}{\partial\theta}\left(k\frac{h_\alpha h_\beta}{r}\frac{\partial T}{\partial\theta}\right)\right]. \qquad (C19)$$

There transfer equation of total energy defined by $E=(1/2)(u^2+v^2+w^2)+e+(p/\rho)+\Omega$ is given by addition of Eqs. (C16) and (C18).

$$\frac{DE}{Dt}=\frac{\partial\Omega}{\partial t}+\frac{1}{\rho}\frac{\partial p}{\partial t}+\frac{1}{\rho}[H+\Phi+\Psi], \qquad (C20)$$

where $\Phi+\Psi$ represents the rate of total work done by adjacent fluid.

Appendix D

Fundamental Relations of Fluid Dynamics for a Viscous Fluid Referred to the Cylindrical Coordinates

Fundamental relations referred to the cyrindrical coordinates shown in Fig. D1 are obtained by taking

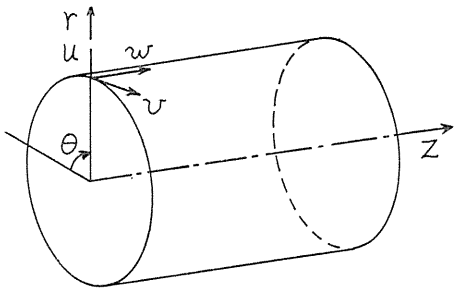

Fig. D1. Velocity components in cylindrical coordinates.

$$\alpha=r,\quad \beta=\theta,\quad \gamma=Z;\quad h_\alpha=1,\quad h_\beta=r,\quad h_\gamma=1. \tag{D1}$$

Denoting r, θ and z components of velocity by u, v and w, respectively, formulae are shown in order in the followings.

1. Fundamental relations of coordinates

1. 1. Conditions of orthogonality

The Gauss' condition is automatically satisfied.

1. 2. Differentials of vector

$$\begin{gathered}\frac{\partial u}{\partial x}=\frac{\partial u}{\partial r},\quad \frac{\partial u}{\partial y}=\frac{1}{r}\frac{\partial u}{\partial \theta}-\frac{v}{r},\quad \frac{\partial u}{\partial z}=\frac{\partial u}{\partial z};\\ \frac{\partial v}{\partial y}=\frac{1}{r}\frac{\partial v}{\partial \theta}+\frac{u}{r},\quad \frac{\partial v}{\partial z}=\frac{\partial v}{\partial z},\quad \frac{\partial v}{\partial x}=\frac{\partial v}{\partial r};\\ \frac{\partial w}{\partial z}=\frac{\partial w}{\partial z},\quad \frac{\partial w}{\partial x}=\frac{\partial w}{\partial r},\quad \frac{\partial w}{\partial y}=\frac{1}{r}\frac{\partial w}{\partial \theta}.\end{gathered} \tag{D2}$$

1. 3. The Euler derivative

The Euler derivative of a vector $\boldsymbol{A}(A_r, A_\theta, A_z)$ are given by

$$\begin{aligned}\frac{DA_r}{Dt}&=\frac{\partial A_r}{\partial t}+u\frac{\partial A_r}{\partial r}+\frac{v}{r}\frac{\partial A_r}{\partial \theta}+w\frac{\partial A_r}{\partial z}-A_\theta\frac{v}{r},\\ \frac{DA_\theta}{Dt}&=\frac{\partial A_\theta}{\partial t}+u\frac{\partial A_\theta}{\partial r}+\frac{v}{r}\frac{\partial A_\theta}{\partial \theta}+w\frac{\partial A_\theta}{\partial z}+A_r\frac{v}{r},\\ \frac{DA_z}{Dt}&=\frac{\partial A_z}{\partial t}+u\frac{\partial A_z}{\partial r}+\frac{v}{r}\frac{\partial A_z}{\partial \theta}+w\frac{\partial A_z}{\partial z}.\end{aligned} \tag{D3}$$

The operator of Euler derivative of a scaler is

$$\frac{D}{Dt}=\frac{\partial}{\partial t}+u\frac{\partial}{\partial r}+\frac{v}{r}\frac{\partial}{\partial \theta}+w\frac{\partial}{\partial z}. \tag{D4}$$

2. Fundamental relations on the infinitesimal fluid element

2. 1. The strain of fluid element

$$\begin{gathered}e_{rr}=\frac{\partial u}{\partial r},\quad e_{\theta\theta}=\frac{1}{r}\frac{\partial v}{\partial \theta}+\frac{u}{r},\quad e_{zz}=\frac{\partial w}{\partial z};\\ e_{\theta z}=\frac{1}{r}\frac{\partial w}{\partial \theta}+\frac{\partial v}{\partial z},\quad e_{zr}=\frac{\partial u}{\partial z}+\frac{\partial w}{\partial r},\quad e_{r\theta}=r\frac{\partial}{\partial r}\left(\frac{v}{r}\right)+\frac{1}{r}\frac{\partial u}{\partial \theta}.\end{gathered} \tag{D5}$$

The rate of expansion of fluid volume is

$$\operatorname{div}\boldsymbol{V}=\frac{1}{r}\frac{\partial(ur)}{\partial r}+\frac{1}{r}\frac{\partial v}{\partial \theta}+\frac{\partial w}{\partial z}. \tag{D6}$$

The r, θ and z components of vorticity are

$$\xi=\frac{1}{r}\frac{\partial w}{\partial\theta}-\frac{\partial v}{\partial z},\quad \eta=\frac{\partial u}{\partial z}-\frac{\partial w}{\partial r},\quad \zeta=\frac{1}{r}\frac{\partial(vr)}{\partial r}-\frac{1}{r}\frac{\partial u}{\partial\theta}. \tag{D7}$$

2. 2. The relation between stress and strain

The Stokes law reduces to

$$\begin{aligned}
&\sigma_{rr}=-p+\tau_{rr},\quad \sigma_{\theta\theta}=-p+\tau_{\theta\theta},\quad \sigma_{zz}=-p+\tau_{zz};\\
&\tau_{rr}=\lambda\ \mathrm{div}\ \boldsymbol{V}+2\mu e_{rr},\quad \tau_{\theta z}=\mu e_{\theta z}=\mu e_{z\theta}=\tau_{z\theta},\\
&\tau_{\theta\theta}=\lambda\ \mathrm{div}\ \boldsymbol{V}+2\mu e_{\theta\theta},\quad \tau_{zr}=\mu e_{zr}=\mu e_{rz}=\tau_{rz},\\
&\tau_{zz}=\lambda\ \mathrm{div}\ \boldsymbol{V}+2\mu e_{zz},\quad \tau_{r\theta}=\mu e_{r\theta}=\mu e_{\theta r}=\tau_{\theta r}.
\end{aligned} \tag{D8}$$

2. 3. Dissipation function

$$\begin{aligned}
\Phi&=\tau_{rr}e_{rr}+\tau_{\theta\theta}e_{\theta\theta}+\tau_{zz}e_{zz}+\tau_{r\theta}e_{r\theta}+\tau_{\theta z}e_{\theta z}+\tau_{zr}e_{zr}\\
&=\lambda\ \mathrm{div}^2\ \boldsymbol{V}+\mu(2e_{rr}^2+2e_{\theta\theta}^2+2e_{zz}^2+e_{r\theta}^2+e_{\theta z}^2+e_{zr}^2).
\end{aligned} \tag{D9}$$

3. Fundamental equations for the flow of a viscous fluid

3. 1. Equation of state

$$p/\rho=RT \qquad \text{(for a perfect gas)}, \tag{D10}$$

$$\rho=\text{constant} \quad \text{(for an incompressible fluid)}. \tag{D11}$$

3. 2. Equation of continuity

$$D\rho/Dt+\rho\ \mathrm{div}\ \boldsymbol{V}=0, \tag{D12}$$

gives

$$\frac{\partial\rho}{\partial t}+\frac{1}{r}\frac{\partial(\rho ur)}{\partial r}+\frac{1}{r}\frac{\partial(\rho v)}{\partial\theta}+\frac{\partial(\rho w)}{\partial z}=0. \tag{D13}$$

3. 3. Equations of motion

$$\begin{aligned}
\frac{Du}{Dt}&=X-\frac{1}{\rho}\frac{\partial p}{\partial r}+\frac{1}{\rho}\left[\frac{1}{r}\frac{\partial(\tau_{rr}r)}{\partial r}+\frac{1}{r}\frac{\partial\tau_{\theta r}}{\partial\theta}-\frac{1}{r}\tau_{\theta\theta}+\frac{\partial\tau_{zr}}{\partial z}\right],\\
\frac{Dv}{Dt}&=Y-\frac{1}{\rho}\frac{1}{r}\frac{\partial p}{\partial\theta}+\frac{1}{\rho}\left[\frac{1}{r}\frac{\partial(\tau_{r\theta}r)}{\partial r}+\frac{1}{r}\frac{\partial\tau_{\theta\theta}}{\partial\theta}+\frac{1}{r}\tau_{\theta r}+\frac{\partial\tau_{z\theta}}{\partial z}\right],\\
\frac{Dw}{Dt}&=Z-\frac{1}{\rho}\frac{\partial p}{\partial z}+\frac{1}{\rho}\left[\frac{1}{r}\frac{\partial(\tau_{rz}r)}{\partial r}+\frac{1}{r}\frac{\partial\tau_{\theta z}}{\partial\theta}+\frac{\partial\tau_{zz}}{\partial z}\right].
\end{aligned} \tag{D14}$$

Substitution of Eqs. (D8) and (D5) gives

$$\frac{\partial u}{\partial t}+u\frac{\partial u}{\partial r}+\frac{v}{r}\frac{\partial u}{\partial\theta}+w\frac{\partial u}{\partial z}-\frac{v^2}{r}$$

$$=X-\frac{1}{\rho}\frac{\partial p}{\partial r}+\frac{1}{\rho}\left\{\frac{1}{r}\frac{\partial}{\partial r}\left[\lambda r\ \mathrm{div}\ \boldsymbol{V}+2\mu r\frac{\partial u}{\partial r}\right]\right.$$

$$\left.+\frac{1}{r}\frac{\partial}{\partial\theta}\left[\mu\left(r\frac{\partial(v/r)}{\partial r}+\frac{1}{r}\frac{\partial u}{\partial\theta}\right]\right)\right.$$

$$\left.-\frac{1}{r}\left[\lambda\ \mathrm{div}\ \boldsymbol{V}+2\mu\left(\frac{1}{r}\frac{\partial v}{\partial\theta}+\frac{u}{r}\right]\right)+\frac{\partial}{\partial z}\left[\mu\left(\frac{\partial u}{\partial z}+\frac{\partial w}{\partial r}\right)\right]\right\},$$

$$\frac{\partial v}{\partial t}+u\frac{\partial v}{\partial r}+\frac{v}{r}\frac{\partial v}{\partial\theta}+w\frac{\partial v}{\partial z}+\frac{uv}{r}$$

$$=Y-\frac{1}{\rho}\frac{1}{r}\frac{\partial p}{\partial\theta}+\frac{1}{\rho}\left\{\frac{1}{r}\frac{\partial}{\partial r}\left[\mu r\left(r\frac{\partial(v/r)}{\partial r}+\frac{1}{r}\frac{\partial u}{\partial\theta}\right)\right]\right.$$

$$\left.+\frac{1}{r}\frac{\partial}{\partial\theta}\left[\lambda\ \mathrm{div}\ \boldsymbol{V}+2\mu\left(\frac{1}{r}\frac{\partial v}{\partial\theta}+\frac{u}{r}\right)\right]\right. \tag{D15}$$

$$\left.+\frac{1}{r}\left[\mu\left(r\frac{\partial(v/r)}{\partial r}+\frac{1}{r}\frac{\partial u}{\partial\theta}\right)\right]+\frac{\partial}{\partial z}\left[\mu\left(\frac{1}{r}\frac{\partial w}{\partial\theta}+\frac{\partial v}{\partial z}\right)\right]\right\},$$

$$\frac{\partial w}{\partial t}+u\frac{\partial w}{\partial r}+\frac{v}{r}\frac{\partial w}{\partial\theta}+w\frac{\partial w}{\partial z}$$

$$=Z-\frac{1}{\rho}\frac{\partial p}{\partial z}+\frac{1}{\rho}\left\{\frac{1}{r}\frac{\partial}{\partial r}\left[\mu r\left(\frac{\partial u}{\partial z}+\frac{\partial w}{\partial r}\right)\right.\right.$$

$$\left.\left.+\frac{1}{r}\frac{\partial}{\partial\theta}\left[\mu\left(\frac{1}{r}\frac{\partial w}{\partial\theta}+\frac{\partial v}{\partial z}\right)\right]+\frac{\partial}{\partial z}\left[\lambda\ \mathrm{div}\ \boldsymbol{V}+2\mu\frac{\partial w}{\partial z}\right]\right]\right\}.$$

The tranfer equation of kinetic energy is

$$\frac{D}{Dt}\left(\frac{u^2+v^2+w^2}{2}\right)=(Xu+Yv+Zw)$$

$$-\frac{1}{\rho}\left(u\frac{\partial p}{\partial r}+\frac{v}{r}\frac{\partial p}{\partial\theta}+w\frac{\partial p}{\partial z}\right)+\frac{1}{\rho}\Psi, \tag{D16}$$

where Ψ represents the work done by adjacent fluid for the translational motion of the concerning fluid element.

3. 4. Energy equation

The first law of thermodynamics is expressed by

$$\frac{De}{Dt}+p\frac{D}{Dt}\left(\frac{1}{\rho}\right)=\frac{1}{\rho}(H+\Phi), \tag{D17}$$

where

$$H=\frac{1}{r}\frac{\partial}{\partial r}\left(kr\frac{\partial T}{\partial r}\right)+\frac{1}{r}\frac{\partial}{\partial\theta}\left(\frac{k}{r}\frac{\partial T}{\partial\theta}\right)+\frac{\partial}{\partial z}\left(k\frac{\partial T}{\partial z}\right). \tag{D18}$$

The transfer equation of total energy is given by addition of Eqs. (D16) and (D18).

$$\frac{DE}{Dt}=\frac{\partial \Omega}{\partial t}+\frac{1}{\rho}\frac{\partial p}{\partial t}+\frac{1}{\rho}[H+\Phi+\Psi], \tag{D19}$$

where

$$\begin{aligned}\Phi+\Psi=&\frac{1}{r}\frac{\partial(ur\tau_{rr})}{\partial r}+\frac{1}{r}\frac{\partial(u\tau_{\theta r})}{\partial\theta}+\frac{\partial(u\tau_{zr})}{\partial z}\\&+\frac{1}{r}\frac{\partial(vr\tau_{r\theta})}{\partial r}+\frac{1}{r}\frac{\partial(v\tau_{\theta\theta})}{\partial\theta}+\frac{\partial(v\tau_{z\theta})}{\partial z}\\&+\frac{1}{r}\frac{\partial(wr\tau_{rz})}{\partial r}+\frac{1}{r}\frac{\partial(w\tau_{\theta z})}{\partial\theta}+\frac{\partial(w\tau_{zz})}{\partial z},\end{aligned} \tag{D20}$$

represents the rate of total work done by adjacent fluid.

Appendix E

Fundamental Relations of Fluid Dynamics Referred to Orthogonal Curvilinear Coordinates Consisting of a Reference Surface and Normal Straight Lines

A Coordinate system, which consists of the orthogonal curvilinear coordinates α, γ on a reference surface and of straight lines $n(=\beta)$ normal to $\alpha\gamma$-surface as shown in Fig. E1, is conveniently used for the three-dimensional boundary layer flows. Denoting the curvature of α axis in $\alpha\beta$-surface by $K_\alpha=1/R_\alpha$ and that of γ axis in $\beta\gamma$-surface by $K_\gamma=1/R_\gamma$, we have

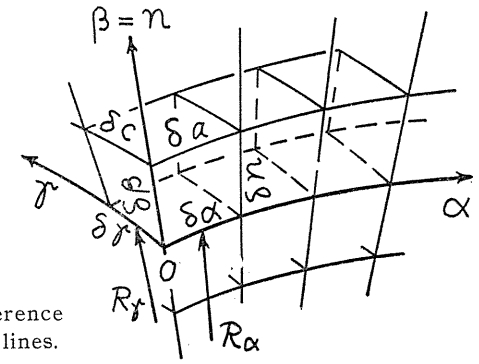

Fig. E1. Coordinates consist of a reference surface and normal straight lines.

$$\begin{aligned}h_\alpha&=\partial a/\partial\alpha=(R_\alpha+n)/R_\alpha=1+K_\alpha n,\quad h_\beta=1,\\h_\gamma&=\partial c/\partial\gamma=(R_\gamma+n)/R_\gamma=1+K_\gamma n,\end{aligned} \tag{E1}$$

where K_α and K_γ are functions of α and γ.

Coordinate surfaces normal to $n(=\beta)$ are parallel to the reference $\alpha\gamma$.

1. Fundamental relation of coordinates

1. 1. Condition of orthogonality

$$\frac{\partial}{\partial\gamma}\left(\frac{1}{1+K_\gamma n}\frac{\partial K_\alpha}{\partial\gamma}\right)+\frac{\partial}{\partial\alpha}\left(\frac{1}{1+K_\alpha n}\frac{\partial K_\gamma}{\partial\alpha}\right)=0. \tag{E2}$$

Other components of Gauss' condition are automatically satisfied. In the case of two-dimensional flow, where $K_\tau=0$ and $\partial/\partial\gamma=0$, Eq. (E2) is automatically satisfied.

1. 2. Differentials of vector

$$\frac{\partial u}{\partial x}=\frac{1}{1+K_\alpha n}\frac{\partial u}{\partial\alpha}+\frac{K_\alpha}{1+K_\alpha n}v+\frac{(\partial K_\alpha/\partial\gamma)n}{(1+K_\tau n)(1+K_\alpha n)}w,\quad \frac{\partial u}{\partial y}=\frac{\partial u}{\partial n},$$

$$\frac{\partial u}{\partial z}=\frac{1}{1+K_\tau n}\frac{\partial u}{\partial\gamma}-\frac{(\partial K_\tau/\partial\alpha)n}{(1+K_\tau n)(1+K_\alpha n)}w;\quad \frac{\partial v}{\partial y}=\frac{\partial v}{\partial n},$$

$$\frac{\partial v}{\partial z}=\frac{1}{1+K_\tau n}\frac{\partial v}{\partial\gamma}-\frac{K_\tau}{1+K_\tau n}w,\quad \frac{\partial v}{\partial x}=\frac{1}{1+K_\alpha n}\frac{\partial v}{\partial\alpha}-\frac{K_\alpha}{1+K_\alpha n}u;\qquad (E3)$$

$$\frac{\partial w}{\partial z}=\frac{1}{1+K_\tau n}\frac{\partial w}{\partial\gamma}+\frac{(\partial K_\tau/\partial\alpha)n}{(1+K_\tau n)(1+K_\alpha n)}u+\frac{K_\tau}{1+K_\tau n}v,$$

$$\frac{\partial w}{\partial x}=\frac{1}{1+K_\tau n}\frac{\partial w}{\partial\alpha}-\frac{(\partial K_\alpha/\partial\gamma)n}{(1+K_\tau n)(1+K_\alpha n)}u,\quad \frac{\partial w}{\partial y}=\frac{\partial w}{\partial n}.$$

1. 3. The Euler derivative

The Euler derivative of a vector A (A_α, A_n, A_τ) are given by

$$\frac{DA_\alpha}{Dt}=\frac{\partial A_\alpha}{\partial t}+\frac{u}{1+K_\alpha n}\frac{\partial A_\alpha}{\partial\alpha}+v\frac{\partial A_\alpha}{\partial n}+\frac{w}{1+K_\tau n}\frac{\partial A_\alpha}{\partial\gamma}$$

$$-A_n\left[-\frac{K_\alpha}{1+K_\alpha n}u\right]+A_\tau\frac{1}{(1+K_\tau n)(1+K_\alpha n)}\left]\frac{\partial K_\alpha}{\partial\gamma}nu-\frac{\partial K_\tau}{\partial\alpha}nw\right],$$

$$\frac{DA_n}{Dt}=\frac{\partial A_n}{\partial t}+\frac{u}{1+K_\alpha n}\frac{\partial A_n}{\partial\alpha}+v\frac{\partial A_n}{\partial n}+\frac{w}{1+K_\tau n}\frac{\partial A_n}{\partial\gamma}$$

$$-A_\tau\left[\frac{K_\tau}{1+K_\tau n}w\right]+A_\alpha\left[-\frac{K_\alpha}{1+K_\alpha n}u\right],\qquad (E4)$$

$$\frac{DA_\tau}{Dt}=\frac{\partial A_\tau}{\partial t}+\frac{u}{1+K_\alpha n}\frac{\partial A_\tau}{\partial\alpha}+v\frac{\partial A_\tau}{\partial n}+\frac{w}{1+K_\tau n}\frac{\partial A_\tau}{\partial\gamma}$$

$$-A_\alpha\frac{1}{(1+K_\tau n)(1+K_\alpha n)}\left[\frac{\partial K_\alpha}{\partial\gamma}nu-\frac{\partial K_\tau}{\partial\alpha}nw\right]+A_n\left[\frac{K_\tau}{1+K_\tau n}w\right].$$

The Euler derivative of a scalar ρ is

$$\frac{D\rho}{Dt}=\frac{\partial\rho}{\partial t}+\frac{u}{1+K_\alpha n}\frac{\partial\rho}{\partial\alpha}+v\frac{\partial\rho}{\partial n}+\frac{w}{1+K_\tau n}\frac{\partial\rho}{\partial\gamma}.\qquad (E5)$$

2. Fundamental relations on the infinitesimal fluid element

2. 1. The strain of a fluid element

$$e_{\alpha\alpha}=\frac{1}{1+K_\alpha n}\frac{\partial u}{\partial\alpha}+\frac{K_\alpha}{1+K_\alpha n}v+\frac{(\partial K_\alpha/\partial\gamma)n}{(1+K_\tau n)(1+K_\alpha n)}w,$$

$$e_{nn}=\partial v/\partial n,$$

$$e_{\gamma\gamma}=\frac{1}{1+K_\gamma n}\frac{\partial w}{\partial\gamma}+\frac{(\partial K_\gamma/\partial\alpha)n}{(1+K_\gamma n)(1+K_\alpha n)}u+\frac{K_\gamma}{1+K_\gamma n}v;$$

$$e_{n\gamma}=(1+K_\gamma n)\frac{\partial}{\partial n}\left(\frac{w}{1+K_\gamma n}\right)+\frac{1}{1+K_\gamma n}\frac{\partial v}{\partial\gamma}=e_{\gamma n}, \tag{E6}$$

$$e_{\gamma\alpha}=\frac{1+K_\alpha n}{1+K_\gamma n}\frac{\partial}{\partial\gamma}\left(\frac{u}{1+K_\alpha n}\right)+\frac{1+K_\gamma n}{1+K_\alpha n}\frac{\partial}{\partial\alpha}\left(\frac{w}{1+K_\gamma n}\right)=e_{\alpha\gamma},$$

$$e_{\alpha n}=\frac{1}{1+K_\alpha n}\frac{\partial v}{\partial\alpha}+(1+K_\alpha n)\frac{\partial}{\partial n}\left(\frac{u}{1+K_\alpha n}\right)=e_{n\alpha}.$$

The rate of expansion of fluid element is

$$\text{div } V=\frac{1}{(1+K_\alpha n)(1+K_\gamma n)}\left\{\frac{\partial[u(1+K_\gamma n)]}{\partial\alpha}\right.$$

$$\left.+\frac{\partial[v(1+K_\gamma n)(1+K_\alpha n)]}{\partial n}+\frac{\partial[w(1+K_\alpha n)]}{\partial\gamma}\right\}. \tag{E7}$$

The α, n and γ components of vorticity are, respectively,

$$\xi=\frac{1}{1+K_\gamma n}\left\{\frac{\partial[w(1+K_\gamma n)]}{\partial n}-\frac{\partial v}{\partial\gamma}\right\},$$

$$\eta=\frac{1}{(1+K_\gamma n)(1+K_\alpha n)}\left\{\frac{\partial[u(1+K_\alpha n)]}{\partial\gamma}-\frac{\partial[w(1+K_\gamma n)]}{\partial\alpha}\right\}, \tag{E8}$$

$$\zeta=\frac{1}{1+K_\alpha n}\left\{\frac{\partial v}{\partial\alpha}-\frac{\partial[u(1+K_\alpha n)]}{\partial n}\right\}.$$

which satisfy $div\,V=0$ automatically.

2. 2. The relation between stress and strain

The Stokes' law reduces

$$\sigma_{\alpha\alpha}=-p+\tau_{\alpha\alpha},\quad \sigma_{nn}=-p+\tau_{nn},\quad \sigma_{\gamma\gamma}=-p+\tau_{\gamma\gamma};$$

$$\tau_{\alpha\alpha}=\lambda\,\text{div}\,V+2\mu e_{\alpha\alpha};\quad \tau_{n\gamma}=\mu e_{n\gamma}=\mu e_{\gamma n}=\tau_{\gamma n},$$

$$\tau_{nn}=\lambda\,\text{div}\,V+2\mu e_{nn};\quad \tau_{\gamma\alpha}=\mu e_{\gamma\alpha}=\mu e_{\alpha\gamma}=\tau_{\alpha\gamma}, \tag{E9}$$

$$\tau_{\gamma\gamma}=\lambda\,\text{div}\,V+2\mu e_{\gamma\gamma};\quad \tau_{\alpha n}=\mu e_{\alpha n}=\mu e_{n\alpha}=\tau_{n\alpha}.$$

2. 3. Dissipation

$$\Phi=\tau_{\alpha\alpha}e_{\alpha\alpha}+\tau_{nn}e_{nn}+\tau_{\gamma\gamma}e_{\gamma\gamma}+\tau_{\alpha n}e_{\alpha n}+\tau_{n\gamma}e_{n\gamma}+\tau_{\gamma\alpha}e_{\gamma\alpha}. \tag{E10}$$

3. Fundamental equations for the flow of a viscous fluid

3. 1. Equation of state

The equation of state for a perfect gas is

$$p/\rho=RT, \tag{E11}$$

and that for an incompressible fluid is

$$\rho=\text{constant}. \tag{E12}$$

3. 2. Equation on continuity

$$D\rho/Dt+\rho \operatorname{div} \boldsymbol{V}=0, \tag{E13}$$

gives

$$\frac{\partial\rho}{\partial t}+\frac{1}{(1+K_\alpha n)(1+K_\gamma n)}\left\{\frac{\partial[\rho u(1+K_\gamma n)]}{\partial\alpha}\right.$$

$$\left.+\frac{\partial[\rho v(1+K_\gamma n)(1+K_\alpha n)]}{\partial n}+\frac{\partial[\rho w(1+K_\alpha n)]}{\partial\gamma}\right\}=0. \tag{E14}$$

3. 3. Equations of motion

$$\frac{\partial u}{\partial t}+\frac{u}{1+K_\alpha n}\frac{\partial u}{\partial\alpha}+v\frac{\partial u}{\partial n}+\frac{w}{1+K_\gamma n}\frac{\partial u}{\partial\gamma}$$

$$-v\left[-\frac{K_\alpha}{1+K_\alpha n}u\right]+w\frac{1}{(1+K_\gamma n)(1+K_\alpha n)}\left[\frac{\partial K_\alpha}{\partial\gamma}nu-\frac{\partial K_\gamma}{\partial\alpha}nw\right]$$

$$=X-\frac{1}{\rho}\frac{1}{1+K_\alpha n}\frac{\partial p}{\partial\alpha}+\frac{1}{\rho}\frac{1}{(1+K_\alpha n)(1+K_\gamma n)}\left\{\frac{\partial[\tau_{\alpha\alpha}(1+K_\gamma n)]}{\partial\alpha}\right.$$

$$+\tau_{\alpha n}(1+K_\gamma n)K_\alpha+\tau_{\alpha\gamma}\frac{\partial K_\alpha}{\partial\gamma}n+\frac{\partial[\tau_{n\alpha}(1+K_\gamma n)(1+K_\alpha n)]}{\partial n}$$

$$\left.+\frac{\partial[\tau_{\gamma\alpha}(1+K_\alpha n)]}{\partial\gamma}-\tau_{\gamma\gamma}\frac{\partial K_\gamma}{\partial\alpha}n\right\},$$

$$\frac{\partial v}{\partial t}+\frac{u}{1+K_\alpha n}\frac{\partial v}{\partial\alpha}+v\frac{\partial v}{\partial n}+\frac{w}{1+K_\gamma n}\frac{\partial v}{\partial\gamma}$$

$$-w\left[\frac{K_\gamma}{1+K_\gamma n}w\right]+u\left[-\frac{K_\alpha}{1+K_\alpha n}u\right] \tag{E15}$$

$$=Y-\frac{1}{\rho}\frac{\partial p}{\partial n}+\frac{1}{\rho}\frac{1}{(1+K_\alpha n)(1+K_\gamma n)}\left\{\frac{\partial[\tau_{\alpha n}(1+K_\gamma n)]}{\partial\alpha}-\tau_{\alpha\alpha}(1+K_\gamma n)K_\alpha\right.$$

$$+\frac{\partial[\tau_{nn}(1+K_\tau n)(1+K_\alpha n)]}{\partial n}+\frac{\partial[\tau_{\tau n}(1+K_\alpha n)]}{\partial \gamma}-\tau_{\tau\tau}(1+K_\alpha n)K_\tau\Big\},$$

$$\frac{\partial w}{\partial t}+\frac{u}{1+K_\alpha n}\frac{\partial w}{\partial \alpha}+v\frac{\partial w}{\partial n}+\frac{w}{1+K_\tau n}\frac{\partial w}{\partial \gamma}$$

$$-u\frac{1}{(1+K_\alpha n)(1+K_\tau n)}\left[\frac{\partial K_\alpha}{\partial \gamma}nu-\frac{\partial K_\tau}{\partial \alpha}nw\right]+v\left[\frac{K_\tau}{1+K_\tau n}w\right]$$

$$=Z-\frac{1}{\rho}\frac{1}{1+K_\tau n}\frac{\partial p}{\partial \gamma}+\frac{1}{\rho}\frac{1}{(1+K_\alpha n)(1+K_\tau n)}\Big\{\frac{\partial[\tau_{\alpha\tau}(1+K_\tau n)]}{\partial \alpha}$$

$$-\tau_{\alpha\alpha}\frac{\partial K_\alpha}{\partial \gamma}n+\frac{\partial[\tau_{n\tau}(1+K_\tau n)(1+K_\alpha n)]}{\partial n}+\frac{\partial[\tau_{\tau\tau}(1+K_\alpha n)]}{\partial \gamma}$$

$$+\tau_{\tau\alpha}\frac{\partial K_\tau}{\partial \alpha}n+\tau_{\tau n}(1+K_\alpha n)K_\tau\Big\}.$$

The transport equation of kinetic energy is

$$\frac{D}{Dt}\left(\frac{u^2+v^2+w^2}{2}\right)=(Xu+Yv+Zw)$$

$$-\frac{1}{\rho}\left(\frac{u}{1+K_\alpha n}\frac{\partial p}{\partial \alpha}+v\frac{\partial p}{\partial n}+\frac{w}{1+K_\tau n}\frac{\partial p}{\partial \gamma}\right)+\frac{1}{\rho}\Psi, \qquad \text{(E16)}$$

where Ψ is the work for translating fluid element reduced from

$$\Psi=\left(\frac{\partial \tau_{\alpha\alpha}}{\partial x}+\frac{\partial \tau_{n\alpha}}{\partial y}+\frac{\partial \tau_{\tau\alpha}}{\partial z}\right)u$$

$$+\left(\frac{\partial \tau_{\alpha n}}{\partial x}+\frac{\partial \tau_{nn}}{\partial y}+\frac{\partial \tau_{\tau n}}{\partial z}\right)v+\left(\frac{\partial \tau_{\alpha\tau}}{\partial x}+\frac{\partial \tau_{n\tau}}{\partial y}+\frac{\partial \tau_{\tau\tau}}{\partial z}\right)w. \qquad \text{(E17)}$$

3. 4. Equation of energy

The first law of thermodynamic is expressed by

$$\frac{De}{Dt}+p\frac{D}{Dt}\left(\frac{1}{\rho}\right)=\frac{1}{\rho}(H+\Phi), \qquad \text{(E18)}$$

where

$$H=\frac{1}{(1+K_\alpha n)(1+K_\tau n)}\left\{\frac{\partial}{\partial \alpha}\left[k\frac{1+K_\tau n}{1+K_\alpha n}\frac{\partial T}{\partial \alpha}\right]\right.$$

$$\left.+\frac{\partial}{\partial n}\left[k(1+K_\tau n)(1+K_\alpha n)\frac{\partial T}{\partial n}\right]+\frac{\partial}{\partial \gamma}\left[k\frac{1+K_\alpha n}{1+K_\tau n}\frac{\partial T}{\partial \gamma}\right]\right\}. \qquad \text{(E19)}$$

The transport equation of total energy defined by $E=(1/2)(u^2+v^2+w^2)+e+(p/\rho)+\Omega$ is given by addition of Eqs. (E16) and (E18).

$$\frac{DE}{Dt}=\frac{\partial Q}{\partial t}+\frac{1}{\rho}\frac{\partial p}{\partial t}+\frac{1}{\rho}[H+\Phi+\Psi], \tag{E20}$$

where $\Phi+\Psi$ represents the rate of total work done by adjacent fluid.

References

1) Uchida, S., A New Approximate Solution in Boundary Value Problems by the Use of Orthogonal Curvilinear Coordinates, J. Phys. Soc. Japan, Vol. 3, pp. 33-40, 1948.
2) Flügel, G., Ein neues Verfahren der graphischen Integration, angewandt auf Strömungen idealer Flüssigkeiten in Kreiselrädern, Ztschr. f. d. gesamte Turbinenwesen, Vol. 12, pp. 73-77, 89-91, 100-103, 1915.
3) Flügel, G., Mehrdimensionale Strömung von Gasen, Ztschr. f. d. gesamte Turbinenwesen, Vol. 17, pp. 161-165, 178-180, 1919.
4) Bindon, J. P., and Carmichael, A. D., Streamline Curvature Analysis of Compressible and High Mach Number Cascade Flows, J. Mech. Eng. Sci., Vol. 13, pp. 344-357, 1971.
5) Barger R. L., Streamline Curvature Design Procedure for Subsonic and Transonic Ducts, NASA TN D-7368, 1973.
6) McNally, W. D., FORTRAN Program for Generating a Two-dimensional Orthogonal Mesh between Two Arbitrary Boundaries, NASA TN D-6766, 1972.
7) Ferri, A., Elements of Aerodynamics of Supersonic Flows, Mcmillan, New York, 1949.
8) Uchida, S., and Kondo, T., On the Computation of a Nozzle With Arbitrary Distribution of Velocity Along the Wall, 9th Fluid Dynamics Meeting, Paper 1B4, Pre-print pp. 74-77, 1977 (in Japanese).
9) Uchida, S., Calculation of Compressible Cascade Flow by the Method of Flux Analysis, J. Aero. Sci., Vol. 21, pp. 237-250, 1954.
10) Kawasaki, T., Calculation on the Cascade of Symmetrical Joukowski Airfoils, Railway Tech. Lab., Gas Turbine Res., TM No. 9, pp. 1-8, 1948 (in Japanese).
11) Numachi, F., and Kurokawa, T., Model Air Test on Guide Vane Blades of Gas Turbine, Trans. Japan Soc. Mech. Engrs., Vol. 15, pp. 46-52, 1950 (in Japanese).
12) Hudimoto, B., Aerodynamic Research on the Cascades of Turbine Blades, Eng. Res. Inst., Kyoto Univ., Rep. No. 34, pp. 1-35, 1956.
13) Oswatitsch, K., and Ryhming, I., Über den Kompressibilitätseinfluss bei ebenen Schaufelgittern starker Umlenkung, D.V.L. Bericht No. 28, pp. 1-29, 1957.
14) Oswatitsch, K., Basic Formulation for Transonic Flow Problems in Rotors, Transonic Flow Problems in Turbomachinery, ed. by T. C. Adamson, Jr. and M. F. Platzer, Hemisphere, Washington, pp. 6-19, 1977.
15) Nakamura, T., and Otsuka, S., A Study on the Method of Flux Analysis Applied to Cascade Flow, Fluid and Heat Eng. Research (Tokai Inst. Fluid and Heat Eng.), Vol. 11, pp. 27-40, 1976 (in Japanese).
16) Katsanis, T., A Computer Program for Calculating Velocities and Streamlines for Two-Dimensional, Incompressible Flow in Axial Blade Rows, NASA TN D-3762, 1967.
17) Katsanis, T., FORTRAN Program for Calculating Transonic Velocities on a Blade-to-Blade Stream Surface of a Turbomachine, NASA TN D-5427, 1969.
18) Uchida, S., and Yasuhara, M., The Rotational Field Behind a Curved Shock Wave Calculated by the Method of Flux Analysis, J. Aero. Sci., Vol. 23, pp. 830-845, 1956: Correction of Erratum: J. Aero. Sci., Vol. 25, p. 200, 1958.
19) Vazsonyi, A., On Rotational Gas Flows, Quart. Appl. Math., Vol. 3, pp. 29-37, 1945.
20) Eula, A., L'influenza del numero di Reynolds ai grandi numeri di Mach, Aerotecnica, Vol. 20, pp. 20-29, 1940.
21) Gowen, F. E., and Perkins, E, W., Drag of Circular Cylinders for a Wide Range of

Reynolds Numbers and Mach Numbers, NACA TN 2960, 1953.
22) Uchida, S., Nakamura, Y. and Kondo, T., On the Flux Analysis Method and its Application to the Study of Swirling Flows, (to be published).
23) Hall, M. G., The Structure of Concentrated Vortex Cores, Progress in Aeron. Sci., Vol. 7, pp. 53-110, 1966.
24) Hall, M. G., Vortex Breakdown, Ann. Rev. Fluid Mech., Vol. 4, pp. 195-218, 1972.
25) Sarpkaya, T., Vortex Breakdown in Swirling Conical Flows, AIAA J., Vol. 9, pp. 1792-1799, 1971.
26) Sarpkaya, T., Effect of the Adverse Pressure Gradient on Vortex Breakdown, AIAA J., Vol. 12, pp. 602-607, 1974.
27) Leibovich, S., The Structure of Vortex Breakdown, Ann. Rev. Fluid Mech., Vol. 10, pp. 221-246, 1978.
28) Uchida, S., Nakamura, Y., Nakamura, H., Suehiro, F. and Tsuboi, K., Measurments on the Swirling Flow by Laser Velocimeter, J. Japan Soc. Aero. Space Sci., Vol. 25, pp. 510-517, 1977 (in Japanese).
29) Faler, J. H. and Leibovich, S., An Experimental Map of the Internal Structure of a Vortex Breakdown, J. Fluid Mech., Vol. 86, pp. 313-335, 1978.
30) Long, R. R., Steady Motion around a Symmetrical Obstacle Moving along the Axis of a Rotating Liquid, J. Meteor., Vol. 10, pp. 197-203, 1953.
31) Chow, C.-Y., Swirling Flow in Tubes of Non-Uniform Cross-Sections, J. Fluid Mech., Vol. 38, pp. 843-854, 1969.
32) Uchida, S., Nakamura, Y. and Taniguchi Y., Analytical Solutions of Swirling Flow with an Arbitrary distribution of Velocities along the Axis - Exact Solutions, Trans. Japan Soc. Aero. Space Sci., Vol. 20, pp. 75-86, 1977.
33) Uchida, S. and Suzuki, T., On a Similar Solution for a Turbulent Half-Jet along a Curved Streamline, J. Fluid Mech., Vol. 33, pp. 379-395, 1968.
34) Uchida, S., Kuwabara, K. and Kishi, M., On a Similar Solution for the Laminar Half-Jet along a Curved Streamline, Trans. Japan Soc. Aero. Space Sci. Vol. 16, pp. 264-279, 1973.
35) Murao, R. and Uchida, S., On a Similar Solution for a Turbulent Curved Jet, Z.A.M.P., Vol 28, pp. 97-106, 1977.
36) Uchida, S. and Kuwabara, K., On a Particular Solution of the Energy Equation for a Compressible Laminar Boundary Layer Referred to Orthogonal Curvilinear Coordinates, Trans. Japan Soc. Aero. Space Sci., Vol. 14, pp. 1-8, 1971.
37) Uchida, S. and Kuwabara, K., On a Particular Solution of the Energy Equation for a Compressible Turbulent Boundary Layer Referred to Orthogonal Curvilinear Coordinates, Trans. Japan Soc. Aero. Space Sci., Vol. 17, pp. 1-9, 1974.
38) Kuwabara, K., On an Approximate Solution for a Compressible Laminar Half-Jet along a Curved Streamline, J. Japan Soc. Aero. Space Sci., Vol. 26, pp. 541-550, 1978 (in Japanese).
39) Ishii, R., Subsonic-Supersonic Flow in Axially-Symmetric Nozzles, Trans. Japan Soc. Aero. Space Sci., Vol. 23, pp. 18-34, 1980.